PHYSICO-CHEMICAL PROPERTIES OF LIGNIN SULFONATES

A Thesis

by

John Leslie Gardon

Submitted to the Faculty of Graduate Studies and Research of McGill University in partial fulfilment of the requirements for the degree of Doctor of Philosophy.

Department of Chemistry,
McGill University,
Montreal, Canada.

April 1955.

Acknowledgements.

The author would like to express his sincere gratitude and appreciation to:

Dr. S.G. Mason, for his encouragement, helpful guidance and kind patience throughout this work,

Mr. G.J.C. Potter of the Pulp and Paper Research Institute of Canada for the kind assistance in editing the present study,

the National Research Council of Canada for a Studentship,

the Anglo-Canadian Paper Co. for two scholarships,

the Pulp and Paper Research Institute of Canada for accomodation and equipment.

SUMMARY

Lignin sulfonates were separated into eight fractions with molecular weights ranging from 3,700 to 58,000 by means of fractional dialysis and ultrafiltration. All fractions have similar ultraviolet absorption spectra. Their methoxyl contents and neutralization equivalent weights increase with increasing molecular weights. All acid groups on the four highest molecular weight fractions are sulfonic.

The molecular weights were determined in a new type of osmometer of simple design. A method of determining osmotic pressures in the presence of membranes which are permeable to the solute was developed and applied to the low molecular weight fractions.

Results of viscosity, conductivity and dyestuff adsorption measurements suggest that lignin sulfonates are flexible polyelectrolytes. There is in addition, evidence that molecular association occurs in the low molecular weight fractions in a manner analogous to micelle formation in soaps. From correlations between molecular weights and intrinsic viscosities it can be concluded that the degree of molecular branching increases with increasing molecular weight.

TABLE OF CONTENTS

LIST OF FIGURES.

LIST OF TABLES

GLOSSARY OF SYMBOLS

Symbol		Unit
a	constant in equation $[\eta] = k_2 M^a$	
A	membrane area	cm^2
A_η	constants in the Fuoss' equation for the concentration dependence of the reduced viscosity of polyelectrolytes	100cc./g
B_η		$\sqrt{100cc./g}$
b	constant in equation $D_1 = k_1 M^{-b}$	
c'	concentration of solute	g/100cc.
c	concentration of solute	$mole.cm^{-3}$
D_1	diffusion coefficient of solute	$cm^2.\ hour^{-1}$
D_2	membrane dialysis coefficient	$cm^3.\ hour^{-1}$
D_η	constant in the Fuoss' equation for the concentration dependence of the reduced viscosity of polyelectrolytes	100cc./g
d	membrane thickness	cm.
d_s	density of solvent	$g.\ cm^{-3}$
k	constant in equation $z = [\eta] + k[\eta]^2 c$	
k_1	constant, see definition of b	
k_2	constant, see definition of a	
K_s	rate constant of solute diffusion, determined from changes in osmotic pressure difference	$hour^{-1}$
K'_s	rate constant of solute diffusion, determined from concentration changes	$hour^{-1}$

Symbol		Units
K_w	rate constant for viscous solvent flow	$hour^{-1}$
M	molecular weight	g
n	number of solute molecules	
P_1	permeability coefficient of membrane	$cm^2.hour^{-1}.(poise).(cm.solvent)^{-1}$
P_2	permeability of membrane to solvent	$cm.hour^{-1}.(cm.solvent)^{-1}$
p	true osmotic pressure difference	cm. solvent
p_{exp}	osmotic pressure reading extrapolated to zero time	cm. solvent
p_m	theoretically measurable osmotic pressure difference, $(1 - \delta)RT\Delta c$ or $(1 - \delta)RT\Delta c$	cm. solvent
p_r	osmotic pressure reading	cm. solvent
q	ratio between solution and solvent chamber volumes in the osmometer cell	
R	gas constant, $8.48\ 10^4$	$g.cm.^oC.mole^{-1}$
S	volume necessary to equilibrate the osmometer for the change in the difference in osmotic pressure caused by the diffusion of 1 mole solute	cm^3
T	absolute temperature	^oC
t	time	hour
t_{max}	time when the viscous backlog in the osmometer is maximal, $(\ln K_w/K_s)/(K_w-K_s)$	hour
t_o	time of the last external adjustment on the osmometer	hour

Symbol		Units
U	volume ultrafiltrate produced in unit time	$cm^3.hour^{-1}$
V	volume of half cell or of the solvent	cm^3
V_{eff}	$= K'_s V_l / K_s$	cm^3
V_m	volume of one mole solvated solute	cm^3
V_L	volume of the liquor at ultrafiltration	cm^3
x	power of c' in the modified Fuoss' equation for the concentration dependence of the reduced viscosity of lignin sulfonates	
z	reduced viscosity, $= \eta sp/c'$	100cc./g
α	characteristic function $(1 - \gamma)(1 + K_s/K_w)/p_{exp}$	$(cm.solvent)^{-1}$
β	characteristic function $(1 - \gamma)K_s/p_{exp}SK_w$	$(cm.solvent)^{-1}cm^{-3}$
γ	partition coefficient of solute between solutions inside and outside the membrane.	
δ	probability of passage for a molecule hitting the membrane	
Δ	error in the final adjustment of the osmometer	cm.solvent
ϵ_{max}	extinction at the maximum of the ultraviolet absorption spectrum	liter $g^{-1}cm^{-1}$
ϵ_{min}	extinction at the minimum of the ultraviolet absorption spectrum	liter $g^{-1}cm^{-1}$
$\Delta\epsilon_{max}$	maximum extinction difference of ultraviolet absorption spectra of pH 12 and pH 6 solutions at around 300 mμ	liter $g^{-1}cm^{-1}$

Symbol		Units
λ	ratio between concentrations in ultrafiltrate and liquor	
η	viscosity of solvent	poise
η_{sp}	specific viscosity, $= \frac{\eta_{solution} - \eta_{solvent}}{\eta_{solvent}}$	
$[\eta]$	intrinsic viscosity $= \lim_{c' \to 0} \eta_{sp}/c'$	100cc./g
σ	capillary cross section	cm^2
τ	time	hour

Subscripts of c and V

1	refers to solution chamber
2	refers to solvent chamber

I. GENERAL INTRODUCTION

A. ECONOMIC SIGNIFICANCE OF LIGNIN SULFONATES

Pulping of wood by the sulfite process is carried out by digesting wood at about 130°C for several hours with a solution of sulfurous acid and a bisulfite salt, generally calcium bisulfite. During the digestion, lignin is sulfonated and part of the carbohydrate is hydrolysed. The solution of the resulting lignin sulfonates and degraded carbohydrates is termed spent sulfite liquor.

The yearly production of spent sulfite liquor in Canada corresponds to more than two million tons of solids (99), of which 60% are lignin sulfonates, 20% fermentable sugars and 20% acidic degradation products. At present only a small fraction of the available vast quantities of spent sulfite liquor finds practical application; the rest is discarded into rivers and causes a serious water pollution problem. There is naturally great interest in finding profitable large scale applications for the solids present in the liquor.

In the manufacture of vanillin the lignin

sulfonates are used as chemical raw materials. This application, however, is limited for various economic and technical reasons.

Relatively large amounts of lignin sulfonates are used as dispersants and adhesives (99, 63). These applications however, were found more or less by accident and very little systematic investigation has yet been carried out on the basic physico-chemical properties which make these uses possible. The aim of the present investigation was to cast some light on these properties.

B. CHEMICAL CONSTITUTION OF LIGNIN SULFONATES.

Although the organic chemistry of lignin and lignin sulfonates has been subject to a great deal of research, the exact structure of these materials is not yet known. It is generally believed (24, 95) that lignin in wood is formed by enzyme-catalysed oxidative polymerisation of coniferyl alcohol (I). It is probable that the aliphatic chains of the monomers are arranged in furan rings (II) as suggested by Hibbert (22, 42), or in pyran rings (III) as suggested by Freudenberg (25). Phenolic hydroxyl contents (26, 27) and spectrochemical data (4) indicate that lignin is built up from units containing 4 to

I.

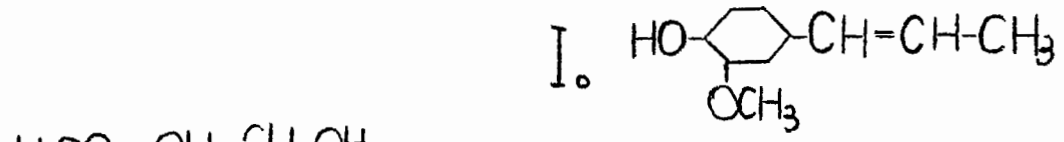

II.

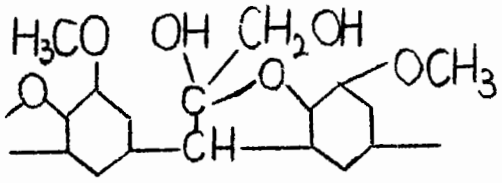

III.

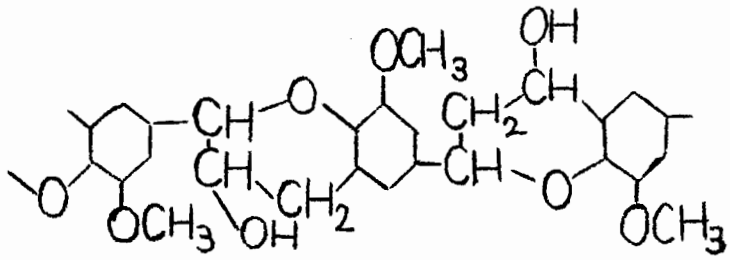

6 coniferyl alcohol monomers. General reviews of other theories of lignin structure are given by Hagglund (35), Brauns (10) and Lindgren et al. (7, 95, 52).

It should be mentioned that only softwood lignins are built of monomers of type (I), hard wood lignins also contain structural elements with two methoxyl and no hydroxyl groups on the aromatic ring.(35)

Model experiments (6, 51) indicate that in the reaction between lignin and sulfurous acid, hydroxyl groups on (II) or (III) are replaced by sulfonate groups according to the following reaction:

$$\geq C\text{-}OH + HSO_3H = \geq C\text{-}SO_3H + H_2O$$

As a confirmation of this view it has been found (21, 27)

that in lignin sulfonates with various degrees of sulfonation, the ratio between the methoxyl and the sum of the hydroxyl and sulfonate groups was constant. The ring formed by the aliphatic chain of the monomer is not split during the sulfonation, as lignin sulfonates with various degrees of sulfonation have the same phenolic hydroxyl contents (55) and similar light absorption spectra (4). There is evidence (21) that there are in lignin two types of group having different reactivities which can be sulfonated.

It is not yet established whether the sulfur of lignin sulfonates is present only as sulfonic groups and whether all acid groups are sulfonic. Lignin sulfonate samples have been prepared with sulfur contents higher than acid group contents (87,88), with solely sulfonic acid groups (19, 53, 78, 79) and with more acid groups than sulfonic groups (27). Some of these variations may be caused by the presence of impurities. In general, the sulfur contents of lignin sulfonate preparations range from one to two sulfur atoms per two monomers.

It must be borne in mind that lignin sulfonates are not chemically well defined substances. Their chemical analyses vary with the molecular weights and also depend on

the cooking conditions and on the species of wood used for the cook. For chemical identification it is customary to determine the methoxyl, sulfur and hydroxyl contents, reducing powers and neutralization equivalent weights. These data are generally considered to give a picture of the functional groups present in the sample under investigation.

C. SCOPE OF THE PRESENT WORK.

The present investigations can logically be divided into a number of stages as follows:

1) Fractionation of lignin sulfonates.

2) Determination of their analytical data.

3) Determination of their molecular weights.

4) Study of the physical structure of the molecules by means of diffusion, viscosity, conductivity and dyestuff adsorption measurements.

This order of presentation is preserved in the ensuing study.

The present approach of studying lignin sulfonates is that of polymer chemistry. In polymer chemistry the materials under investigation are mostly in the molecular weight range of about 20,000 and higher, and soluble in organic solvents. Lignin sulfonate salts are water soluble only and the bulk of the molecular weights was found to be below

20,000. These properties of the lignin sulfonates made it necessary to develop new experimental techniques for fractionation and for molecular weight determination. These techniques are also described in detail.

II. FRACTIONATION OF LIGNIN SULFONATES

A. INTRODUCTION

The dissolved solids in spent sulfite liquor consist largely of lignin sulfonates and the remainder of sugars and acidic degradation products of cellulose and lignin. Various methods of separating lignin sulfonates from the other constituents have been used (8, 39) including precipitation, dialysis and ion exchange. Attempts have also been made to fractionate the highly polydisperse lignin sulfonates according to their molecular weights by fractional dialysis (23, 83), fractional extraction of the free acids by propanol (82), fractional precipitation of the barium salts by ethanol (65) or acetone (69), counter current butanol extraction of free acids and amine salts in water (66), differential sorption on swollen ion-exchange resins (54) and fractionation by the different solubilities of various amine salts (19, 53, 69).

The ultimate aim of our work was to investigate some of the basic physico-chemical properties of lignin sulfonates. For this purpose relatively large quantities of chemically well-defined lignin sulfonate fractions were prepared by a combination of fractional dialysis and ultra-

filtration of a spent sulfite liquor concentrate. The flow sheet of this procedure is presented in Fig. 1.

B. EXPERIMENTAL PROCEDURE

1. Material

Spray dried spent sulfite liquor marketed under the name Lignosol B and supplied by Lignosol Chemicals Ltd. was used as the starting material. The spent liquor was drawn from cooks of a mixture of balsam and spruce in approximately equal amounts.

About 700 gm. Lignosol was dissolved in 2 liters of water, filtered, passed through previously regenerated and well washed Amberlite IR-4B (OH) anion and IR-120 (H) cation exchange resins to remove mineral acids and calcium respectively and finally neutralised to pH 6.5 with sodium hydroxide. The resulting solution contained 633 gm. solids.

2. Dialysis

A Webcell Laboratory Model continuous counter current dialyser (manufactured by Brosites Machine Corp.,N.Y.) was used with denitrated nitrocellulose membranes. This dialyser consists of thirteen lucite rings 17.5 cm. I.D. The membranes are clamped between these rings yielding 7 water and 6 solution chambers connected respectively in series through

Fig. 1.

Flow sheet for fractionation of lignin sulfonates.

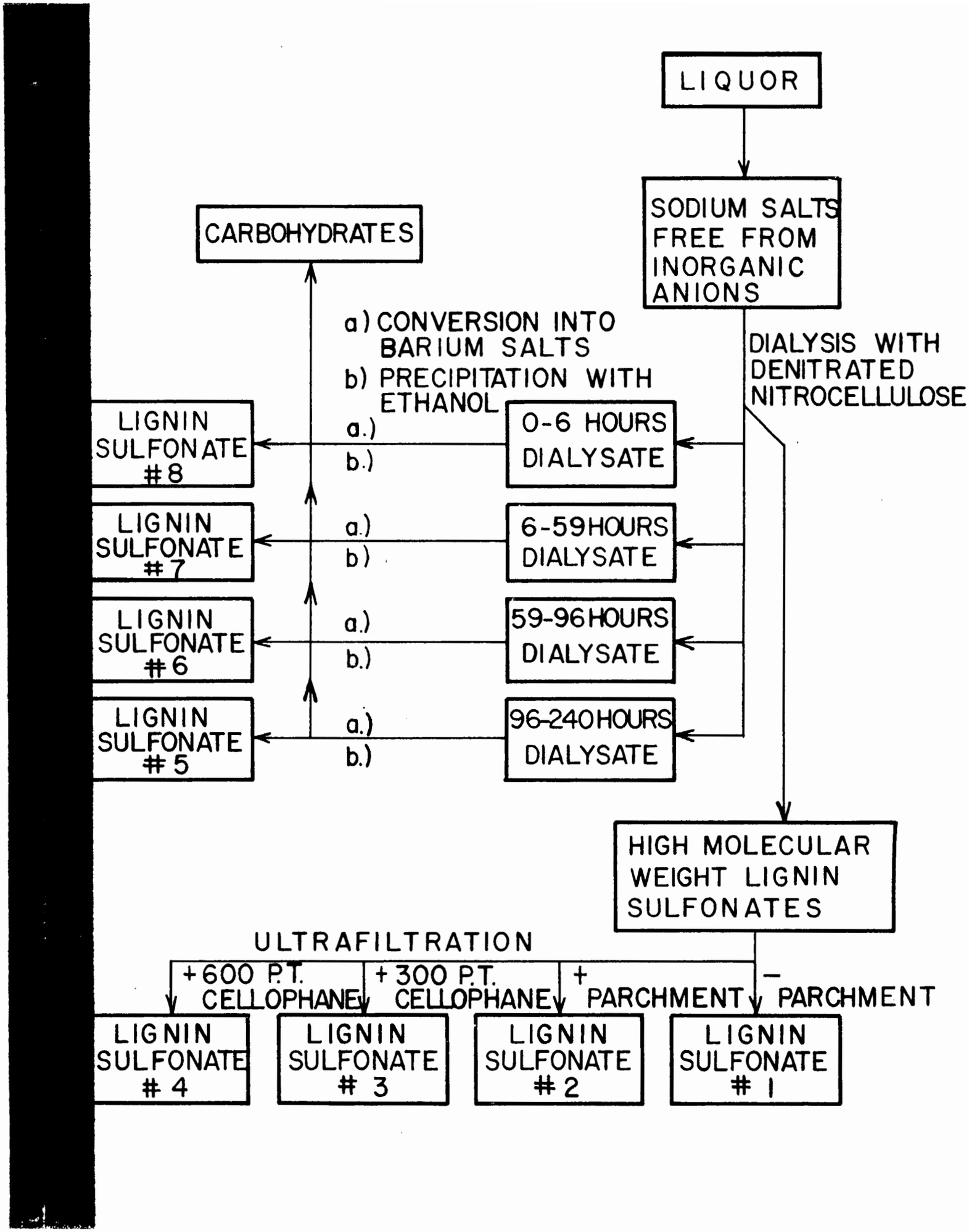
LIQUOR
SODIUM SALTS FREE FROM INORGANIC ANIONS
CARBOHYDRATES
a) CONVERSION INTO BARIUM SALTS
b) PRECIPITATION WITH ETHANOL
DIALYSIS WITH DENITRATED NITROCELLULOSE
LIGNIN SULFONATE #8
LIGNIN SULFONATE #7
LIGNIN SULFONATE #6
LIGNIN SULFONATE #5
a.)
b.)
0-6 HOURS DIALYSATE
6-59 HOURS DIALYSATE
59-96 HOURS DIALYSATE
96-240 HOURS DIALYSATE
HIGH MOLECULAR WEIGHT LIGNIN SULFONATES
ULTRAFILTRATION
+600 P.T. CELLOPHANE
+300 P.T. CELLOPHANE
+ PARCHMENT
− PARCHMENT
LIGNIN SULFONATE #4
LIGNIN SULFONATE #3
LIGNIN SULFONATE #2
LIGNIN SULFONATE #1

suitable channels. These channels were not used as it was found that the apparatus could be controlled better if the corresponding chambers worked in parallel. The design was accordingly altered by drilling holes in the top and bottom of each ring.

As shown in Fig.2, the liquor was circulated from a reservoir through the dialyser, with a continuous counter current flow of distilled water. A membrane pump (A) governed by an oscillating mercury pump was used for this purpose. Details of this pump are shown in Fig. 3.

The construction of the membrane pump (Fig.3,A) is similar to that of the ultrafilter cells to be described later. It is made up of two lucite discs of 12 cm. diameter, two rubber rings 5 mm. thick with 10 cm. outside and 8 cm. inside diameter and of an elastic dental dam membrane disc(c) of 10 cm. diameter clamped between the rubber rings. For accomodating the screws both lucite discs have four holes with centers on an 11 cm. diameter circle concentric with the discs and two 8 mm. bore holes (b), with centers 3.75 cm. from the center of the disc on the same diameter in which tygon tubing is placed in the same manner as described later for the ultrafilters. The membrane is made of two dental dam rubber sheets stuck together with silicone grease. This

Fig. 2.

Dialysis Apparatus.

(A) Membrane pump

(B) Valves

(C) Liquor overflow

(D) Liquor reservoir

(E) Pinchcock to regulate liquor flow

(F) Glass wool filter

(G) T tube

(H) Air inlet

(I) Dialysis cell

(J) Bypass for initial filling of the water chambers

(K) T tube

(L) Constant head device

(M) Air inlet tube

(N) Distilled water reservoir

(O) Pinchcock to regulate water flow

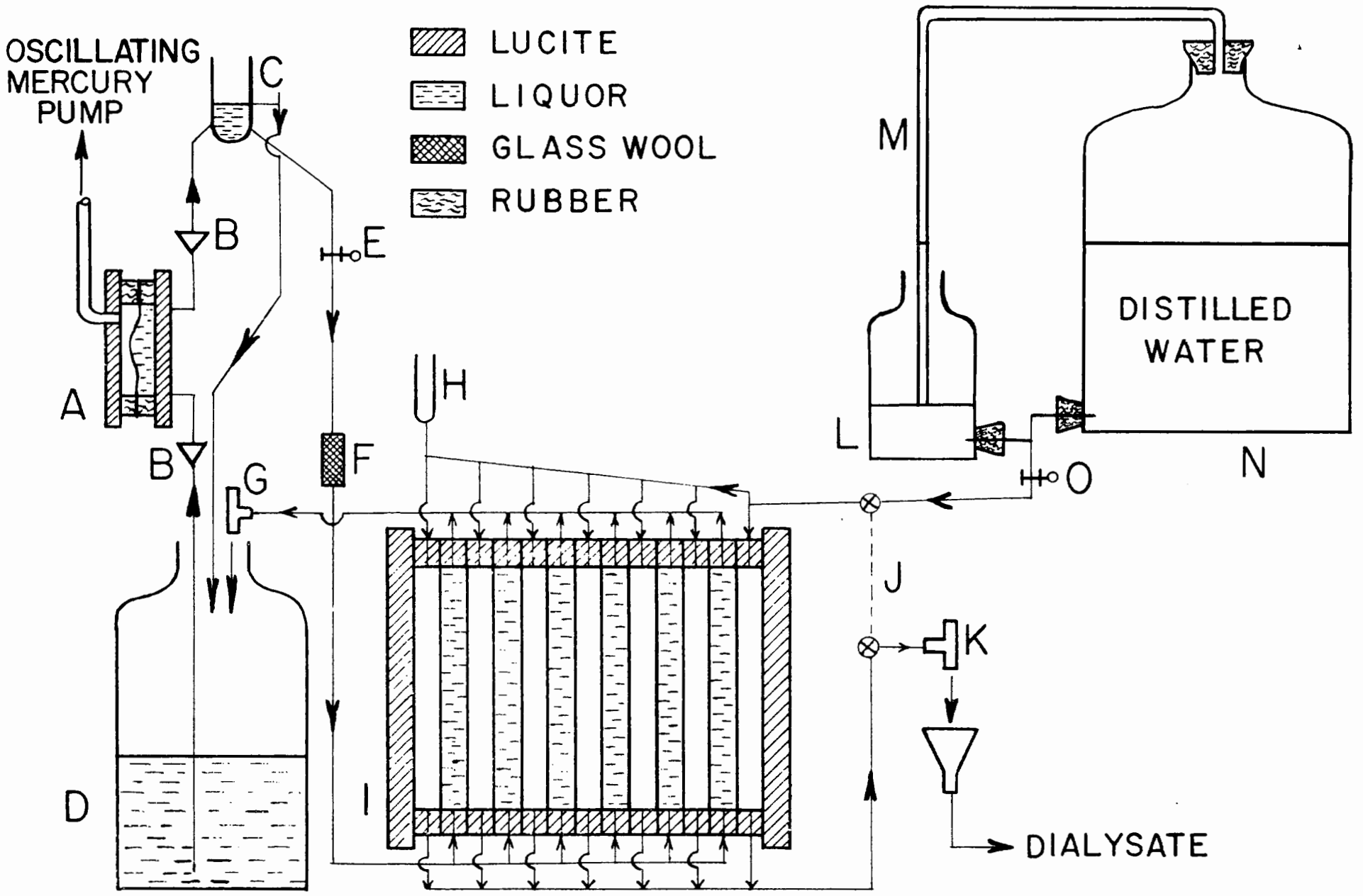
OSCILLATING
MERCURY
PUMP
LUCITE
LIQUOR
GLASS WOOL
RUBBER
A
B
B
C
D
E
F
G
H
I
J
K
L
M
N
O
DISTILLED
WATER
DIALYSATE

Fig. 3.

Details of the circulating pump.

(A) Membrane pump

(a) Stopcock

(b) Inlet holes

(c) Dental dam membrane

(d) Valves

(B) Oscillating mercury pump

(e) Valve

(f) Cork floater.

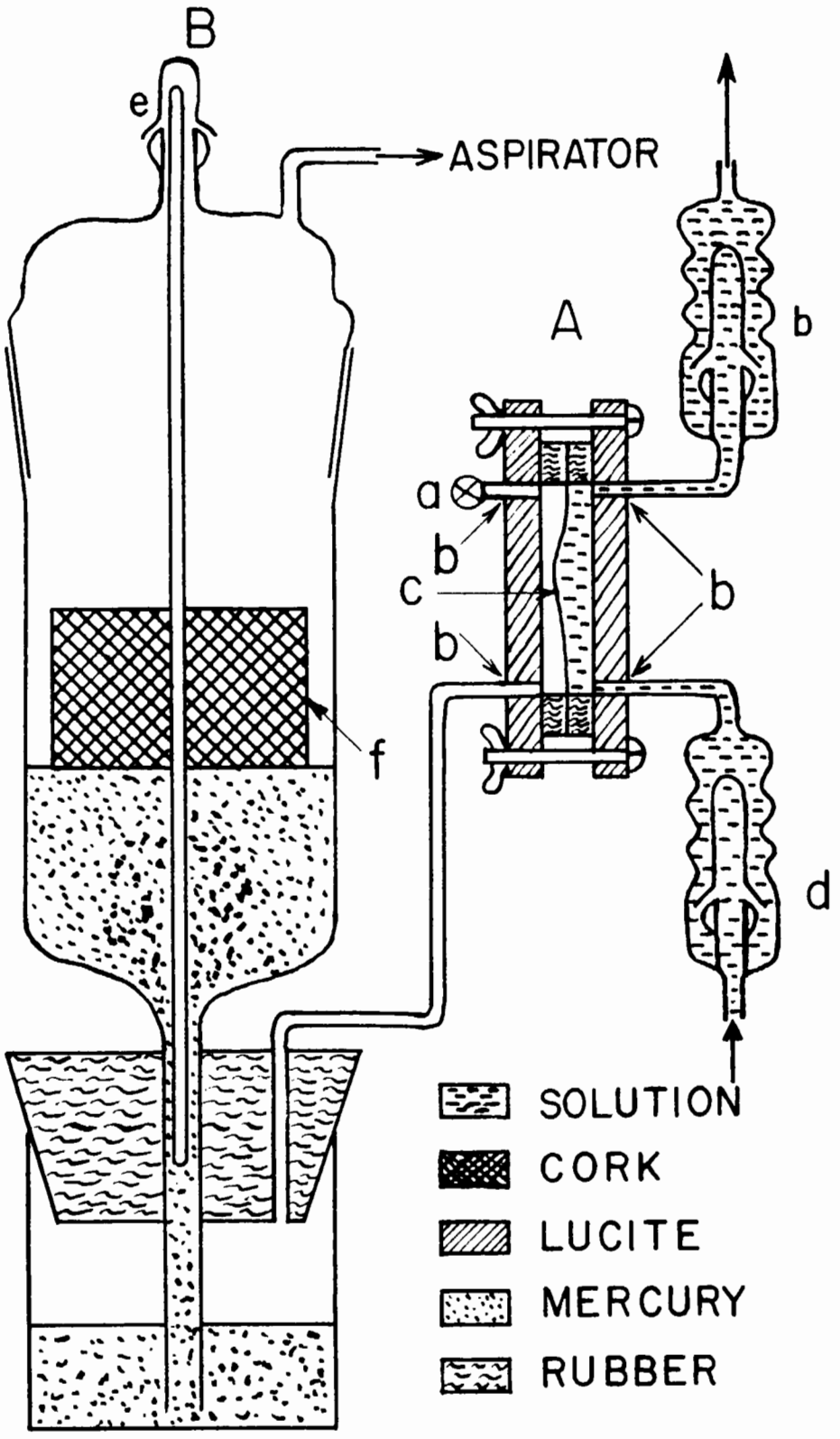
B
e
ASPIRATOR
A
b
a
b
c
b
b
f
d
SOLUTION
CORK
LUCITE
MERCURY
RUBBER

method of preparation gives the membrane a long life. The two check valves (d) are made of spherical glass joints of 12 mm. sphere diameter.

The oscillating mercury pump functions as follows. By applying vacuum in the upper chamber, mercury is sucked into it. The rising mercury raises the cork float (f) and thus opens valve (e). Consequently air enters into the upper chamber, the mercury level drops, valve (e) is closed and a new pumping cycle starts. The lower chamber of this pump is connected with the membrane pump and the membrane in the latter has to follow the movements of the mercury. In practice the oscillating mercury pump is put into operation first, independently of the membrane pump, and stopcock (a) is closed afterwards. The difference in level between the mercury in the lower and upper chambers should alternate between 10 and 14 cm. The diameter of both the upper and the lower chambers of the oscillating mercury pump is 7 cm. and the length of the pump is 25 cm. The valve (e) is made of 12 mm. diameter spherical glass joint.

The capacity of this pumping system is around 200 cc. per minute.

To ensure steady flow the pump did not feed directly

into the dialyser, but passed through an overflow (Fig.2, C) and liquor flowed through the unit by gravity. The flow rate was regulated to 60 cc/min. by a pinch cock (E).

The distilled water came from a reservoir (N) and through a constant head device (L) at 3 cc/min. The free head of the water in the constant head device was maintained by the air inlet tube (M) which controlled the flow of air into and the flow of water from the reservoir (N). In this way the head of water was automatically maintained constant within 2 cm.

The volume of liquor was maintained between 4 and 6 liters. The volume increase due to osmosis amounted to about 2 liters per 12 hours; this excess was periodically removed, neutralized with sodium hydroxide to avoid polymerisation of the lignin sulfonic acids, concentrated by vacuum evaporation at 60° C. and reintroduced into the system.

To avoid growth of fungi during dialysis and the subsequent ultrafiltration, a small amount of toluene was added to the liquor.

The dialysates produced every 12 hours were handled as separate fractions. They were brought to pH 6.5

with sodium hydroxide or with cation exchange resin as required. Their content, reducing power and neutralization equivalent weight of solids were determined. The reducing power of the solids in the residual liquor was calculated from these results by difference and checked by direct determination every 48 hours.

The dialysis was stopped after 19 days when the reducing power of the solids in both dialysate and residual liquor became of the same order of magnitude (Fig. 6, Curves F and G).

To separate the β -lignin sulfonates, i.e. the low molecular weight fractions, from the carbohydrates, the barium salts were precipitated with ethanol as suggested by Erdtman (19). The dialysates corresponding to 0 to 6, 6 to 59, 59 to 98, 98 to 240 hours of dialysis were respectively combined to yield four separate fractions from which sodium was removed by cation exchange. The resulting free acids were neutralized with barium hydroxide, and the solutions were concentrated by vacuum evaporation at 60°C to about 30% solid content and poured dropwise into 4 volumes of ethanol with vigorous stirring. The precipitates were twice dissolved in water and reprecipitated. The barium salts were passed through a cation exchanger and the free

acids obtained were neutralized with sodium hydroxide and dried at 60°C under vacuum yielding fractions Nos. 5 to 8. The alcoholic mother liquors containing the carbohydrates were discarded; it should be noted, however, that in subsequent investigations it would be well worth while to investigate these constituents.

3. Ultrafiltration

Most ultrafilters (14, 29, 60) have perforated or porous plates as membrane supports, use membranes with small area, and to get appreciable rates of filtration, are operated at relatively high pressures. The solution, being under pressure, cannot readily be stirred and, becoming increasingly concentrated on the membrane surface, has a tendency to block the membrane pores (11). Such ultrafilters are not suitable for handling large quantities of materials.

For the purpose of fractionating lignin sulfonates a new type of ultrafilter was developed. This unit uses very large membrane areas, is fully automatic, simple to construct, leakproof and allows thorough stirring of the liquid.

a. The ultrafilter cell.

Each ultrafilter cell consists mainly of two lucite discs and two rubber rings (Fig. 4). The membrane is clamped between the rubber rings, reinforced with fine-mesh stainless steel screens and supported on both sides by two layers of tightly packed glass beads. To avoid leakage at the edges of the screens, rings of dental dam rubber are placed between them and the membrane, and between them and the rubber rings forming the body of the cell. When the unit is compressed, the dental dam penetrates into the meshes of the screen reinforcers and seals the cell effectively. The necessary parts for a typical cell are described in Table I.

A very simple, leakproof connection between the glass parts and the lucite can be made without the use of any cement. For this purpose Tygon tubing with 1.5 mm. wall thickness and 10 mm. O.D. is placed into 8 mm. bore holes in the lucite. To introduce the tubing into the hole the end of it is cut off conically along the length and pulled into the hole by the tongue thus formed, and the tongue is then cut away.

Each lucite disc is equipped with the connectors

Fig. 4.

Details of the ultrafilter cell (expanded view)

(1) Lucite discs
(2) Rubber rings
(3) Glass beads
(4) Dental dam gaskets
(5) Stainless steel screens
(6) Membrane
(7) Inlet hole

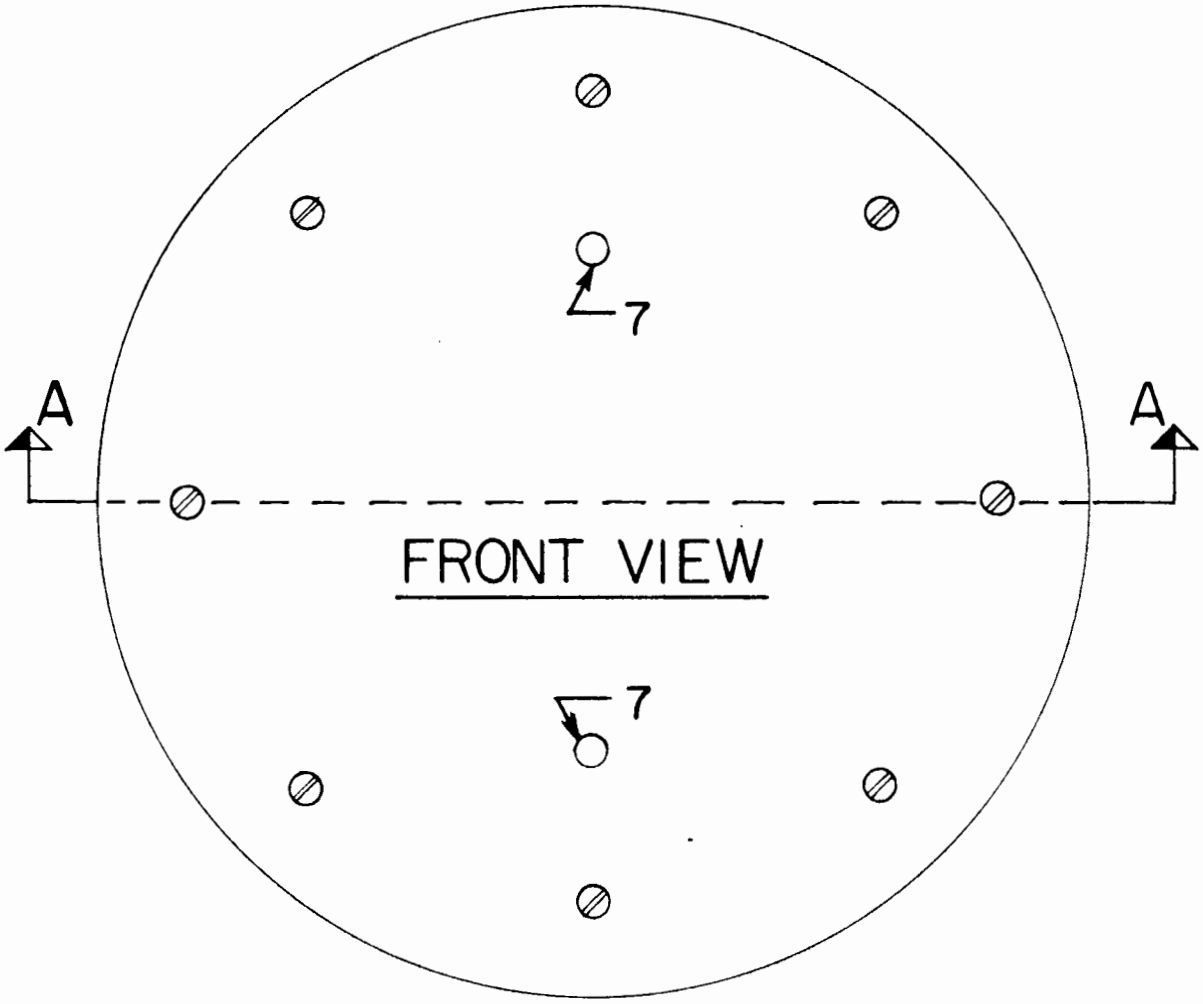

FRONT VIEW

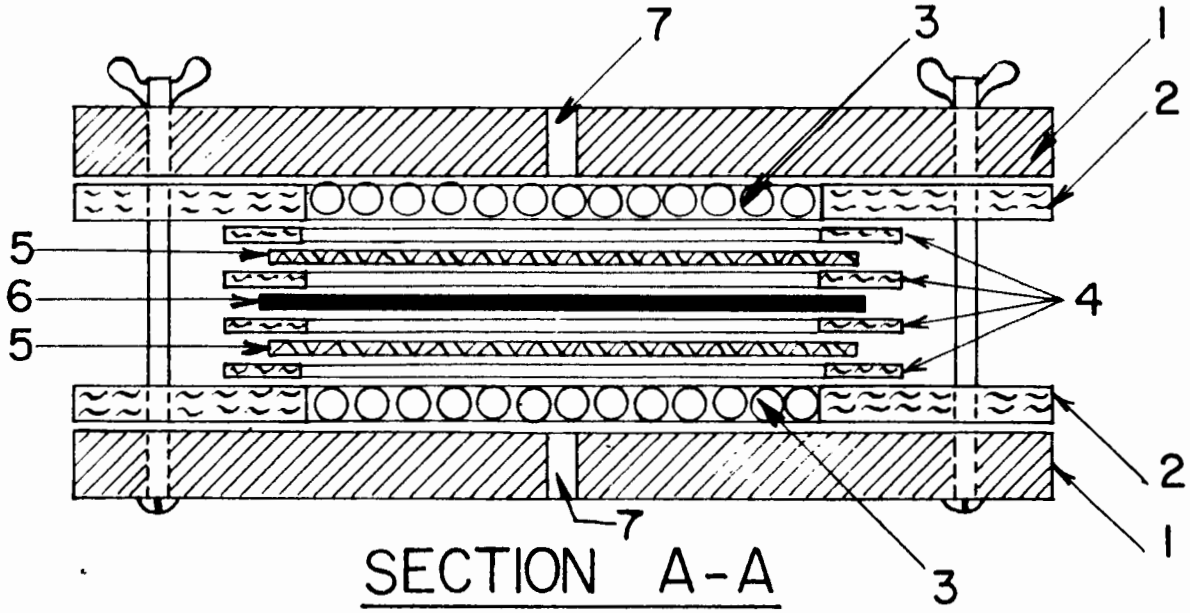

SECTION A-A

TABLE I.

COMPONENTS OF AN ULTRAFILTER CELL

WITH 200 SQ.CM. ACTIVE MEMBRANE AREA.

2 lucite discs

diameter 25 cm.
thickness 1 cm.
8 holes with centers on a 23 cm. diameter circle concentric with the discs to accomodate the screws
2 holes with centers on the same diameter 17.5 cm. apart, bore diameter 8 mm.

2 rubber rings

inside diameter 18 cm.
outside diameter 25 cm.
thickness 0.3 to 0.32 cm.
8 holes drilled in identical positions as in the lucite for holding the screws

4 dental dam gaskets

inside diameter 18 cm.
outside diameter 22 cm.
thickness about 0.03 cm.

2 stainless steel screens

diameter 20 cm.
125 mesh

1 membrane

diameter 21 cm.

glass beads

diameter 0.28 to 0.3 cm.

8 screws, 8 wingnuts, 16 washers

before assembling the cell. To prevent the glass beads from dropping into the Tygon tubing, a small piece of stainless steel screen is placed in the tubing.

b. Operation

The assembled unit is shown on Fig. 5. The solution chambers of the different cells are connected in series and the solution is circulated by a pump as used for dialysis from reservoir (C) to provide adequate stirring.

The volume of the liquor is kept constant by the constant head device (B). If the level in reservoir (C) drops sufficiently to expose the end of the tube (B) to the air, air will enter into the distilled water container (A) and consequently water will flow into reservoir (C). The rising level in the reservoir closes tube (B) and thus stops the water flow. Trap (b) is needed to prevent the solution entering the distilled water container.

The ultrafiltrate is fed into suction flask (F) by gravity.

Evidence presented later indicated that the residual liquor at the end of the dialysis contained pure lignin sulfonates. The residue was separated into four fractions

Fig. 5.

The assembled ultrafiltration unit.

(A) Water reservoir

(B) Constant Head device (b) Solution trap

(C) Solution reservoir

(D) Membrane pump (d) Valves

(E) Ultrafilter cells (e) Stopcocks

(F) Suction flask, reservoir for ultrafiltrate

(G) Glass wool filter.

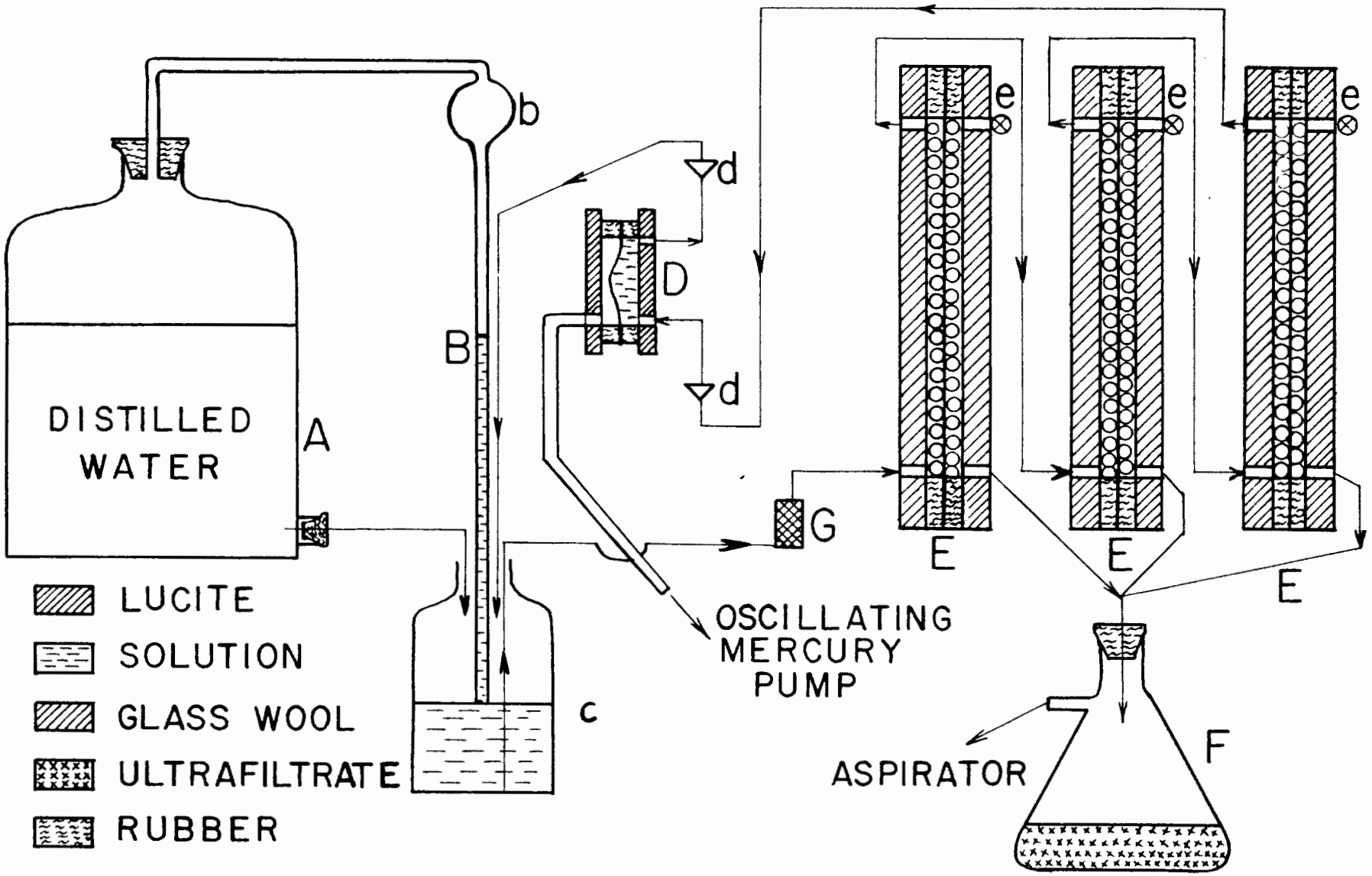
DISTILLED WATER
A
B
b
c
d
D
d
e
e
e
E
E
E
G
OSCILLATING MERCURY PUMP
ASPIRATOR
F
LUCITE
SOLUTION
GLASS WOOL
ULTRAFILTRATE
RUBBER

(Nos. 1 to 4) by means of ultrafiltration using 600 P.T., 300 P.T. cellophane and No. 27 parchment membranes as supplied with the Webcell dialyser. A unit consisting of 6 cells was used for the cellophane membranes, and of 3 cells for the parchment membrane. During the operation, the volume of liquor was kept constant at 1 liter. The ultrafiltration was stopped after 3, 7 and 12 days for the parchment, 300 P.T. and 600 P.T. cellophane membranes respectively, the end points being determined as described later.

The ultrafiltrate of the 600 P.T. cellophane is fraction No. 4 and the fraction that did not pass the parchment is fraction No. 1. Before evaporating the solutions of the different fractions, they were adjusted to pH 6.5 by treating them with cation exchanger and adding hydroxide as required.

All four of these fractions could be quantitatively precipitated with barium and alcohol.

C. CHANGES IN THE ANALYTICAL DATA OF THE SOLIDS IN THE DIALYSED LIQUOR AND IN THE DIALYSATE DURING DIALYSIS

The main problem in fractionation of polydisperse materials by dialysis is to determine when the process is

ended since small amounts continue to diffuse through the membrane after long periods of dialysis. It was not possible to establish firm analytical criteria for the purity of lignin sulfonate fractions because their reducing power, sulfur content, neutralization equivalent weight and methoxyl content change with molecular weights. To complicate matters further, there are other acidic, reducing, sulfur- and probably methoxyl- containing materials present in the liquor. These substances, mostly sugars and degradation products of cellulose and lignin are believed, however, to have lower molecular weights than the bulk of the lignin sulfonates.

In Fig. 6 the control data of the dialysis are shown. All data are plotted against the cumulative percentage of the solids removed during the dialysis. Since the dialysates contained materials with different diffusion rates, no theoretical relation could be derived for the time dependence of the removal of the dialysable solids. It was found that the concentration of the dialysates was about inversely proportional to the dialysis time and that the amount of solids removed was roughly proportional to the logarithm of dialysis time and cumulative dialysate volume (Fig. 3, Curves B and D)

The most significant curves are those of the

reducing power of the solids in the dialysate and in the residual liquor (Curves F and G) and of the neutralization equivalent weights of the solids in the dialysate (Curve E). (The analytical methods which were used will be presented later.) The following distinct stages of dialysis can be observed:

(1) The first 30% solids removed have a progressively increasing reducing power and decreasing neutralization equivalent weight, as can be seen from curves F and G.

(2) In the next dialysis period, 20% solids were removed. The reducing power of the solids in the dialysate passed through a maximum while their neutralization equivalent weight stayed constant.

(3) The reducing power and neutralization weights of the subsequent 2% solids removed decreased sharply, and the neutralization equivalent weights had minimum at 375. At this minimum the reducing power of the dialysate was low, indicating that it contained very little non-ionic sugars. Thus, it is fair to assume that the previous dialysates contained acids with neutralization equivalents of 375 or less.

(4) There is evidence that after the diffusion of 52% solids, the residual liquor consists of carbohydrate-free lignin sulfonates. This is indicated by the fact that the reducing power of the solids in the dialysate and in the rest

Fig. 6.

Dialysis control diagrams showing % reducing substances removed (Curve A), dialysis time (B), % acid equivalents removed (C), cumulative dialysate volume (D), neutralization equivalent weight of the solids in the dialysate (E), reducing power of the solids in the dialysate (F) and the reducing power of the solids in the liquor (G).

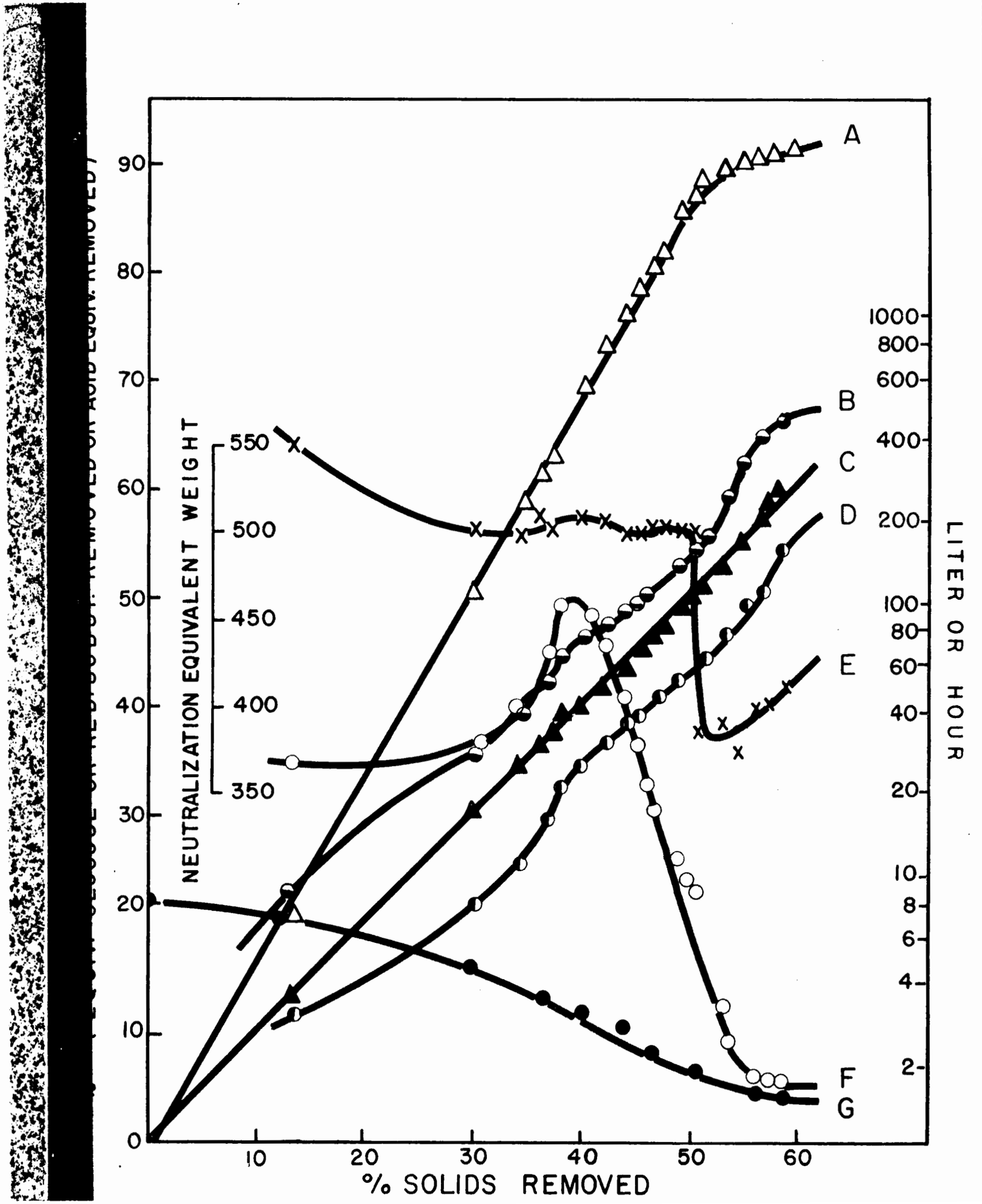
A
B
C
D
E
F
G
90
80
70
60
50
40
30
20
10
0
10
20
30
40
50
60
% SOLIDS REMOVED
NEUTRALIZATION EQUIVALENT WEIGHT
550
500
450
400
350
1000
800
600
400
200
100
80
60
40
20
10
8
6
4
2
LITER OR HOUR

of the liquor is roughly the same and that, with increasing time of dialysis, the neutralization equivalent weights of the dialysates increase; the neutralization equivalent weights of the lignin sulfonates increase with increasing molecular weights.... In the last period of dialysis, the dialysates were very dilute.

The reducing powers of the diffusing and of the residual solids was roughly equal at the end of the dialysis, indicating that the reducing power of the lignin sulfonates investigated was inherent and not due to impurities. In this connection the experiments of Peniston and McCarthy (75) are of interest. These authors plotted the reducing power of dialysed lignin sulfonates, as obtained in a continuous counter-current dialyser, against the reciprocal of the time of dialysis and by extrapolating their data to a value corresponding to infinite time of dialysis, concluded that really pure lignin sulfonates should not be reducing. The present experiments indicate that care must be taken in such an extrapolation. The curve G can be extrapolated to zero from the region of 30 to 52% solids removal but, on the other hand, it runs almost parallel to the horizontal axis later.

D. DEGREE OF FRACTIONATION ACHIEVED BY ULTRAFILTRATION

Neither fractional dialysis nor ultrafiltration as employed allow absolute separation of the different molecular weight fractions; while this is self-evident in fractional dialysis, it needs further explanation for ultrafiltration.

The behaviour of solutes in ultrafiltration depends on the relative size of their molecules to the size of the membrane pores (18). Materials with relatively small molecules can pass through the membrane in unchanged concentration; intermediate molecular size materials pass through the membrane with a decreased concentration, and substances with relatively large molecules are retained by the membrane. If the ratio of concentrations of any component "i" in the ultrafiltrate and in the residual liquor is λ_i, this coefficient $\lambda_i = 0$, if the molecules of "i" are larger than the membrane pores; $0 < \lambda_i < 1$, if both are comparable in size; finally, $\lambda_i = 1$ for molecules much smaller than the pores of the membrane.

If the volume of the residual liquor is kept constant at V_L, as was done in the experiments described here, knowing λ_i the time necessary to remove any arbitrary frac-

tion of component "i" can be calculated. At unchanged pressure differentials, the volume of ultrafiltrate produced in unit time U is constant. The amount of component "i" removed in time dt is

$$- V_L \, dc_i(t) = \lambda_i U \, c_i(t) \, dt$$

where $c_i(t)$ is the concentration of "i" in the residual liquor. By integrating this equation, a relation is obtained for the fraction of "i" remaining in the liquor at time t:

$$\frac{c_i(t)}{c_i(0)} = e^{-\frac{\lambda U}{V_L} t}$$

In principle λ_i may be evaluated by determining $c_i(t)$ at different time periods. This however, cannot be done for polydisperse substances such as lignin sulfonates. To determine the ultrafiltration time it was assumed that the solution to be filtered contained a component which could pass through the membrane in unchanged concentration i.e. its λ_i was unity. The values of V_L and U were determined experimentally and the time necessary for the removal of 99.5% of this component was calculated. Consequently, besides

really high molecular weight substances, a portion of the materials with $0 < \lambda_i < 1$ was left behind, and there has to be some overlapping in the molecular weight distributions, even for the higher fractions.

Despite the imperfections in the methods of fractionation, the fractions represent well-defined molecular weight ranges. As will be shown, in osmotic pressure measurements it was possible to follow the diffusion rates of fractions Nos. 2 to 6 continuously with time. Furthermore, in the diffusion coefficient determinations, the diffusion times were varied up to three fold and it was found that the diffusion rates were independent of the diffusion time. This indicates that the fractions cannot be very heterodisperse.

III. CHEMICAL CHARACTERIZATION OF THE FRACTIONS

A. INTRODUCTION

As already mentioned, the lignin sulfonates cannot be considered as homogeneous, chemically well-defined materials. Their analytical data depend not only on the species of wood used in the digester and on the cooking conditions, but also the number of functional groups on the lignin molecules changes markedly with the molecular weight of the lignin sulfonates. It has been found (65) that the methoxyl contents increased with increasing molecular weights, and with few exceptions (54), the sulfur contents decreased with increasing methoxyl contents.

The variations of the analytical data found in the literature are considerable. It can nevertheless be stated that the methoxyl content of lignin sulfonates may range up to 15%, sulfur content from 3 to 10%, phenolic hydroxyl content up to 2%, and reducing power up to 10% equivalent glucose.

In the present work, the functional groups of the lignin sulfonates were determined and the dependence of

these results on the molecular weights and ultraviolet light absorption characteristics of the fractions is demonstrated.

B. ANALYTICAL PROCEDURE

To determine the neutralization equivalent weights, the sodium was removed by Amberlite IR-100 (H) cation exchanger and the free acid thus obtained was titrated with methyl red as indicator. Separate conductivity and pH titration experiments showed that all fractions have only one titration endpoint at pH 6.5. The titration curves were very similar to the ones presented by Peniston and McCarthy (75).

After oxidizing the lignin sulfonates with nitric acid the sulfur was determined as barium sulfate as suggested by Yorston (94).

The methoxyl content was determined by the method of Peniston and Hibbert (76) adding red phosphorus, as suggested by Vjebock and Schappach (91), instead of phenol to the hydriodic acid lignin sulfonate mixture.

The reducing power of the fraction was compared to that of glucose by means of Fehling solution and expressed as equivalent glucose, as described by Yorston (94).

Ultraviolet absorption spectra were measured in a Beckman Model DU spectrophotometer for pH 6 and pH 12 with the buffers as blanks. It has been verified that Beer's Law is valid for all fractions if ultraviolet light is used.

The results obtained are presented in Table II. The methods of determining the molecular weights and diffusion coefficients also presented in this table will be given later.

C. ANALYTICAL DATA OF THE FRACTIONS

It has already been mentioned that the dialysis method makes it probable that the four high molecular weight fractions are carbohydrate free lignin sulfonates, and further evidence is provided by analytical data in Table II. The acid and sulfur contents are approximately equal, thus indicating that all acid groups are sulfonic. The reducing power of these fractions is low and the methoxyl contents are high.

Some 60% of the total solids of the spent sulphite liquor from which the mineral acids were removed by ion exchange can be precipitated with ethanol as barium salts. It is, however, doubtful whether this technique in itself is

adequate to separate the carbohydrates from the lignin sulfonates quantitatively. If not, there may be considerable impurities present in the low molecular weight fractions.

Fractions 5 to 8 contain more acidic groups than calculated on the basis of their sulfur content. Freudenberg et al. (27) found similar analytical results and suggested that these were due to the presence of carboxyl groups in the lignin sulfonates. An alternative explanation is that the carboxyl groups belong to the contaminating carbohydrates.

The sulfur contents of the fractions increase with decreasing molecular weights up to fraction No. 5 and then decrease. This peculiar drop in sulfur content after fraction No. 5 may be caused by the presence of non sulfur-containing impurities.

Even if the low molecular weight fractions are contaminated, there is no doubt that their bulk is made up of lignin sulfonates chemically similar to the higher fractions. The strongest evidence is furnished by ultraviolet absorption spectra.

It is well known that the ultraviolet absorption spectra of lignin preparations in neutral solution have maxima near 280 mμ and minima near 260 mμ. Not only do all

of the fractions show the same pattern (Fig. 7, Table III) but the ratio of the extinction coefficients (ϵ) at the maximum and minimum is approximately constant at 1.35 for all fractions. The only difference in the shapes of the curves is that the slopes in the lower wavelength region decrease with the molecular weights of the fractions. The ratios of extinctions at 245 and 260 mμ decrease from fraction No. 1 to fraction No. 8 (Table III).

The light absorbing power decreases with the molecular weights of the fractions; this can be noticed by the visual observation of the colors and is expressed quantitatively by the extinction coefficients for 0.1% solutions at 280 mμ (Table III). Nevertheless the ultraviolet light absorbing power per methoxyl bearing unit at 280 mμ is the same for all the fractions except the lowest, for which it is relatively high (Table III).

Aulin-Erdtman (4, 5) found shifts in the characteristic ultraviolet spectra of lignin compounds when determined in neutral and in alkaline solutions, and attributed them to the ionization of the phenolic hydroxyl groups. The minima of the samples shifted from 263 mμ to 266 mμ for the highest, and from 258 to 273 mμ for the lowest fraction. The values of λ_{max} decreased on the average by 1 mμ. The

ratio $\epsilon_{max}/\epsilon_{min}$ was the same for all fractions, the mean value being 1.11, i.e. less than for neutral solutions.

Goldschmied (37) and Aulin-Erdtman (5) suggested that the phenolic hydroxyl contents of lignin and analogous model compounds can be determined from the differential spectra of solutions with pH 6 and pH 12. These spectra were shown to have maxima around 250 and 300 mμ. With model substances, Goldschmied determined the characteristic maximum extinction difference around 300 mμ ($\Delta\epsilon_{max}$) for one mole phenolic hydroxide per liter. According to this value, the unknown phenolic hydroxyl content of a substance can be calculated from the following formula:

$$(\%\ \phi - OH) = 17/41 \wedge \epsilon_{max}$$

The hydroxyl contents of the fractions (Table II) were determined from such differential spectra, characteristic data of which are shown in Table III and three of which are plotted in Fig. 8.

TABLE II.

Analytical Data of Sodium Lignin Sulfonate Fractions

FRACTION NO.	% of total original solids	% of the total of the fractions	% methoxyl	% S	% Phenolic* acid	Reducing power, % eq. glucose	Neutralization eq.wt.	Acid groups / sulfur	S / MeO	Molecular Weight	Diffusion Coefficient sq.cm./day
1	7.3	11.87	10.45	5.22	0.945	3.56	599	1.03	0.53	58,000	0.0314
2	18.7	30.41	10.40	5.58	0.739	3.36	570	1.01	0.56	19,200	0.0849
3	2.8	4.55	10.41	5.40	0.780	3.35	585	1.01	0.55	15,500	0.113
4	10.2	16.58	9.82	5.98	0.870	3.79	535	1.00	0.64	8,500	0.134
5	4.8	7.805	8.80	6.37	0.770	7.18	450	1.11	0.81	5,200	0.178
6	9.5	15.45	7.24	6.25	0.696	9.20	375	1.36	0.89	4,600	0.194
7	3.4	5.53	4.06	5.55	0.672	9.42	289	2.00	1.46	3,700	0.219
8	4.8	7.805	2.25	5.02	0.530	8.47	227	2.81	2.38	3,650	0.221
Total	61.5%	100%									

* Calculated from differential UV extinction coefficient (see text)

TABLE III.

Characteristic Data of the Ultraviolet Adsorption Spectra

FRACTION NO.	pH 6						pH 12			Differential Spectrum	
	280 $cm^{-1}g^{-1}$ liter	Optical density at 280mμ mole methoxyl/liter	λ_{max} mμ	λ_{min} mμ	$\frac{\epsilon_{max}}{\epsilon_{min}}$	$\frac{\epsilon_{245}}{\epsilon_{260m\mu}}$	λ_{max} mμ	λ_{min} mμ	$\frac{\epsilon_{max}}{\epsilon_{min}}$	λ_{max} mμ	$\Delta\epsilon_{max}$ $cm^{-1}g^{-1}$ liter
1	13.9	4200	282	263	1.32	2.28	282	266	1.13	300	2.28
2	13.3	4090	283	263	1.39	2.28	281	267	1.13	298	1.78
3	13.5	4150	282	262	1.38	2.23	281	267	1.12	301	1.88
4	12.4	4020	282	262	1.29	2.20	281	268	1.07	298	2.10
5	11.1	4100	283	263	1.39	2.15	281	268	1.09	299	1.86
6	8.8	3900	283	262	1.38	2.05	282	270	1.10	300	1.68
7	5.8	4200	277	261	1.34	1.89	281	270	1.16	299	1.62
8	4.2	6360	277	258	1.30	1.59	282	273	1.09	297	1.28

Fig. 7.

Ultraviolet absorption spectra of fraction No. 1.

Curve A: pH 12
Curve B: pH 6

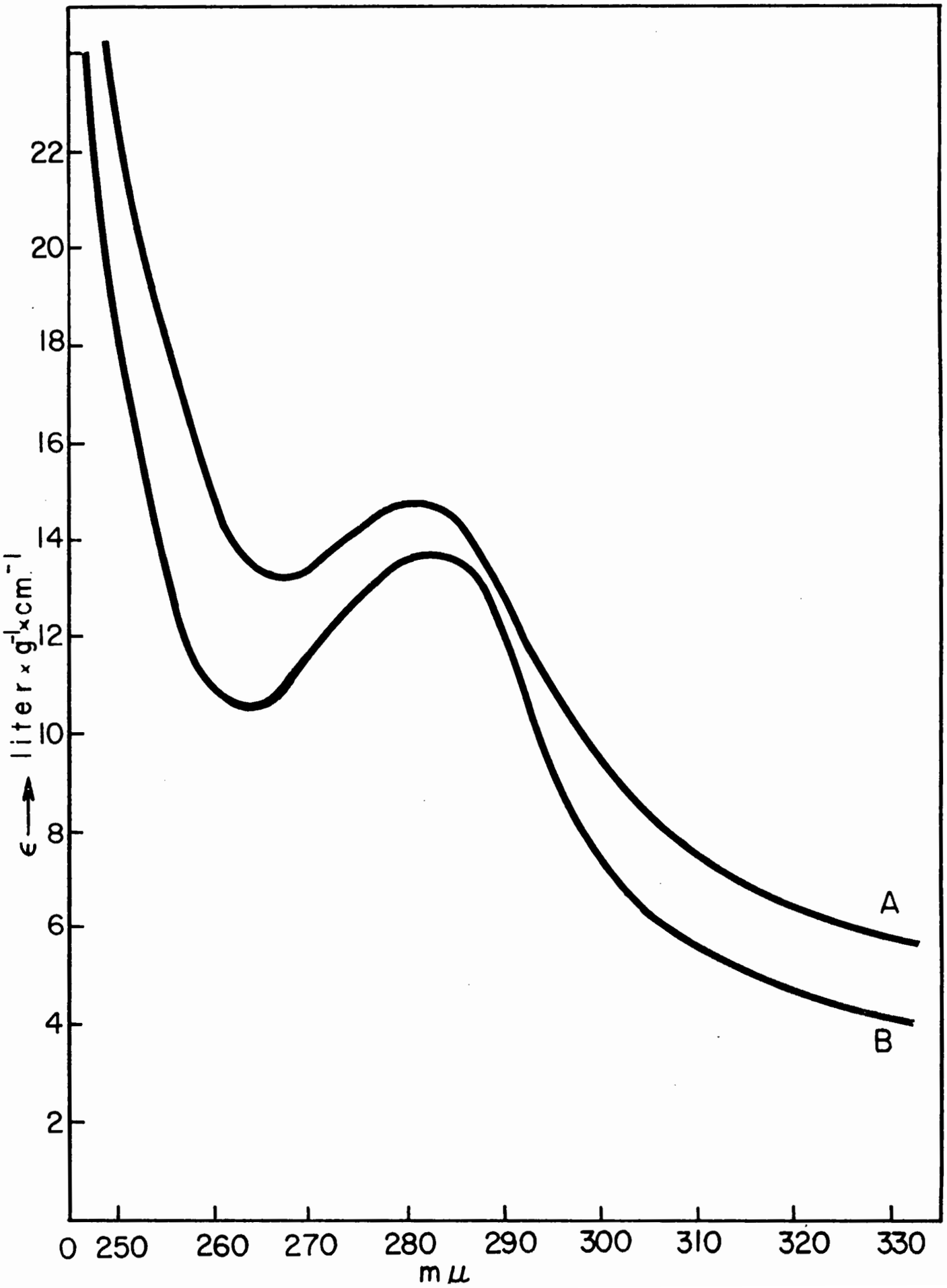
22
20
18
16
14
12
10
8
6
4
2
ε ⟶ liter × g⁻¹ × cm⁻¹
A
B
0 250 260 270 280 290 300 310 320 330
mμ

Fig. 8.

Differential absorption spectra between solutions at pH 12 and pH 6.

Curve A: fraction No. 1
Curve B: fraction No. 6
Curve C: fraction No. 8

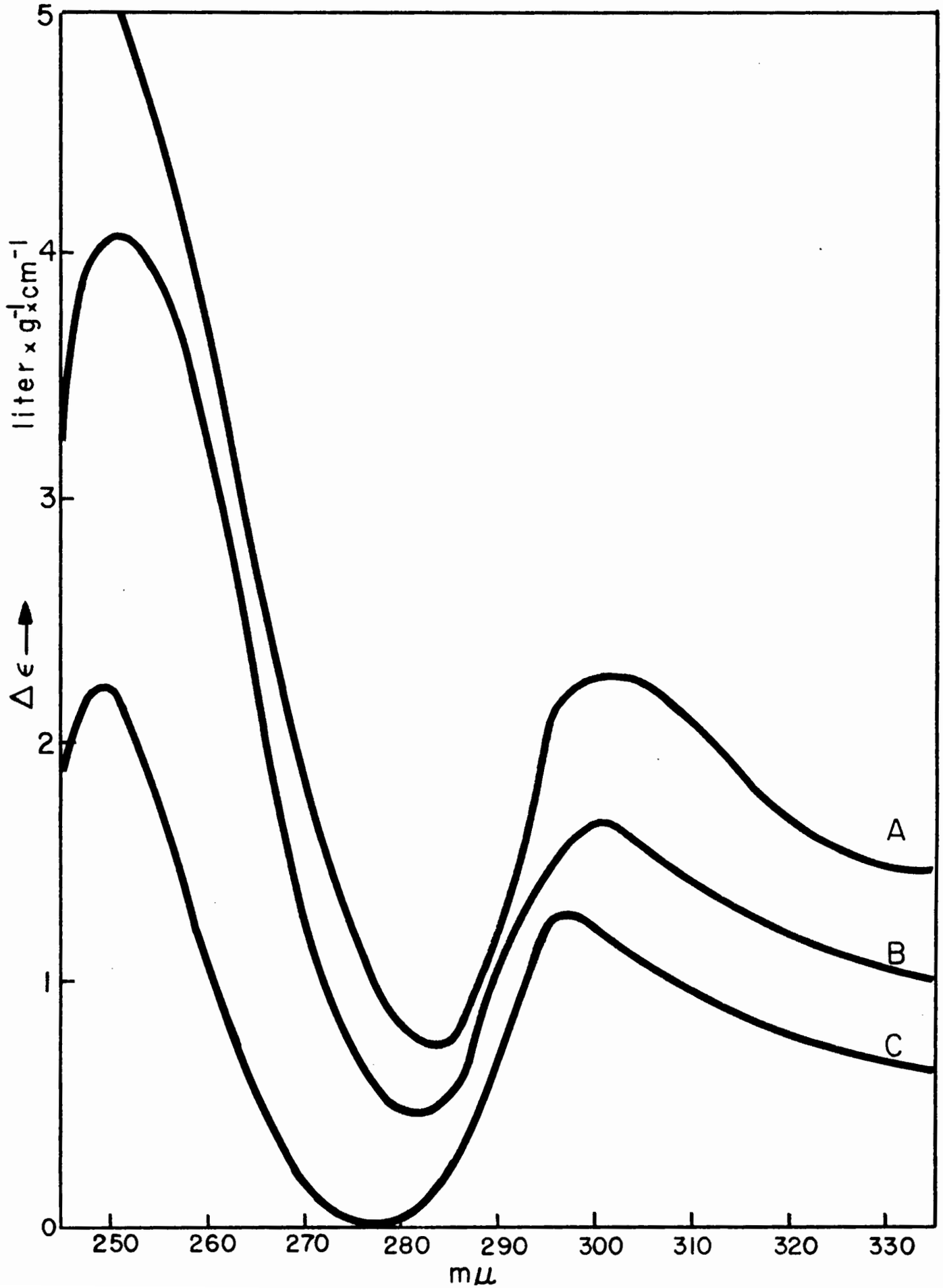
5
4
3
2
1
0
liter × g⁻¹ × cm⁻¹
Δε
250
260
270
280
290
300
310
320
330
mμ
A
B
C

IV. MOLECULAR WEIGHT MEASUREMENTS

A. HISTORY

Various attempts have been made to determine the molecular weights of lignin sulfonates. Cryoscopic and ebullioscopic methods (44, 79) yielded apparent molecular weights in the range of 1,000 to 6,000, but due to electrolytic dissociation of the lignin sulfonates, these values are probably low. Estimates of molecular weights have also been made from the diffusion coefficients (23, 27, 43) and from the dialysis rates (82) either by comparison of the lignin sulfonates with various test substances or by assuming that the lignin sulfonate molecules are spherical and non-solvated, and that the relation between the molecular radius and the diffusion coefficient given by the Sutherland-Einstein equation applies. Molecular weights ranging from 2,000 to 20,000 have thus been obtained. These values agree in order of magnitude with the more careful measurements of McCarthy (66) and Olleman, Pennington and Ritter (69), who were able to determine axial ratios and weight average molecular weights from diffusion and ultracentrifuge sedimentation, respectively from diffusion and viscosity data. McCarthy (66) has obtained molecular weights

ranging up to 100,000.

B. GENERAL REMARKS

In the present investigation the molecular weight of the lignin sulfonates were determined by osmotic pressure measurements. For this purpose it was found necessary to design a new type of osmometer which is suitable for work with aqueous solutions. Even with such an instrument on hand, the molecular weights of the fractions, except the one with the highest molecular weight, could not be determined by the ordinary procedures in osmometry. It was found that the molecular size of all fractions, except of fraction No. 1, was so small that they could permeate through the available lowest porosity membranes. An experimental technique had to be devised to evaluate the true osmotic pressures of their solutions despite the shortcoming of the membranes.

In the present chapter, the osmometer and its operations under conventional conditions with semipermeable membranes is described. Subsequently the theory and practice of osmometry with membranes permeable to the solutes is presented. Finally, the established molecular weights of the fractions are interpreted and discussed.

C. THE OSMOMETER

1. Introduction

Most osmometers for determining molecular weights of macromolecules have metal plate membrane supports and solvent-filled manometers. These units are not convenient for use in aqueous solutions, because the high surface tension causes air bubbles to be trapped at the metal surfaces and also leads to large capillarity errors in the manometer.

The units described in this paper are inexpensive to construct, simple to operate, and have the following advantages:

(1) Measurements can be carried out reasonably fast, even with low porosity membranes, by making use of large membrane areas.

(2) In membranes as big as 200 sq.cm. in area, membrane ballooning is eliminated.

(3) The membrane area per cc. half cell volume is 10 sq. cm., which compares favourably with other designs (92).

(4) The unit is transparent.

(5) Solutions can be changed readily without taking the unit apart.

The osmometer consists essentially of a cell and

a manometer attachment. The cell is similar to that of the ultrafilter, but allows firmer support of the membrane. Its main body consists of two lucite discs and two rubber rings (Fig. 9). The membrane is clamped between two stainless steel screens and is supported by layers of glass rods, not glass beads, closely packed parallel to one another in both cell compartments. The unit is sealed by means of the two rubber rings mentioned above which are compressed to the same thickness as the glass rods when the unit is assembled.

The osmotic pressure is measured in a capillary manometer which is connected to the solvent chamber. A syringe such as that from a glass syringe pipette acts as a levelling device.

All parts are individually clamped to a metal rod which forms the backbone of the unit.

2. Construction of the cell

The stainless steel screens are placed between the rubber rings and the membrane. To avoid leakage through the screen meshes and to protect the membrane, two dental dams are placed between the screens and the membrane and the rubber rings are lubricated with silicone grease where they

are in contact with the screens. As an additional precaution, Pyseal cement can be applied on the outside. If, for any reason, the use of silicone grease is to be avoided, four dental dam gaskets are used on each side of the screens, as in the ultrafilter cells, and Pyseal cement applied on the outside of the cell.

The components of three typical cells having active membrane areas of approximately 200, 60 and 20 sq. cm. are described in Table IV. Standard pyrex rods of 3 mm. diameter are used as membrane supports. When these rods are initially packed into the cell, a 3 mm. clearance is left between them and the rubber rings to allow for expansion of the latter when the cell is tightened. The rods are vertical when the cell is in use. In the present work this method of membrane stabilization was used for the largest and medium osmometer cell.

There is an alternative method of stabilizing the membranes and the stainless steel screen reinforcers. Discs of 5 mm. diameter, cut out of the same rubber sheet as used to prepare the body of the cell, can also be used as stabilizers. These discs are placed in pairs opposite to each other on both sides of the membrane, using 2 to 3 such pairs per 10 sq. cm. membrane area. This method does not provide as

Figure 9.

Details of the osmometer cell (Exploded view)

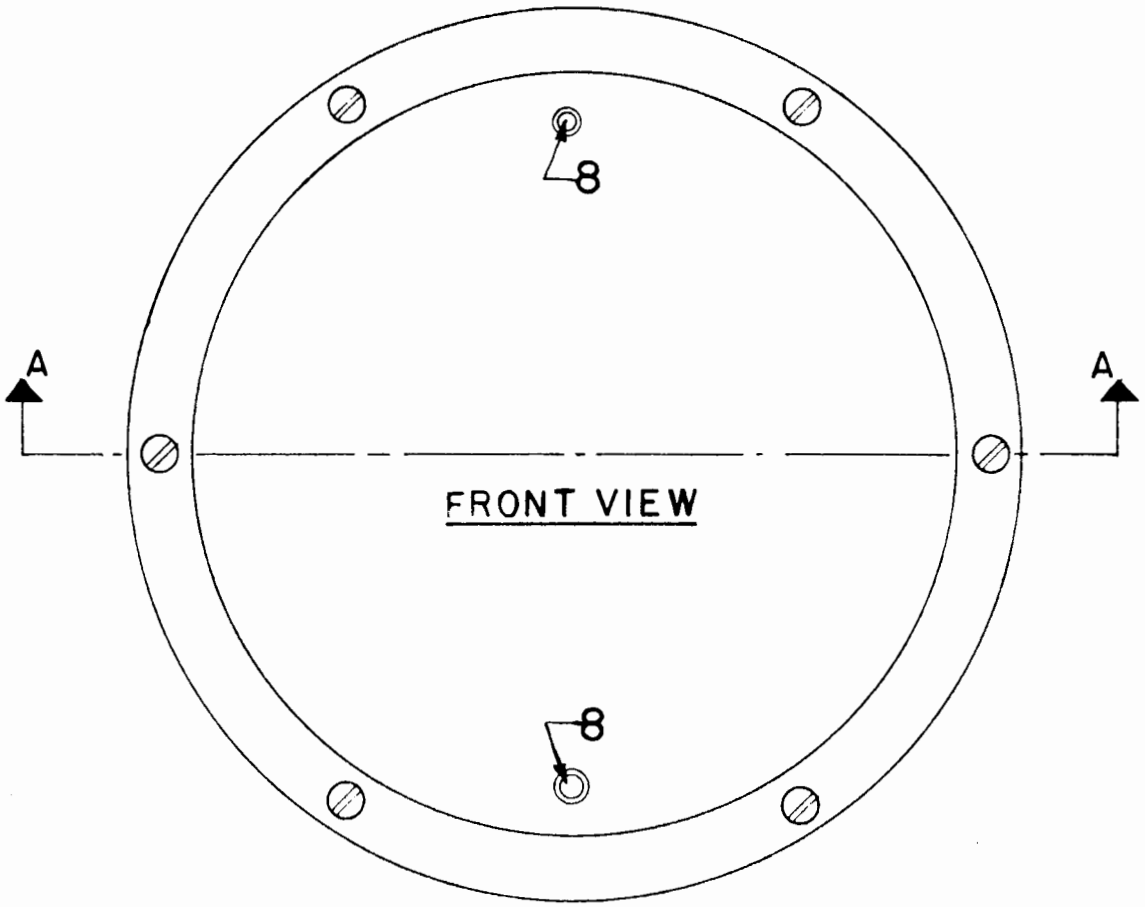

FRONT VIEW

① — BRASS RING
② — LUCITE
③ — GLASS RODS
④ — RUBBER RING
⑤ — STAINLESS STEEL SCREEN
⑥ — DENTAL DAM GASKET
⑦ — MEMBRANE

⑧ — INLET HOLE

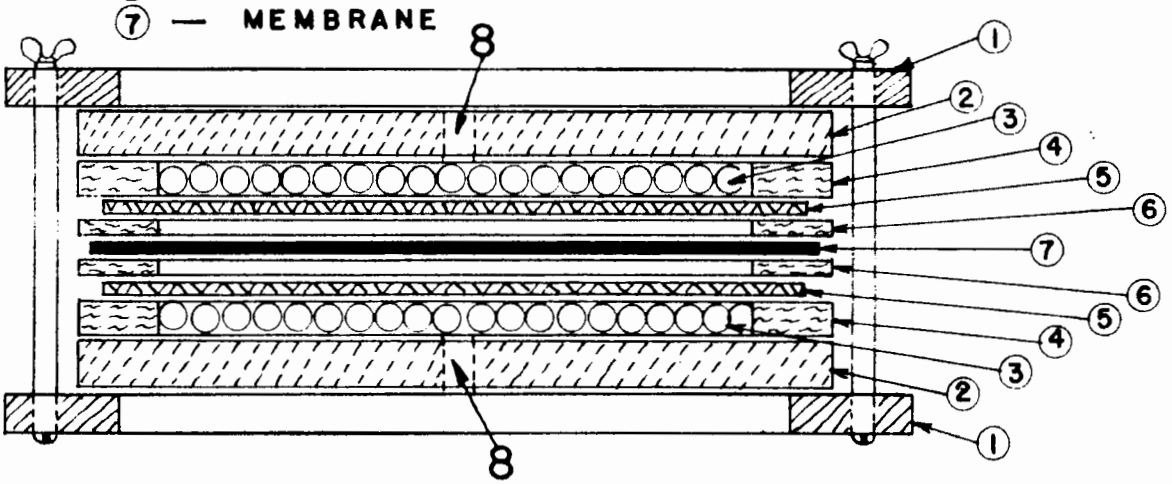

SECTION A—A

TABLE IV.

Dimensions of the osmometer cell components

Cell designation	C	B	A
Active membrane area, sq. cm.	200	60	20
2 brass rings			
inside diameter, cm.	18.0	11.5	6.5
outside diameter, cm.	25.5	15.0	11.5
number of holes for screws	8	6	4
2 lucite discs			
diameter, cm.	20.5	12.5	7.5
thickness, 1 cm.			
2 holes with centers on the same diameter; bore diameter 8 mm.; distance of the centers of the holes from the center of the disc, cm.	7.4	4.9	2.4
2 rubber rings			
thickness 3.1 $\pm$ 0.1 mm.			
inside diameter, cm.	15.0	10.0	5.0
outside diameter, cm.	20.5	12.5	7.5
2 or 4 dental dam gaskets			
inside diameter, cm.	15.0	10.0	5.0
outside diameter, cm.	20.5	12.5	7.5
2 stainless steel screens			
diameter, cm.	16.5	11.0	6.0
125 mesh			
membrane			
full diameter, cm,	17.5	11.5	6.5

firm a membrane support as the other and was used only for the smallest cell.

The cell is clamped to the metal rod backbone through two short metal rods pressed into drilled holes in one of the brass rings. When the largest cell is assembled there is a tendency for the lucite and consequently for the membrane to balloon, since the pressure is applied only at the edges of the lucite discs. This can be overcome by providing additional compression at the center of the discs by means of a suitable clamp which is independent of the brass rings.

The lucite discs are simply and tightly connected with the stopcocks and the glass parts leading to the manometer attachment by Tygon tubing without any cement, in the same manner as the ultrafilter cells. The lucite discs are equipped with the connectors before assembling the cell, and for this purpose, each lucite disc has two holes near the opposite ends of its vertical diameter.

3. The manometer

The design of the glass parts assembled with the cell is shown in Fig. 10 and as can be seen, the cells can be changed without taking the manometer unit apart. The

different glass parts are connected by spherical ground glass joints of 12 mm. sphere diameter. These joints are lubricated with silicone grease and clamped together. The glass parts can also be connected by tygon tubing. All connecting capillaries have 1 mm. bore. To ensure a constant capillary rise effect, the measuring capillary (E) should be of uniform bore; it was found that the most satisfactory bore diameter was 0.3 $\pm$ 0.003 mm. The tubes (A) and (B) are 1 cm. in diameter and cut from the same piece of tubing. The syringe is lubricated with silicone grease and its plunger is firmly wired to a levelling screw. The toluene water interface is in the 1.5 cm. diameter bulb below the measuring capillary. The ground glass joint (D) is lubricated with toluene insoluble lubricant (e.g. Fisher's Nonaq Grease) and waterproofed by coating the outside with Pyseal cement. All stopcocks have 1 mm. bore.

4. Operation with semipermeable membranes

The measuring capillary is attached to the unit after the other parts have been filled with water. The bulb (D) is then filled with toluene, the capillary is sealed in, the stopcock (C) is opened and toluene is allowed to rise into the dry capillary.

The unit is filled with solution from a pipette

Figure 10.

Assembled osmometer showing details of the manometer system.

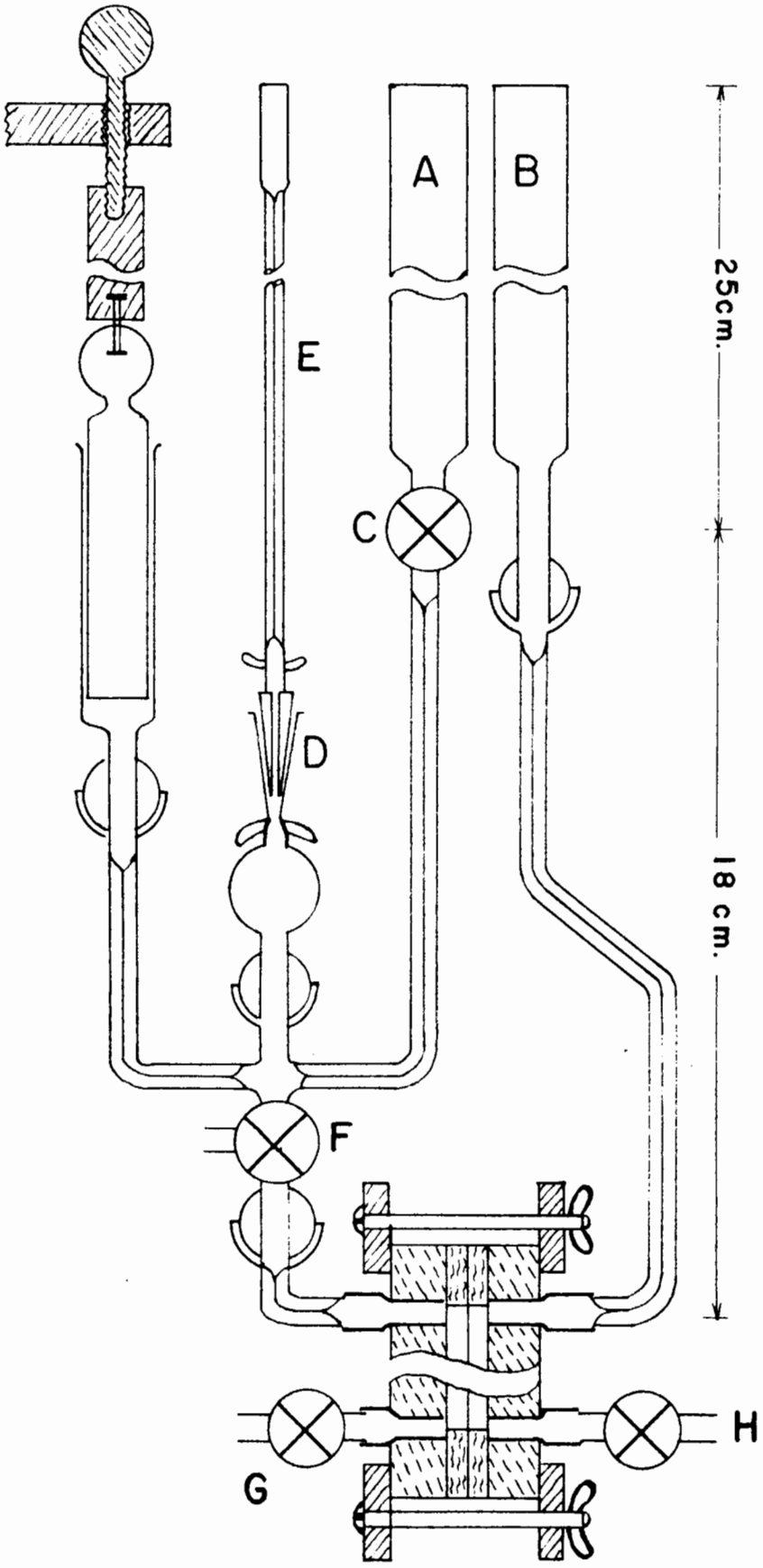
A
B
E
C
D
F
G
H
25cm.
18 cm.

which is connected to the stopcock (H) by rubber tubing. To change solutions, the solution chamber is emptied and rinsed three times with the new solution. If necessary the water in the solvent chamber can be changed too without disturbing the toluene-water interface, through stopcocks (G) and (F).

The measurements are carried out slightly above the room temperature in a water thermostat controlled to 0.001°C. Temperature equilibrium is established in the cell within 0.5 to 1.5 hours.

The readings are made on a scale with 0.5 mm. subdivisions behind the measuring capillary and are estimated to 0.01 cm. To avoid parallax, the scale is viewed through a cathetometer. The level difference in tubes (A) and (B) is established on the cathetometer scale.

The levels in tubes (A) and (B) are brought within 0.1 mm. of one another and the meniscus height in the measuring capillary is recorded. Stopcock (C) is then closed and the osmotic equilibrium is established by the half-sum method suggested by Fuoss and Mead (33). The difference between the original capillary meniscus reading and the one corresponding to the equilibrium is equal to the

osmotic pressure in cm. toluene. No correction is necessary, since the density difference between water and the solution is negligible.

It is desirable to avoid excessive dilution of the solution by osmotic diffusion of solvent while the temperature equilibrium is being established. The measuring technique described above can be used only when the osmotic pressure of the solution is small, in our experience less than 3 cm. of toluene. In the case of larger osmotic pressures, it is preferable to adjust a level difference roughly corresponding to the expected osmotic pressure in tubings (A) and (B) when filling the instrument. Thus the driving pressure acting on the solvent is kept small till the actual measurement can be started. When temperature equilibrium is reached, stopcock (C) is closed and the osmotic equilibrium is established by the half sum method. If the levels in tubes (A) and (B) are e and f respectively, and the meniscus levels in the capillary with stopcock (C) open and at equilibrium are g and h respectively, the osmotic pressure in gm./sq.cm. (cm. water) is given by the following formula:

$$p = (f - e)d_{solvent} + (g - h)d_{toluene} \qquad ..IV\ (1)$$

where d is the density.

The reproducibility of the capillary rise along the length of a 0.3 mm. bore capillary is $\pm$ 0.02 cm., if the precision of the bore is within 1%. If necessary, the accuracy can be improved by using thicker capillaries; this however, can only be done at the expense of a longer time to osmotic equilibrium.

In addition, the accuracy of the measurements depends on the reproducibility of the so-called "zero pressure", i.e. of the finite apparent osmotic pressure existing when solutions of identical composition are placed on both sides of the membrane. In some instances, the solute may be adsorbed on the membrane and this leads to considerable difference in zero pressure before and after the measurements.

The speed of the measurements depends mainly upon the ratio of the capillary cross section to membrane area. Using the small cell with 300 p.t. cellophane, the medium cell with 600 p.t. cellophane and the large cell with denitrated nitrocellulose and a capillary of 0.3 mm. bore, equilibrium osmotic pressures can be established to $\pm$ 0.02 mm. by the half-sum method within four hours after the temperature equilibrium is reached. This compares favourably with other designs of osmometers.

To avoid ionic dissociation of the sodium lignin sulfonates, the measurements were carried out using 1/2 N sodium chloride solution instead of pure water as solvent. The half-sum method could only be applied for the highest molecular weight fraction (No. 1) because all other fractions leaked through the available membranes. The results obtained for fraction No. 1 are shown in Table XI.

D. OSMOTIC PRESSURE MEASUREMENTS WITH MEMBRANES PERMEABLE TO SOLUTE.

1. Introduction

The main difficulty in determining osmotic pressures of polydisperse materials, and especially of materials with molecular weights less than 20,000, lies in the selection of suitable semipermeable membranes. It is suggested in this paper that even if the solute leaks through the membrane, the true osmotic pressure of the solution initially placed in the osmometer can be determined from the variation with time of the osmotic pressure readings. As there exists the need of a method of evaluating number average molecular weights in the region of 1,000 to 20,000, the procedure described here can fill at least part of this gap.

2. Theoretical Part

a. Permeability and semipermeability of membranes

At the present it is generally believed (50, 89, 93, 96) that the permeability of organocolloid membranes to solutes is determined by their solubility in the membrane or in the solvent present in the membrane. This solubility can be measured by the partition coefficient γ between the solutions inside and outside the membrane. If $\gamma = 0$, the solute is insoluble in the membrane and the membrane is said to be semipermeable. If $\gamma = 1$, the membrane pores are much larger than the solute molecules and do not stericly hinder the dissolution of the latter in the solvent present in the pores. In the intermediate case, when $0 < \gamma < 1$, the solute can pass through the membrane but the diffusion process is partially hindered by the limited solubility of the solute in the solvent present in the membrane pores.

In a system consisting of a membrane which separates the solution from the pure solvent and is permeable to the solvent, the solute will show a tendency to distribute itself equally in all available solvent. This can be accomplished in one of three ways:

(1) If the membrane is semipermeable, solvent diffuses into the solution and dilutes it.

(2) If the membrane is completely permeable to both solvent and solute, no osmotic solvent diffusion occurs (50), only the solute diffuses from the solution into the solvent.

(3) In the intermediate case, when $0 < \gamma < 1$, both solvent and solute diffusion take place simultaneously.

b. The effect of solute leakage on the measured osmotic pressure.

If the membrane separating the solvent from the solution is semipermeable, the pressure that forces the solvent to pass through the membrane is equal under ideal conditions to the true osmotic pressure of the solution. According to Van't Hoff (36) this pressure is due to the bombardment of the membrane by the solute molecules. An alternative theory (36) suggests that the difference in the impacts of the bombardment of the semipermeable membrane by the solvent molecules on both sides causes the pressure difference between the solvent and solution.

If the membrane or capillary system separating the

solvent from the solution is completely permeable to both solvent and solute, i.e. the partition coefficient is equal to unity, no boundary exists between the membrane and the solution, on which the impacts of the bombarding molecules are transformed into pressure. This explains why no osmotic solvent diffusion occurs when solutions of different concentrations are separated by porous plates, capillaries or membranes with sufficiently big pore sizes. This fact was mentioned, but not explained, by Kuhn (50) and is common experience in transference number determinations.

It can readily be seen from the foregoing that, when $0 < \gamma < 1$, the driving pressure acting on the solvent is less than the true osmotic pressure difference between the solutions present on both sides of the membrane. When $\gamma < 1$ a boundary always exists between the membrane and the solution. If the concentration of the solution on one side of the membrane is c_1, the concentration in the membrane at the interface is γc_1. The osmotic pressure difference existing at that interface for an ideal solution is $RTc_1(1 - \gamma)$ and, similarly at the interface on the other side of the membrane $RTc_2(1 - \gamma)$. Hence the actual driving pressure acting on the solvent through such membranes, i.e. the pressure that can be experimentally measured (p_m), is given by:-

$$p_m = RT\,(c_1 - c_2)(1 - \gamma) = (1 - \gamma)p \qquad \ldots IV(2)$$

where p is the true ideal osmotic pressure difference, R the gas constant and T the absolute temperature.

It is not necessary to assume the presence of the solute in the membrane and to assign finite thickness to the membrane to arrive at a conclusion similar to the one presented above. If δ is the probability of passage of each molecule colliding with the membrane, the portion of the molecules which are reflected and so induce a pressure is $(1 - \delta)$. The driving pressure p_m acting on the solvent in the ideal conditions is

$$p_m = RT\,(c_1 - c_2)(1 - \delta) = (1 - \delta)p$$

The identity of this expression and equation IV (2) indicates that γ and δ are identical.

In osmometry, the hydrostatic pressure, which counteracts p_m in such a way that no osmotic solvent diffusion occurs, is measured. When the membrane is semipermeable, i.e. $\gamma = 0$, this pressure is the true osmotic pressure.

As will be shown, it is possible, when $0 < \gamma < 1$,

to establish in an osmometer the hydrostatic pressure which counterbalances the p_m prevailing at the time. When the osmometer is adjusted to this pressure, no driving pressure acts on the solvent. Due to solute diffusion, the osmotic pressure difference between the solutions on both sides of the membrane decreases progressively. As a result, with increasing time, a driving pressure comes into existence tending to decrease the preadjusted hydrostatic pressure difference between the solutions of higher and lower concentrations, i.e. the osmometer follows the changes in concentrations. Under these conditions both solvent and solute diffuse in the same direction.

Furthermore, it will be shown that after a certain period of time the logarithm of the measured pressures decreases linearly with time and can be extrapolated to zero time. If the osmometer is initially filled with a solution on one side and with the solvent on the other side of the membrane, this extrapolated pressure, under ideal conditions, is a measure of the true osmotic pressure of this solution. To obtain the true osmotic pressure from the extrapolated pressure in the first approximation, it is necessary to know

a) the value of δ ,

b) the value of a constant related to the rate of solute

diffusion, and

c) the value of a constant related to permeability of the membrane to the solvent.

Actually to obtain a more accurate value, a number of measurements must be carried out on the same solution under different experimental conditions. From the results obtained it is possible to calculate the true osmotic pressure more accurately and, in principle also, the solvated molar volume of the solute.

The theoretical treatment presented below consists of the following steps:

(1) The time dependence of the concentration changes in the cell is evaluated.

(2) An equation is derived for the time dependence of the experimental pressure readings and a correction is evaluated to calculate $(1 - \gamma)\, p(0)$ from the extrapolated pressure.($p(0)$ is the true osmotic pressure of the solution initially placed into the osmometer). This is necessary because, owing to the viscous resistance of the membrane to the solvent, the osmometer cannot follow the concentration (i.e. osmotic pressure) changes instantaneously.

(3) A procedure is suggested to establish the value of the partition coefficient γ .

c. The Time Dependence of the Pressure Readings in an Osmometer.

i. The time dependence of the changes in the true osmotic pressure difference.

In the general practice of osmometry, the pressure is measured in a capillary manometer. Because of the small diameter of the capillary, the volume changes due to osmotic solvent diffusion are extremely small compared to the volume of the cell, and it can be assumed that they are negligible from the point of view of the concentration changes. Consequently concentration changes in the cell are due only to solute diffusion in the membrane.

It will also be assumed that concentration changes in the osmometer occur in the cell alone. For an osmometer with the manometer system connected to the cell by long capillaries this assumption is justified.

Under experimental conditions there is a linear concentration gradient $\gamma (c_1 - c_2)/d$ in the membrane when γ is the partition coefficient, c_1 and c_2 are the concentions in the solution and solvent chambers respectively and d is the thickness of the membrane. If D_1 and D_2 are the diffusion and dialysis coefficients respectively of the solute

in the membrane, V_1 is the volume of the solution chamber and A is the area of the membrane, Fick's law for the membrane has the following form:-

$$\frac{dn}{dt} = V_1 \frac{dc_1}{dt} = \frac{D_1 \gamma A}{d} (c_1 - c_2) \qquad \ldots IV(3)$$

$$= D_2 A (c_1 - c_2)$$

If one chamber of the cell is initially filled with solution and the other with solvent, the following relation holds:-

$$V_1 c_o = V_1 c_1 + V_2 c_2 = V_1 c_1 + q V_1 c_2 \qquad \ldots IV(4)$$

where q is the ratio between the half cell volumes. By combining equations IV (3) and IV (4) and integrating, the time dependence of both c_1 and c_2 can be evaluated. The difference between $c_1(t)$ and $c_2(t)$ multiplied by RT gives the time dependence of the osmotic pressure differences under ideal conditions:

$$p(t) = p(0)\, e^{-(1 + q)\frac{D_2 A}{V_1} t}$$

$$= p(0)\, e^{-K_s t} \qquad \ldots IV(5)$$

K_s is a constant characteristic for the rate of solute diffusion in the cell.

If the osmometer is adjusted to $(1 - \sigma)p(0)$ at zero time, $(1 - \sigma)p(t)$ will only describe the time dependence of the osmotic pressure reading if the osmometer were able to follow the concentration changes instantaneously. Because of the resistance of the unit due to the viscosity of the solvent there will be a difference between recorded pressure readings and the values of $(1 - \sigma)p(t)$ prevailing at the same time.

ii) Evaluation of the resistance of the osmometer to the flow of the solvent.

If we know how any arbitrary hydrostatic pressure difference is equilibrated in the osmometer, we shall be able to conclude how any osmotic pressure difference change Δp is compensated in it.

The calculations presented below are valid for an osmometer design having the following characteristics:

(1) The free head of the solvent is in a capillary and that of the solution in a relatively large tube. Thus if solvent diffuses through the membrane, it affects only the capillary meniscus; the level changes in the thick tubing are negligible.

(2) Membrane ballooning is eliminated. Consequently

the total volume of the solvent diffusing through the membrane contributes to level changes in the capillary.

Both chambers of the osmometer are filled with solvent only and the meniscus in the capillary is adjusted in such a way that there is a hydrostatic pressure difference Π (0) between the free heads of the solvent present in the two chambers. The permeation of the solvent through a membrane of thickness d and area A under the influence of a hydrostatic pressure difference Π can be described in terms of viscous flow:-

$$\frac{dV}{dt} = -\sigma \frac{d\Pi}{dt} = \frac{P_1 A}{d\eta} \Pi = P_2 A \Pi \qquad ..IV(6)$$

In this equation dV is the volume of the liquid passing through the membrane in time dt, P_1 is the permeability coefficient, P_2 the permeability of the membrane to the solvent, and η is the viscosity of the solvent. If σ is the capillary cross section and Π is measured in cm. solvent, the product $\sigma d\Pi$ is equal to dV in the osmometer described above. The integrated form of equation IV (6) gives the time dependence on the equilibration of any

hydrostatic pressure difference in the osmometer.

$$\overline{\Pi}(t) = \overline{\Pi}(0)\, e^{-K_w t} \qquad \ldots IV(7)$$

In this formula, AP/σ is substituted by the constant K_w.

The value of this constant can be determined by filling the osmometer with solvent only and by measuring how the preadjusted hydrostatic pressure difference decreases with time. The plot of the natural logarithm of the pressure readings vs. time is a straight line with K_w as slope.

The cell constant K_w is equal to AP/σ only if the membrane alone contributes to the solvent flow resistance of the osmometer. In practice, the resistance of the capillary and, perhaps, of the other parts of the unit is an appreciable part of the whole. Experimental results show that the product $K_w\sigma$ increases when determined in the same units but with different capillaries with increasing capillary cross sections. A semi-empirical formula can be derived for K_w which is approximately in accordance with the experimental data. For the same liquid at the same temperature, the resistance of a capillary is inversely proportional

to the fourth power of its radius or to the square of its cross section. The dependence of the K_w for the same manometer liquid and solvent in the same cell is given by equation IV (8):-

$$\frac{1}{K_w \sigma} = \frac{1}{\Delta P_2} + \frac{v}{\sigma^2} + w \qquad \ldots \text{IV (8)}$$

Both v and w are empirical constants characteristic of the cell and the solvent; w is the resistance of the osmometer without the measuring capillary and the membrane.

iii. The time dependence of the osmotic pressure readings when the molar volume of the solvated solute is negligible.

The following assumptions have to be made for the calculations presented below:

(1) The osmometer has such characteristics that equations IV (5) and IV (7) are valid.

(2) The osmometer is so adjusted when filled with solution and solvent that a hydrostatic pressure difference equal to $(1 - \gamma)p(0)$ counteracts the osmotic pressure exerted on the solvent. The solvent diffusion with increasing time is due to the osmotic pressure changes alone, and

proceeds in the same direction as the diffusion of the solute.

(3) Changes in the position of the capillary meniscus are solely due to the solvent passing through the membrane and the volume changes due to the volume of solute diffusing from one half cell to the other are neglected. (A correction for the volume of the solute will be made later).

(4) The flowing solvent does not entrain solute particles with it and the solute molecules do not carry more solvent than attached to them by solvation. (The validity of this assumption was justified experimentally).

As mentioned before, if the osmometer had no resistance to the flow of solvent, the time dependence of the osmotic pressure reading p_r would be described by the time dependence of the true osmotic pressure difference p (equation IV (5)) corrected for the partition coefficient γ. Using equation IV (5) as a basis, we shall now calculate the value of the osmotic pressure reading at fixed time t after filling the instrument, keeping in mind that according to the second assumption $p_r(0) = (1 - \gamma)p(0)$. Each change in osmotic pressure difference $(1 - \gamma)\Delta p(\tau)$

occurring at time τ when $0 < \tau < t$, equilibrates itself for a time period $(t - \tau)$ according to equation IV (7). The viscous backlog in the osmometer can be calculated accordingly:

$$p_r(t) - (1 - \gamma)p(t) = \lim_{\Delta p \to 0} \sum_{p=p(0)}^{p=p(t)} \Delta p(\tau) e^{-(t - \tau)}(1-\gamma) \quad \text{...IV(9)}$$

The value of $\Delta p(\tau)$ can be calculated by putting $t = \tau$ in equation IV (5) to give

$$\Delta p(\tau) = -p(0)\, K_s e^{-K_s \tau}\, \Delta \tau$$

Equation IV (9) can now be rewritten:

$$p_r(t) = (1 - \gamma)p(0)\, e^{-K_s t} - \int_0^t p(0)(1 - \gamma)\, K\, e^{-K_s \tau} e^{-K_w(t - \tau)}\, d\tau$$

$$p_r(t) = (1 - \gamma)p(0)e^{-K_s t} +$$

$$+ (1 - \gamma)p(0)\frac{K_s}{K_w - K_s}(e^{-K_s t} - e^{-K_w t}) \qquad \ldots \text{IV(10)}$$

The relative error of the osmotic pressure readings which is due to the viscous backlog alone is given by:

$$\frac{p_r(t) - (1 - \gamma)p(t)}{(1 - \gamma)\ p(t)} = \frac{K_s}{K_w - K_s}\ (\ 1 - e^{(K_s - K_w)t}) \quad \text{IV(11)}$$

The difference between $p_r(t)$ and $(\ 1 - \gamma)p(t)$ reaches a maximum at t_{max}:

$$t_{max} = \frac{\ln.\frac{K_w}{K_s}}{K_w - K_s} \qquad \ldots \text{IV (12)}$$

An interesting property of these equations is that the value of the relative error given in equation IV (11) is K_s/K_w at time t_{max}.

On Fig. 11 the logarithm of the calculated pressure reading is plotted against time. In these particular plots $(1 - \gamma)p(0)$ and K_s are kept constant having values of 10 and 0.01 respectively and K_w is varied; these values are selected arbitrarily and are of the same order of magnitude as under experimental conditions.

If K_w is larger than K_s, the term $e^{-K_w t}$ vanishes sooner with increasing time than the term $e^{-K_s t}$. If the difference between K_w and K_s is large enough, the log $p_r(t)$ vs. time plot yields a straight line with K_s as slope after a certain period. From a great number of such plots, as presented in Fig. 11, it has been concluded that the plots are straight lines always after t_{max} if the ratio K_s/K_w does not exceed 0.3 and after 1.5 t_{max} if the value of K_s/K_w is between 0.3 and 0.5. Actually the slopes of the straight line portions decrease very slightly with increasing values of K_w. If the straight line portions within the period of $2t_{max}$ are extrapolated to zero time, the difference between the extrapolated value p_{exp} and $(1 - \gamma)p(0)$ is equal within 5% to $(1 - \gamma) K_s/K_w p_o$. This means that the relative error due to the resistance to solvent flow for the extrapolated value is the same as at t_{max}.

Figure 11.

Theoretical log p_r vs. t plots, calculated from equation IV (10)

$$(1 - \gamma)p(0) = 10$$

$$K_s = 0.01$$

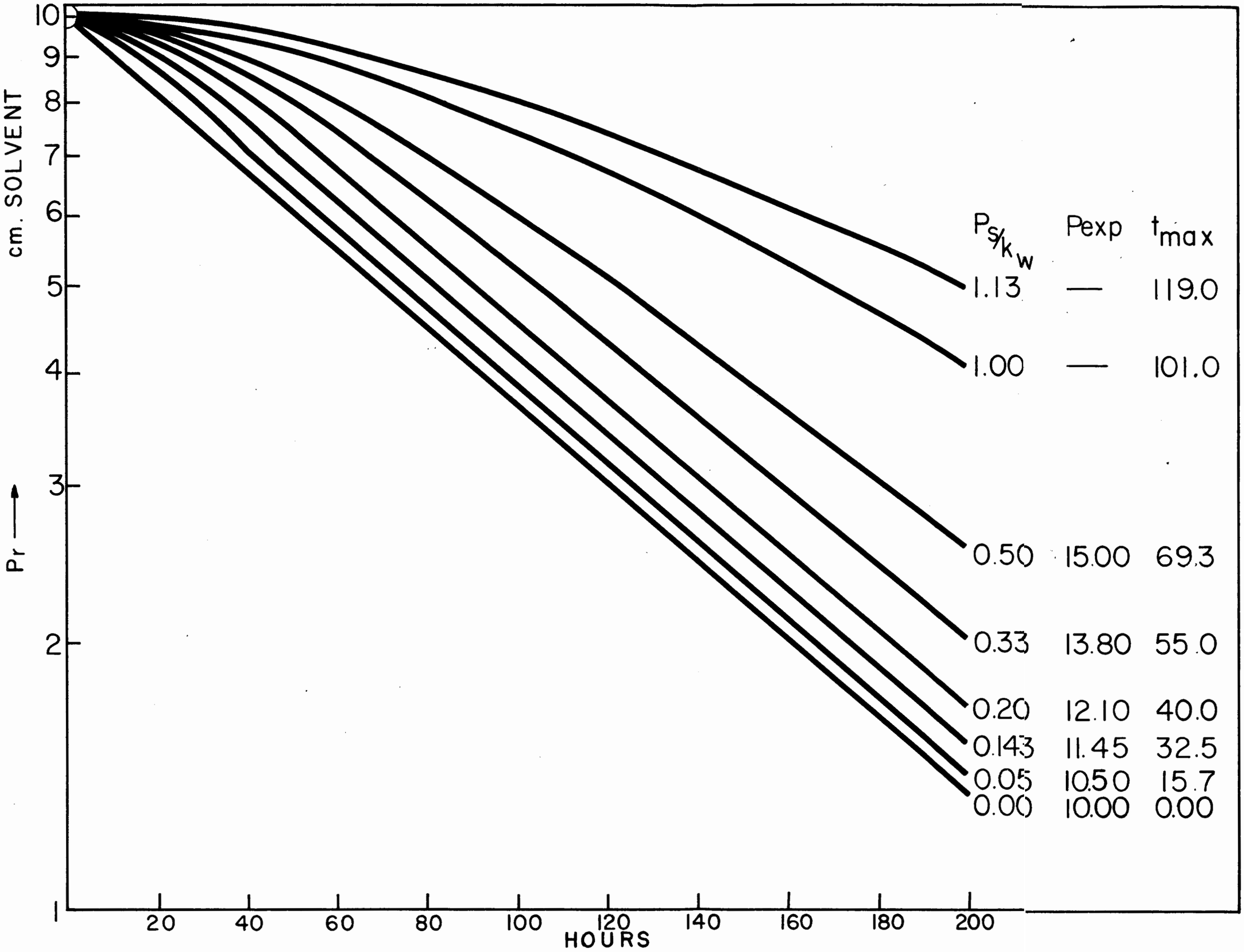
cm. SOLVENT
Pr
10
9
8
7
6
5
4
3
2
1
20
40
60
80
100
120
140
160
180
200
HOURS
P_{s/k_w}
Pexp
t_{max}
1.13 — 119.0
1.00 — 101.0
0.50 15.00 69.3
0.33 13.80 55.0
0.20 12.10 40.0
0.143 11.45 32.5
0.05 10.50 15.7
0.00 10.00 0.00

The formula to compute the true osmotic pressure from the extrapolated value is given below:

$$p(0) = \frac{p_{exp}}{(1 + K_s/K_w)(1 - \gamma)} \qquad \ldots IV(13)$$

It should be mentioned that equation IV (10) describes the time dependence of the osmotic pressure readings for any theoretically conceivable values of K_s and K_w. If these constants are identical, this equation yields a ratio with zero both in the numerator and in the denominator. The value of this ratio can be evaluated according to the L'Hôpital Rule:

$$\lim_{K_w \to K_s} p_r(t) = (1 - \gamma)p(0)e^{-K_s t} + (1 - \gamma)p(0)\frac{K_s}{1 - K_s}\, t\, e^{-K_s t}$$

The values for the curve with $K_s/K_w = 1$ in Fig.11 were calculated according to the equation above.

In practice it is impossible to adjust the osmometer to the initial osmotic pressure at the time of filling, as this osmotic pressure is unknown and some time is needed to be able to establish it. It is possible, however, to

establish the osmotic pressure prevailing at a certain time t_o and to measure the time dependence of the osmotic pressure readings in succeeding times. If the error in this initial adjustment at time t_o is Δ, this will theoretically correspond to an error $\Delta e^{K_w t_o}$ in the initial adjustment at time zero according to equation IV (7). To obtain the actual time dependence of the osmotic pressure readings, the term $\pm\Delta e^{K_w(t_o - t)}$ has to be added to the right hand side of equation IV (10). In most practical cases both Δ and K_s can be kept much smaller than $p(0)$ and K_w respectively. Thus this error term soon becomes negligible, sometimes even within t_{max} and does not interfere with the extrapolation.

iv. Correction for the molar volume of the solvated solute.

In the derivation of equation IV (10) it is assumed that the meniscus in the capillary moves under the influence of the solvent diffusion alone. As both solvent and solute diffuse in the same direction, it is important to account for the volume of the latter.

The osmotic pressure of an ideal 1 M solution in a solvent with density d_s is $2.528 \times 10^4/d_s$ cm. solvent at 25°C. The diffusion of one mole of solute through the

membrane when the volume of both cell chambers is 1 cc. causes a change of $2 \times 2.528 \times 10^7/d_s$ cm. solvent osmotic pressure. If the volumes of the solution and the solvent chambers are V_1 and V_2 respectively, and the capillary cross section is σ, the volume needed to equilibrate the osmometer for each mole solute passing through the membrane is

$$S = (1 + V_1/V_2)\frac{1}{d_s} 2.528 \times 10^7 \times \frac{\sigma}{V_1} \quad ..IV(14)$$

In osmometers generally used (93) σ is in the range of 10^{-4} to 10^{-2} sq. cm. and the half cell volume is 2 to 20 cc. The value of S in practice varies between 2,000 to 200,000cc., i.e. it is of the same order of magnitude as the molar volumes of polymers.

In deriving equation IV (10) it is assumed that the osmotic pressure changes are compensated by the solvent diffusion alone. If V_m is the molar volume of the solvated solute, not S, but $(S - V_m)$ cc. solvent has to diffuse through the membrane for each mole solute passing from one chamber to the other. Hence the true viscous backlog is $(S - V_m)/S$ times the value predicted in equations IV (9)

and IV (10). Both equations IV (10) and IV (13) have to be corrected accordingly:

$$p_r(t) = (1 - \gamma)e^{-K_s t} + (1 - \gamma)p(0)\frac{K_s}{K_w - K_s}\left(1 - \frac{V_m}{S}\right)\left(e^{-K_s t} - e^{-K_w t}\right) \quad \text{..IV(15)}$$

$$p(0) = \frac{p_{exp}}{\left(1 + \frac{K_s}{K_w} - \frac{V_m}{S}\frac{K_s}{K_w}\right)(1 - \gamma)} \quad \text{... IV (16)}$$

In equation IV (16) both $p(0)$ and V_m are characteristic of the solute and are unknown. The other quantities can be determined experimentally. It can readily be seen that neither $p(0)$ nor V_m can be established from one experiment alone. To be able to correlate a number of experiments, it is desirable to rearrange equation IV (16).

$$\frac{1}{p(0)} = \frac{1 - \gamma}{p_{exp}}\left(1 + \frac{K_s}{K_w}\right) - \frac{(1 - \gamma)V_m}{p_{exp}}\frac{K_s}{S}\frac{K_s}{K_w}$$

$$\frac{1 - \gamma}{p_{exp}}\left(1 + \frac{K_s}{K_w}\right) = \frac{1}{p(0)} + V_m\frac{(1 - \gamma)K_s}{p_{exp}S\ K_w}$$

$$\alpha = \frac{1}{p_o} + V_m \beta \qquad \ldots \text{IV (17)}$$

Both α and β can be evaluated from experimental results, and when these values obtained under different experimental conditions are plotted, they yield a straight line with V_m as slope and $1/p(0)$ as intercept on the α axis.

As V_m is the volume of one mole solvated solute, the degree of solvation can theoretically be determined from the difference between V_m and the partial molar volume.

d. Determination of the partition coefficient

The partition coefficients can be simply determined by comparing the dialysis and diffusion coefficients of the solute. A convenient way to determine the diffusion coefficient is given by the porous plate method (58, 68). When two solutions are separated by a porous plate the linear concentration gradient in the plate is similar to that assumed in a membrane. If such a type of cell is filled with solution and solvent, and after a certain time the concen-

trations in both chambers are determined, the value of K'_s can be evaluated. (The value K'_s is used instead of K_s because the latter notation is reserved for osmotic pressure measurements. Theoretically both should be identical for membranes). From equations IV (3) and IV (5), the following relation can be derived:

$$K'_s = \frac{\gamma A D_1}{d} (1 + q) =$$

$$= \frac{\ln c(0) - \ln[c_1(t) - c_2(t)]}{t} \quad \ldots IV(18)$$

In the case of the porous plate γ is unity for any type of solute. The diffusion cell can be calibrated with the solution of a substance with known diffusion coefficient, e.g. with 0.1 N potassium chloride solution, and the cell constant can be determined from the ratio of the known diffusion coefficient and the determined value of K'_s. The product of this cell constant and of K'_s determined for another substance gives the diffusion coefficient of the latter.

The same procedure can be repeated in the osmometer cell. It can be assumed that the partition coefficient of the potassium chloride solutions with respect to water present in the membrane is equal to unity, and the value of K'_s for potassium chloride can be determined. If the solute has a much higher molecular weight than the potassium chloride, its partition coefficient with respect to water in the membrane will be less than one. As can readily be seen, the partition coefficient can be determined from the K'_s values of potassium chloride and the polymer in both the osmometer and in a separate diffusion cell equipped with a porous plate:

$$\frac{D_{i,\ KCl}}{D_{i,\ polymer}} = \left[\frac{K'_{s\ KCl}}{K'_{s\ polymer}}\right]_{\substack{porous\\plate}} =$$

$$= \gamma \left[\frac{K'_{s\ KCl}}{K'_{s\ polymer}}\right]_{membrane} \qquad \ldots IV\ (19)$$

Even if the diffusion coefficients in the solution inside

the membrane are not identical with the diffusion coefficients in water, this would affect the results very little because it is probable that the diffusion coefficients would change in the same sense for both the calibrating potassium chloride and the polymer.

Theoretically, one is justified in using the K_s value obtained from the slope of the ln p_r vs. t plots instead of the K'_s value evaluated for the polymer and membrane from concentration changes. In practice there is very often a difference between these values, probably because of insufficient stirring. K_s is indicative of concentration changes in the immediate membrane neighbourhood while K'_s for the average concentration changes in the half cells. As in the calibration with potassium chloride only the K'_s value can be determined, it is more correct to compare it with a value determined under similar conditions for the polymer.

3. Experimental Part

a. Experimental procedure

Three types of experiments are necessary to deter-

mine the osmotic pressure of a solution, viz. the actual osmotic pressure measurement, the determination of the K_w values of the osmometer and finally the evaluation of the partition coefficient. It is necessary to make at least three osmotic pressure measurements to make an α vs. β plot according to equation IV (17).

i. Determination of p_{exp}

The connecting capillaries between the manometers and the cells of the osmometers were at least 5 cm. long, ensuring that solute diffusion caused concentration changes solely in the cell. Some characteristic data of the three instruments used are given in Table V. From the γ values obtained it can be concluded that the denitrated nitrocellulose membrane had the smallest, and the 300 P.T. cellophane, the largest, pore size. Precision-bore capillaries (Table V) with diameters ranging from 0.3 to 2 mm. were employed with these units. The membranes and the stainless steel screen reinforcers were supported by rubber discs in the smallest, and by glass rods in the two bigger units. All measurements were carried out in a water thermostat at 30°C.

The osmometer readings were corrected for the "zero pressure", that is for the finite pressure reading

TABLE V.

Characteristic Data of the Osmometers and Capillaries

Cell	membrane	solution chamber volume V_1 cc.	solvent chamber volume V_2 cc.	effective membrane area sq. cm.	$K'_{s,KCl}$ $hour^{-1}$
A	300 P.T. Cellophane	13.5	13.5	30	0.97
B	450 P.T. Cellophane	8	8	80	2.03
C	denitrated nitro-cellulose	21	24.3	200	2.85

Capillary	diameter cm.	crossection sq.cm.	cell A K_w $hour^{-1}$	cell B K_w $hour^{-1}$	cell C K_w $hour^{-1}$
a	0.0324	8.20×10^{-4}	0.275	0.725	0.375
b	0.0418	1.38×10^{-3}	0.223	0.623	0.346
c	0.0702	3.75×10^{-3}	0.193	0.371	0.303
d	0.0864	5.85×10^{-3}	0.154	0.267	0.283
e	0.113	1.01×10^{-2}	0.112	0.165	0.196
f	0.144	1.63×10^{-3}	-	0.099	0.140
g	0.191	2.85×10^{-3}	-	0.061	0.112

that was observed when solvent was placed on both sides of the membrane. This zero pressure tended to change when substance was adsorbed on the membrane, but the original value was reestablished by periodically rinsing the membrane on both sides with solvent for periods ranging from 12 to 24 hours. This had to be done after one to three osmotic measurements. The zero pressure for denitrated nitrocellulose was 0.8 and for 450 P.T. cellophane 0.5 cm. toluene. No zero pressure could be measured with the osmometer equipped with the 300 P.T. cellophane.

The osmometer was filled in such a way that the hydrostatic pressure difference between the free heads in the large tubings connected with the solution and the solvent was within 3 cm. of the expected osmotic pressure. This hydrostatic pressure was maintained in the initial 0.5 to 2 hours needed to establish the temperature equilibrium within the units. The purpose of this adjustment was to avoid dilution effects due to excessive solvent diffusion in this period.

After the temperature equilibrium in the unit was established, the measuring capillary was put into operation. The prevailing osmotic pressure difference (actually $(1 - \delta)p(t_0)$) was established by a trial and

error method. The meniscus in the capillary was adjusted to a certain level by making use of the levelling device on the osmometer, and it was observed whether this level rose or fell. This procedure was repeated till two meniscus levels were consecutively found not further than 0.5 cm. apart, one rising and the other falling, indicating that the osmotic pressure difference (actually $(1 - \gamma)p(t)$) prevailing at the time lay within that limit. The osmometer was finally adjusted between these levels and the variations in the pressures were followed with time, at least up to $2t_{max}$, that is for 24 to 48 hours. Readings were taken every 1 to 8 hours. Both level changes in the capillary and in the solution free head were recorded. (The level changes in the solution free head were mainly due to evaporation and occasionally to imperfections in the membrane support). The recorded pressures were calculated in cm. toluene according to equation IV (1).

ii. Determination of K'_s values in the osmometers

At the end of the experiments, the solution and solvent chambers were emptied in such a way that the liquids present in the manometer system did not interfere. The lignin sulfonate concentrations were determined from the

optical densities at 280 mμ in a Beckman Spectrophotometer and the values of K'_s were calculated according to formula IV (18).

The membranes were calibrated with 0.1 N potassium chloride and distilled water in the osmometer cell, the other parts of the unit being closed off by stopcocks. These experiments had to be carried out at room temperature, because the diffusion of the potassium chloride was so rapid that in about half an hour the experiment was ended and there could not have been enough time for temperature equilibration in the thermostat. The potassium chloride concentrations were determined by titration with silver nitrate according to Mohr's method. The evaluated K'_s KCl values were corrected for the difference between room temperature and 30°C according to the differences of the diffusion coefficients of potassium chloride at these temperatures (44).

iii. Determination of the diffusion coefficients

For the determination of the diffusion coefficients, medium grade sintered glass discs of 30 sq.cm area were used. These discs were ground from Gooch filters and placed into the smallest osmometer cell in place of the membrane. The

four inlets to the cell were closed by stopcocks. During the diffusion measurements the cell was in a horizontal position. The experimental procedure was the same as suggested by other authors (58, 68). The diffusion coefficient of 0.1N potassium chloride was taken as 0.00742 sq.cm./hour by correcting the value given by Gordon (97) for the difference between 25°C and 30°C according to the equation in the International Critical Tables (44).

iv. Determination of the values of K_w

The K_w values of the osmometers were determined for each capillary separately. Both cell chambers were filled with distilled water, toluene was placed in the capillary and the unit was put into the thermostat. Plots of $\log \Pi$ against time yielded straight lines of slope $0.4342\ K_w$. Typical plots of this kind are shown on Fig. 12. The values of K_w thus evaluated were independent of the initial pressure. The solvent used in the osmotic pressure measurements was sodium chloride solution, but this could not be used for the determination of the K_w values. The semi-logarithmic plots with sodium chloride solution showed breaks, because the relatively rapid water flow changed the concentration in the immediate membrane neighbourhood and

Figure 12.

$\log \pi$ vs. t plots for osmometer cell B and capillaries a, c, e, g (Compare to Table V)

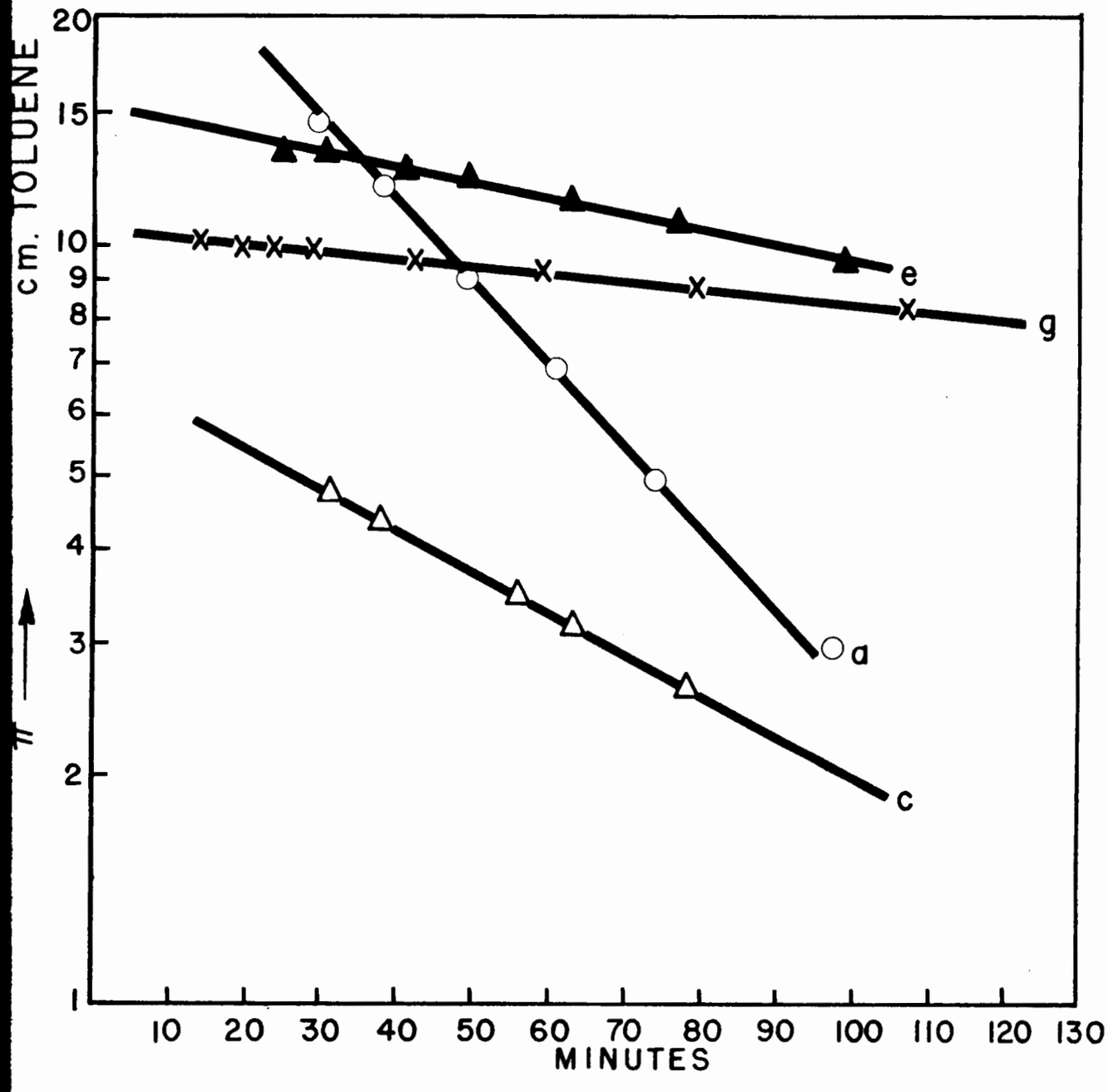
cm. TOLUENE
20
15
10
9
8
7
6
5
4
3
2
1
a
c
e
g
10 20 30 40 50 60 70 80 90 100 110 120 130
MINUTES

the resulting osmotic pressures diminished the actual driving heads.

v. Correction for uneven concentration distribution in the half cells

It has been found very often that the value of K_s from osmotic pressure measurements was greater than K'_s determined from concentration changes. Because of insufficient stirring, the rate of concentration changes in the immediate membrane neighbourhood, indicated by K_s, was greater than the rate of the average concentration changes in the half cells measured by K'_s. For the purpose of determining the values of S an effective half cell volume V_{eff} was used. This V_{eff} is defined as the size of a half cell in which the rate of the average concentration changes is the same as that measured for the immediate membrane neighbourhood with the same membrane. As the rate constants K_s and K'_s are inversely proportional to the half cell volumes, V_{eff} can be computed from the following formula:

$$V_{eff} = \frac{K'_s}{K_s} V_1$$

vi. Determination of molecular weights

The molecular weights were evaluated from the determined true osmotic pressures according to the following equation:-

$$M = 2.942 \times 10^5 \times c'_0 / p(0)$$

where M is the molecular weight, c'_0 is the concentration of the solution in gm./100 cc. and p is the true osmotic pressure in cm. toluene.

b. Results and Discussion.

Typical series of log p_r vs. time plots are shown in Fig. 13 and, as can be seen, they follow the same pattern as the theoretical curves of Fig. 11. The fact that the straight line portions of the curves are parallel to one another is significant. The differences between the values of S, i.e. the volumes of water that passed through the membrane simultaneously with one solute molecule, were up to thirty fold; nevertheless, the rate of solute diffusion remained unchanged. In other words the rate of solute diffusion was not affected by the solvent flowing simul-

taneously through the membrane. This proves the correctness of one of our basic assumptions.

The resistance of the units to solvent flow had the predicted influence on the extrapolated values. As can be seen from Tables VI and VII, p_{exp} increased with increasing K_s / K_w ratio.

The effects ascribed to the molar volume of the solvated solute and to the partition coefficients were at least qualitatively demonstrated by the α vs. β plots (Fig. 14). Owing to experimental imperfections to be discussed later, no straight line could be obtained. Nevertheless, on the average α clearly tended to increase with increasing β, indicating that the volume of the solute diffusing through the membrane effectively contributed to changes in the capillary meniscus level.

The molecular weights shown in Tables VI and VII were calculated from the osmotic pressure values obtained from the treatment of the α and β values by the method of least squares. For fraction No. 5 (Table VII), a great amount of data was available and it was assumed that the maximum deviations of α from the least square average plots corresponded to the maximum possible error in the

evaluated molecular weight. (Both α and the molecular weight are inversely proportional to the osmotic pressure). The precision of the molecular weight determined for fraction No. 6 (Table VI) is probably similar.

The slopes of the α vs. β plots should theoretically be equal to the molar volumes of the solvated solutes. The experiments described were hardly suitable for determining these volumes as the values of α were changed only in a narrow range and the scattering of the results was considerable. The values of V_m obtained by the least square average treatment are given in Tables VI and VII and are probably very inaccurate.

Results obtained for higher molecular weight fractions are presented in Tables VIII, IX and X. The K_s values were so small that the corrections K_s/K_w were within experimental error. Thus it was neither possible nor necessary to use the α vs. β plots for evaluating the osmotic pressures. The p_{exp} values were corrected for the partition coefficient alone. It is significant that the results thus corrected are independent of the membrane used. This proves that the solute present in the membrane (indicated by the finite distribution coefficients) has the

Figure 13.

Experimental log p_r vs. t plots of fraction No. 5 in Osmometer cell B (Compare to Table VII)

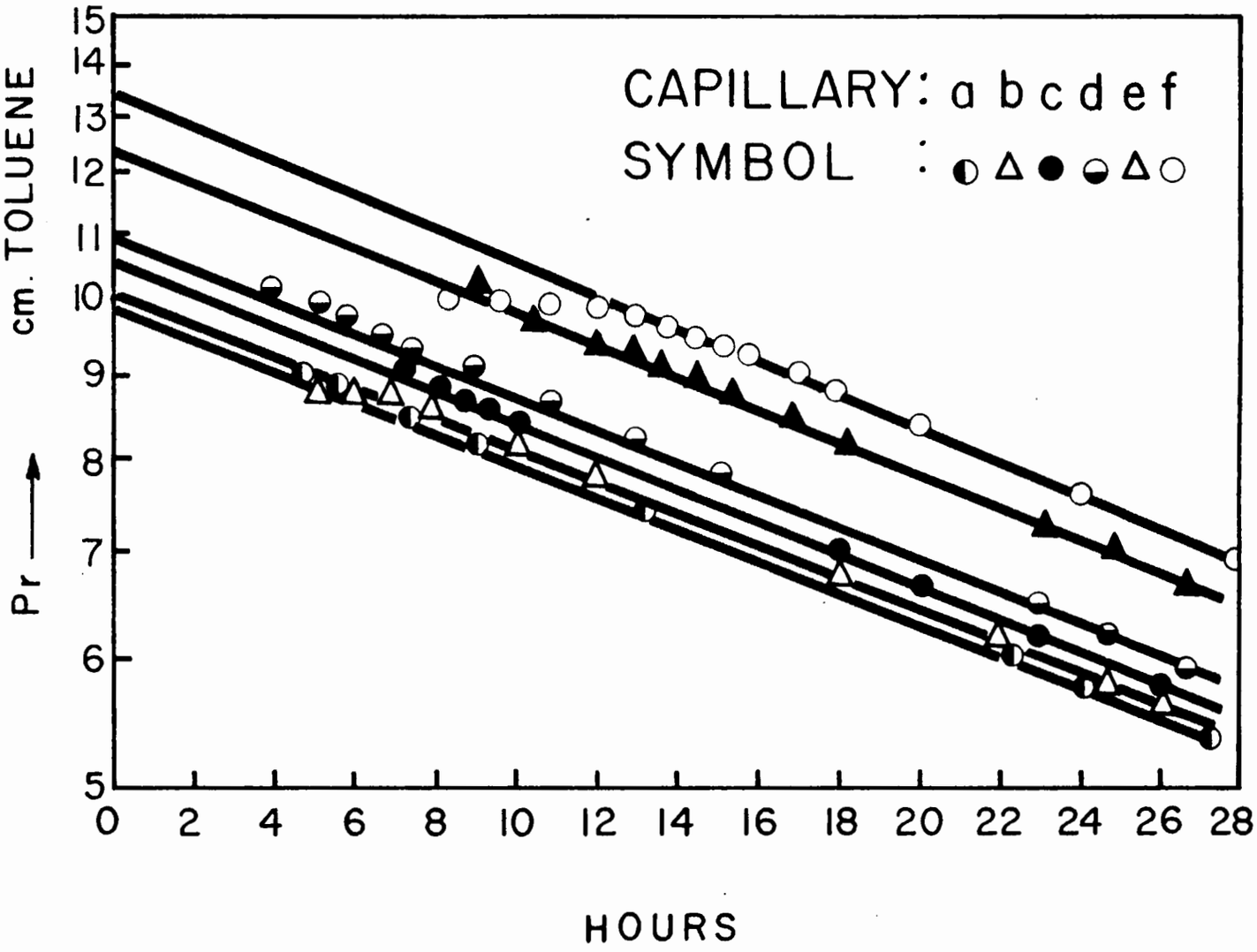
CAPILLARY: a b c d e f
SYMBOL : ◐ △ ● ◒ △ ○
cm. TOLUENE
Pr ⟶
15
14
13
12
11
10
9
8
7
6
5
0 2 4 6 8 10 12 14 16 18 20 22 24 26 28
HOURS

Figure 14.

α vs. β plots for fractions No. 5 and 6. The straight lines were calculated by the method of least squares (Compare to Tables VI and VII)

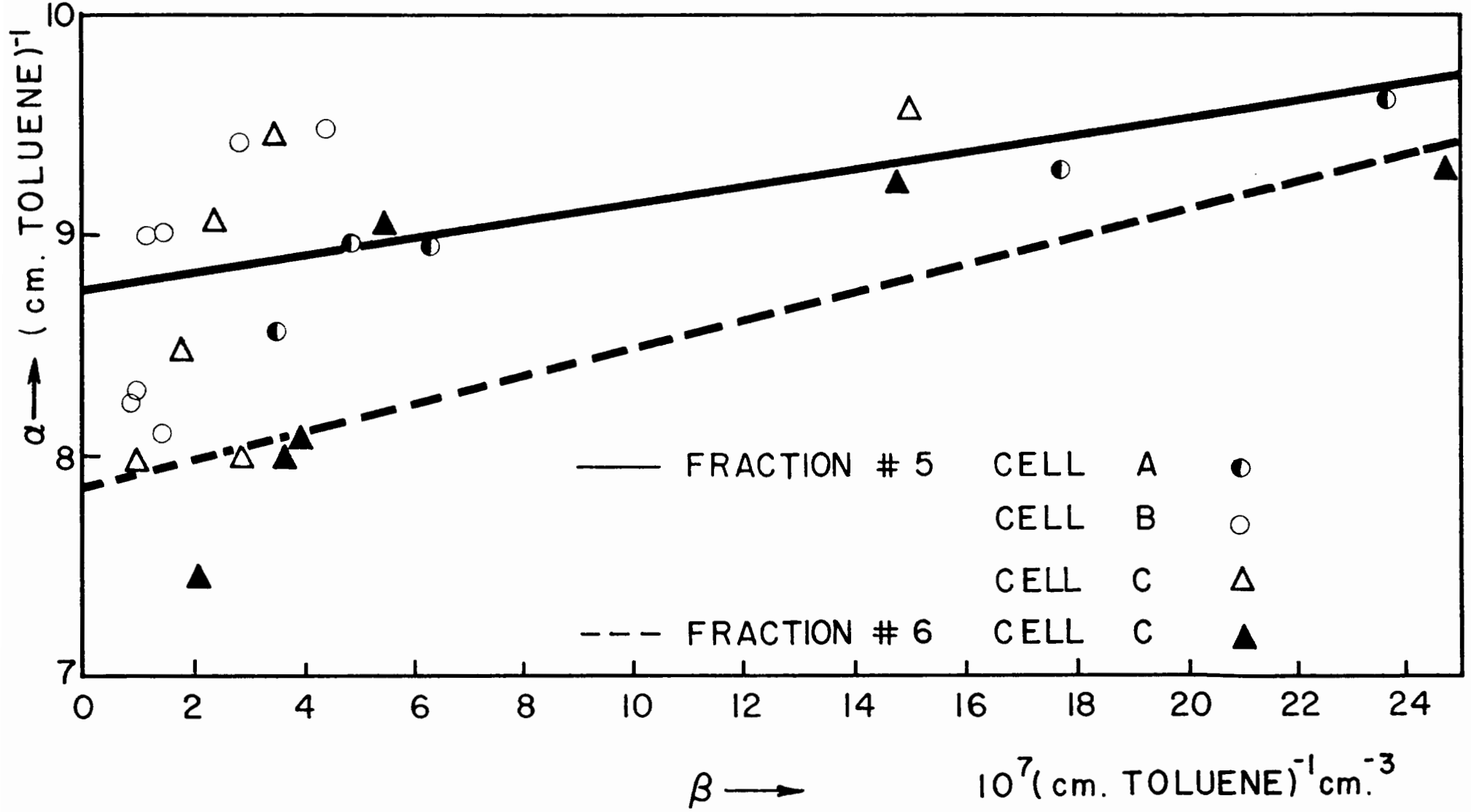
10
9
8
7
α ⟶ (cm. TOLUENE)⁻¹
0
2
4
6
8
10
12
14
16
18
20
22
24
β ⟶
10⁷(cm. TOLUENE)⁻¹cm.⁻³
FRACTION # 5 CELL A
CELL B
CELL C
FRACTION # 6 CELL C

TABLE VII.

Results of Osmotic Pressure Measurements. Fraction No. 5.

Diffusion coefficient: 8.34 x 10^{-3} cm^2 $hours^{-1}$

Concentration 0.2 g./100 cc.

Capillary	K_s/K_w	$p_{exp.}$ cm. toluene	S cm^3	α $(cm.\,toluene)^{-1}$	β $(cm.\,toluene)^{-1}cm^{-3}$
UNIT A.	K_s = 0.0304 $hours^{-1}$			V_{eff} = 11.5 cc.	
	K'_s = 0.0259 $hours^{-1}$			γ = 0.238	
a	0.110	8.8	4,000	0.0962	2.38 x 10^{-6}
b	0.136	9.3	6,700	0.0928	1.78 x 10^{-6}
c	0.158	9.9	19,200	0.0892	6.32 x 10^{-7}
d	0.197	10.2	29,800	0.0892	4.93 x 10^{-7}
e	0.272	11.4	51,500	0.0855	3.53 x 10^{-7}
UNIT B.	K_s = 0.0231 $hours^{-1}$			V_{eff} = 6.7 cc.	
	K'_s = 0.0193 $hours^{-1}$			γ = 0.0849	
a	0.032	9.9	6,800	0.0949	4.34 x 10^{-7}
b	0.037	10.1	11,500	0.0943	2.91 x 10^{-7}
c	0.062	10.6	32,800	0.0922	1.65 x 10^{-7}
d	0.085	10.9	51,000	0.0906	1.39 x 10^{-7}
e	0.14	12.4	88,000	0.0838	1.17 x 10^{-7}
f	0.23	13.6	144,000	0.0830	1.06 x 10^{-7}
UNIT C.	K_s = 0.0188 $hours^{-1}$			$V_{eff.}$ = 15.8 cc.	
	K'_s = 0.0137 $hours^{-1}$			γ = 0.0427	
a	0.052	10.7	3,150	0.0955	1.5 x 10^{-6}
c	0.061	10.9	15,200	0.0944	3.55 x 10^{-7}
d	0.067	11.4	23,500	0.0906	2.46 x 10^{-7}
e	0.096	12.5	40,500	0.0847	1.84 x 10^{-7}
f	0.134	13.5	65,500	0.0814	1.48 x 10^{-7}
g	0.167	14.5	104,000	0.0792	1.07 x 10^{-7}
	p(0) = 11.4 cm. toluene			M = 5,170 (+6% - 9%)	
	V_m = 3,790 cc.				

TABLE VIII.

Results of Osmotic Pressure Measurements. Fraction No.4

Diffusion coefficient: 6.30×10^{-3} cm.^{2} hour^{-1}
Concentration 0.5 gm./100 cc.

UNIT A	K_s = 0.010 hours^{-1}			γ = 0.08
	K'_s = 0.0087 hours^{-1}			
Capillary	a	c	d	e
K_s/K_w	0.036	0.052	0.065	0.089
p_{exp}	15.5	15.3	14.9	16.1
$p/(1-\gamma)$	16.86	16.7	16.2	17.5
UNIT B	K_s = 0.008 hours^{-1}			γ = 0.031
	K'_s = 0.007 hours^{-1}			
Capillary	a	c	d	e
K_s/K_w	0.011	0.021	0.03	0.061
p_{exp}	16.7	16.7	16.3	17.0
$p/(1-\gamma)$	17.2	17.2	16.8	17.5
UNIT C	K_s = 0.006 hours^{-1}			γ = 0.016
	K'_s = 0.005 hours^{-1}			
Capillary	a	c	d	f
K_s/K_w	0.016	0.019	0.021	0.043
p_{exp}	18.4	18.3	17.4	17.6
$p_{exp}/(1-\gamma)$	18.7	18.6	17.7	17.9

$\overline{p(0)}$ = 17.4 cm. toluene M = 8,450 (+3.7%-6.4%)

TABLE IX.

Results of Osmotic Pressure Measurements. Fraction No.3

Diffusion coefficient: 5.26×10^{-3} cm.^{2} hour^{-1}			
Concentration 0.8 g./100 cc.			
UNIT A.	$K_s = K'_s = 0.0038$ hours^{-1}		$\gamma = 0.0632$
Capillary	a	d	e
p_{exp}	13.6	13.9	14.2
$p_{exp}/(1 - \gamma)$	14.5	14.8	15.1
UNIT B .	$K_s = K'_s = 0.0052$ hours^{-1}		$\gamma = 0.0292$
Capillary	a	d	e
p_{exp}	14.3	14.1	14.7
$p_{exp}/(1 - \gamma)$	14.7	14.5	15.3
UNIT C.	$K_s = K'_s = 0.00077$hours^{-1}		$\gamma = 0.00027$
Capillary	a	d	e
p_{exp}	15	15.4	15.4
	$\overline{p(0)} = 14.95$ cm. toluene		
	$M = 15{,}500 \pm 3.7\%$		

TABLE X.

Results of Osmotic Pressure Measurements. Fraction No. 2.

Diffusion coefficient: 3.97×10^{-3} cm.^{2} hour^{-1}

Concentration: 1g./100cc.

UNIT A.	$K_s = K_s' = 0.0028$ hour^{-1}		$\gamma = 0.0542$
Capillary	a	d	e
p_{exp}	14.5	14.8	14.7
$p_{exp}/(1 - \gamma)$	15.3	15.6	15.5
UNIT B.	$K_s = K_s' = 0.0035$ hours^{-1}		$\gamma = 0.0321$
Capillary	a	d	e
p_{exp}	14.5	14.3	14.9
$p_{exp}/(1 - \gamma)$	14.95	14.7	15.4
UNIT C.	$K_s = K_s' = 0.0004$ hours^{-1}		$\gamma = 0.0025$
Capillary	a	d	e
p_{exp}	15.6	15.4	15.8

$\overline{p(0)} = 15.36$ $\qquad$ $M = 19{,}200 \pm 3\%$

TABLE XI.

Concentration Dependence of the reduced Osmotic Pressure of various fractions.

Fraction	Concn. $\frac{gm.}{100cc.}$	Unit	Capillary	p cm. toluene	$\frac{p}{c}$	p_{exp} cm. toluene	$\frac{p_{exp.}}{c.}$
1	0.3	B	a	1.48	4.94	-	-
1	0.5	B	a	2.55	5.10	-	-
1	0.8	A	a	4.25	5.30	-	-
1	1.0	C	b	5.11	5.11	-	-
1	2.0	B	a	10.14	5.07	-	-
3	0.4	A	a	-	-	6.9	17.2
3	0.8	A	a	-	-	13.6	17.0
3	1.2	A	a	-	-	21.0	17.5
5	0.15	B	a	-	-	7.3	48.7
5	0.2	B	a	-	-	9.9	50.45
5	0.3	B	a	-	-	15.0	50.00

effect on the recorded osmotic pressure predicted in the theoretical part. In this connection it should be mentioned that the scattering of the α values from the average was random in the case of fraction No. 5 for all three membranes used (Fig. 14).

The ratios p_{exp}/c'_o proved to be within experimental error, independent of the concentration of all lignin sulfonate fractions determined in the same unit with the same capillary (Table XI). Consequently the molecular weights could be determined from data as obtained at one particular concentration, and extrapolation to zero concentration was not necessary. Osmotic pressures of solutions of fraction No. 1 are also shown in Table XI. The molecular weight of this fraction was 58,000 and all three membranes used were impermeable to it.

Attempts were made to measure osmotic pressures of solutions of fraction No. 6 using cellophane membranes, and of other lower fractions by using denitrated nitrocellulose and cellophane membranes. Higher porosity parchment membranes were also tried for high molecular weight fractions. In these experiments the log p_r vs. time curves deviated more or less from straight lines, the extrapolated values had poor reproducibility, and the values of the

partition coefficients were relatively high, ranging up to 0.3. The failure of these attempts indicate that there are very definite limits in the applicability of permeable membranes to osmotic pressure measurements.

c. Sources of Experimental Errors

The main source of experimental error is the existence of concentration gradients in both half cells. There are two types of concentration disturbances. Due to the solute diffusion there is a concentration gradient across the solution and the solvent cell. Evidence of these gradients is provided by the difference between the values of K_s and K'_s (Tables VI, VII and VIII). Such gradients have an adverse effect on the accuracy of the p_{exp} and S determinations.

Another type of concentration disturbance is caused by solvent diffusion and is more or less confined to the immediate membrane surroundings. As solvent flows through the membrane, the concentration of the solution at the membrane increases on the solution chamber side and decreases on the other side. The effect of solvent diffusion is opposite to that of solute diffusion: it tends to increase the measured osmotic pressure.

The ratio between the amount of solute and solvent simultaneously passing through the membrane under the experimental conditions can be expressed in terms of an apparent concentration in moles per cc., and it has the value of $1/(S - V_m)$. If the concentration gradients are not entirely eliminated by stirring and the value of $1/(S - V_m)$ is smaller than the average of the concentrations on both sides of the membrane, i.e. $c_o /(1 + q)$, the measured osmotic pressures are higher than predicted by the theory. This happens when thick capillaries are used and consequently the α values corresponding to small β values are probably too low.

It has been shown by Schulz (90) that in osmometers with horizontally placed membranes, stirring by convection is considerable. It does not seem to be adequate, however, when the membranes used are permeable to the solute.

The need for membrane support for permeable membranes is greater than for semipermeable membranes. The ballooning of semipermeable membranes has an adverse effect on the speed of the measurements but not on their accuracy. The slightest membrane ballooning in membranes permeable to the solute has an adverse effect on the accuracy of both K_w and S determinations. When the membrane moves, one part

of the solvent diffusing through the membrane causes changes in the hydrostatic pressure, and the other part is needed to compensate for the volume changes in the half cells. In the medium-sized osmometer used (unit B) the membrane support was practically perfect. The reproducibility of the K_w determinations was within 1% and the dependence of the values of K_w on the capillary cross section was in good agreement with equation IV (8). This can be shown by calculating the values of $1/K_s\sigma$ and $1/\sigma^2$ from the data given on Table V and plotting them against one another. The plot is a straight line. In the other two units the K_w determinations were reproducible to $\pm 3\%$ only.

Theoretically, membrane ballooning should also change the value of K_s during the measurements by changing the ratio between the half cells. This could not be verified experimentally.

Another source of experimental error is due to the fact that the measurements could not be started immediately after filling the osmometer, and at the beginning of the determination of the time dependence of the pressure readings there was up to 3% error in the initial adjustment.

As it has been shown in the theoretical part, this error is negligible if K_s/K_w is small.

The scatter of the $\alpha-\beta$ values (Fig. 14) is due to the fact that in calculating each of these values a great number of independently determined data had to be used, some of which were known only inaccurately. The estimated errors of the various quantities are $\pm 3\%$ for p_{exp}, ± 1 to 3% for K_w, ± 1 to 5% for K_s, ± 2 to 10% for S and ± 1 to 10% for δ.

The accuracy of the measurements is better the smaller the capillary and the smaller the value of K_s/K_w. Under the experimental conditions described here, measurements cannot be made with any accuracy if the value of K_s/K_w exceeds 0.20 to 0.25.

4. Conclusions on the applicability of the technique described in this chapter.

It would seem that the theory presented may be used to correct for leakage in osmometers of the type generally used. In aqueous solutions, cellophane-type membranes are impermeable only to substances in the molecular weight range greater than 20,000 to 30,000. It is however possible

to determine osmotic pressures of solutions of substances with molecular weights as low as 5,000 with the same membranes by proceeding as suggested in this paper.

The main drawback of the generally used osmometers equipped with membranes permeable to the solute is that convection alone does not provide sufficient stirring. Full use of the procedure described here could be made only if an osmometer with well-supported membrane and built in stirrer were used. Errors due to concentration gradients in the cell could thus be eliminated and it would probably be possible to extend the applicability of this method to molecular weight regions even lower than 5,000 and also to evaluate the molar volumes of solvated substances.

E. DETERMINATION OF THE MOLECULAR WEIGHTS OF THE TWO LOWEST MOLECULAR WEIGHT FRACTIONS.

As shown above, molecular weights of all but the two lowest fractions were determined by the osmotic pressure method; these values are tabulated in Tables II and XII. When the logarithm of the molecular weights are plotted against the logarithm of the diffusion coefficients (Fig. 23), the points corresponding to fraction Nos. 4, 5 and 6 fall on

a straight line which can be extrapolated to the measured diffusion coefficients of the lowest fractions, from which the molecular weights were calculated. It must be borne in mind that the ultraviolet extinction coefficients of the solutions were used to determine the concentrations in the diffusion experiments. Should the lower fractions be mixtures of ultraviolet light absorbing lignin sulfonates and relatively transparent carbohydrates, the diffusion coefficients would be indicative of the lignin sulfonates alone.

In a homologous polymer series the following relation holds between the weight-average molecular weights and diffusion coefficients D_1 (36):

$$D_1 = K_1 M^{-b}$$

where "b" is a constant depending on the shape of the molecules and K_1 is a constant characteristic for the homologous series. The error involved in using number average molecular weights and the diffusion coefficients for estimating the molecular weights of the lowest lignin sulfonates should be small. As can be seen from the integral molecular weight distribution plot (Fig. 15) the degree of polydispersity of the fractions except the highest (No. 1) is relatively low.

Hence there is only a slight difference between the weight average and the number average molecular weights.

F. DISCUSSION OF THE MOLECULAR WEIGHTS OF LIGNIN SULFONATES

The integral molecular weight distribution plot (Fig. 15) indicates that the molecular weights of the lignin sulfonates investigated range from about 3,700 to about 100,000. Around 30% of the material has molecular weights between 3,700 and 5,000 and also between 15,000 and 25,000.

It is beyond the scope of this study to give a critical survey of the numerous attempts to determine the molecular weights of different lignin preparations. The accumulated data (9, 34) present a confusing picture because in the isolation of lignin or lignin sulfonates the original lignin in the wood can be considerably degraded or polymerized. Furthermore, as will be shown later, there is indication that in the lower molecular weight region association may occur in the solutions; if this occurs the molecular weights obtained for the lower fractions would also be too high.

Nevertheless it is interesting to note that some investigators (13, 38, 57, 81) have found that lignin

preparations isolated under mild conditions have molecular weights not lower than 3,500 to 4,000 which correspond well to the lower limit of the data presented here. According to Gralen (38) there is some indication that lignins with degrees of polymerization corresponding to the molecular weights 4,000 and 8,000 are the most stable. In the light of this, it is significant that 30% of our fractions have molecular weights in the 4,000 range.

Considerably lower molecular weights of lignin, however, have also been reported (9,34). Until a study is made of how the D.P. of lignin is changed in the various isolation techniques it will be difficult to interpret the available data. Since the highest reported native lignin molecular weight is 27,000 (38), there is strong indication that during the sulfite cook at least part of the lignin becomes considerably polymerized.

Figure 15.

Integral molecular weight distribution of lignin sulfonates.

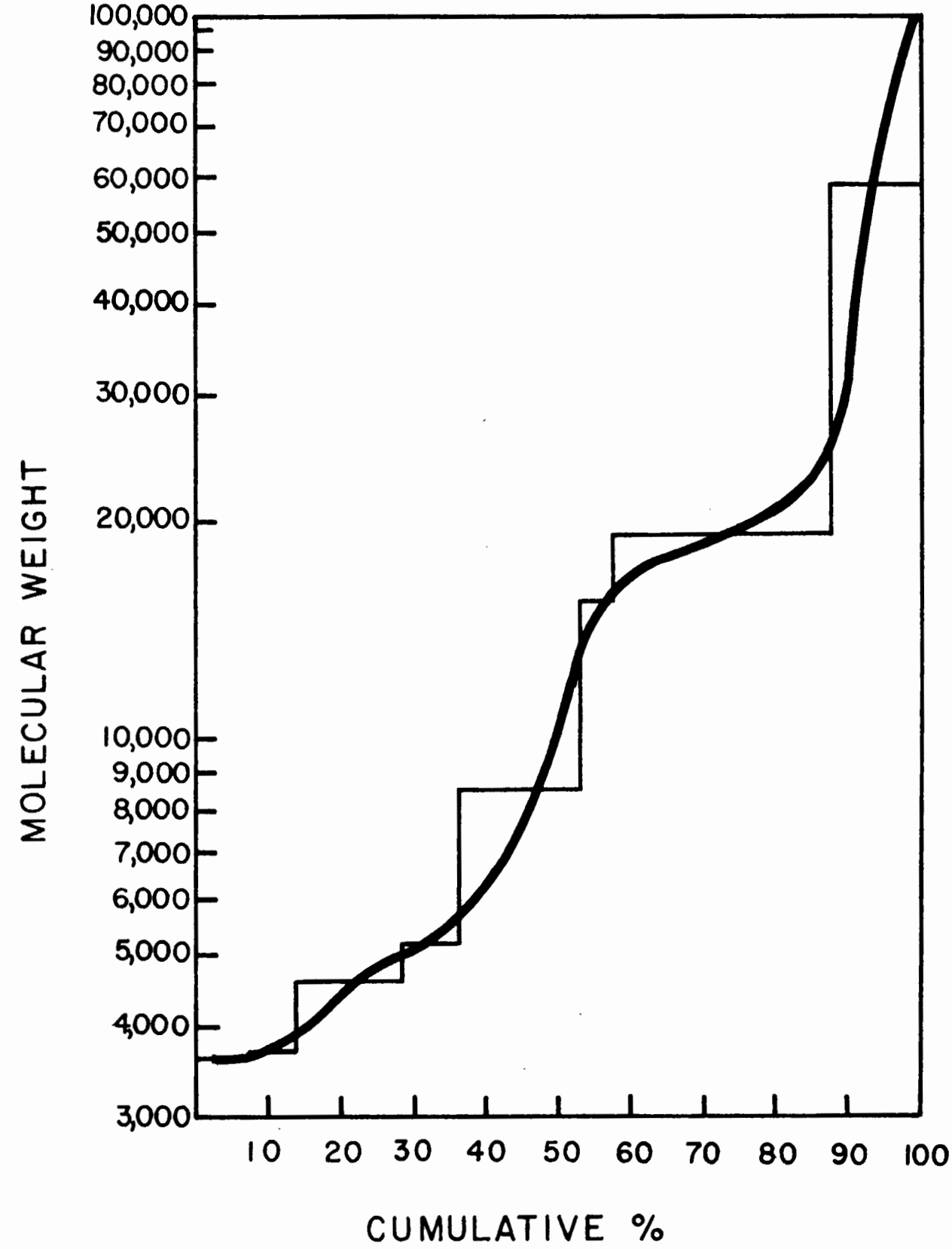
100,000
90,000
80,000
70,000
60,000
50,000
40,000
30,000
20,000
10,000
9,000
8,000
7,000
6,000
5,000
4,000
3,000
MOLECULAR WEIGHT
10
20
30
40
50
60
70
80
90
100
CUMULATIVE %

V. POLYELECTROLYTIC NATURE OF LIGNIN SULFONATES

A. INTRODUCTION

The theories on the molecular structure of lignin sulfonates and the results of the experiments described below, indicate that the lignin sulfonates can be considered as substances consisting of flexible chain molecules with ionizable groups attached to them, i.e. they are polyelectrolytes.

Recently considerable research has been carried out on polyelectrolytes, general accounts of which are given by Fuoss (30, 32), Flory (28) and Katchalsky (46). The most important characteristic is that in solution their molecular shape depends upon the net electrical charge on their molecules. In uncharged state the molecule curls up. If the ionic groups are dissociated, the polyelectrolyte molecule extends owing to the electrostatic repulsion between neighbouring groups.

The degree of ionization of the polyelectrolyte depends on its concentration and also upon the presence of simple electrolytes in the solution. At low polyelectrolyte concentrations, the molecules occupy only a small part of the

available space in the solution. This favours the escape of the counter-ions, e.g. the sodium ions of the lignin sulfonates, from polymer molecules, leaving the latter charged. The equilibrium between the counter-ions associated with the polymer molecules and in the part of the solvent free of polymer molecules, i.e. in the free space, is analogous to a Donnan-type equilibrium. Consequently when the free space becomes smaller as the polyelectrolyte concentration is increased, the counter-ion concentration in this free space greatly increases, inhibiting further ionic dissociation. The polyelectrolyte molecules can also lose their charge, even at low concentrations, if the concentration of the counter-ions in the free space is increased by the addition of simple electrolytes containing the same counter-ion as the solution.

The dependence of the charge of the molecules of the polyelectrolyte on its concentration can be shown by conductivity measurements. As the molecules progressively lose their charge with increasing concentration, less and less current can be carried by each molecule. The specific conductivity decreases with increase of the square root of the concentration, but not linearly, as predicted by the Onsager equation for simple electrolytes. The corresponding plot is curved and is steep at low concentration.

The flexible coiling of the molecules as they progressively lose their charge can be demonstrated by the dependence of the reduced viscosity (η_{sp}/c) on the concentration. As the effect of an extended molecule on the viscosity of the solution is greater than that of a molecular coil, the reduced viscosity of the polyelectrolyte decreases with increasing concentration. If, however, determinations are made of the viscosities of solutions containing different amounts of polyelectrolyte and always the same sufficiently large amount of simple electrolyte, the reduced viscosity of the polyelectrolyte, like the viscosity of uncharged polymers, increases linearly with concentration.

B. CONDUCTIVITY MEASUREMENTS

From the considerations given above it may be expected that variations of the specific conductivity with concentration of lignin sulfonates and of simple electrolytes is different. This apparent anomaly has been observed but not adequately explained by a number of investigators (23, 48, 64, 81). The results obtained by Samec and Ribaric (81) and Koenig (48) did not conform with the pattern predicted for polyelectrolytes and, oddly enough, the specific conductivity curves had maxima at very low concentrations. These results could not be reproduced in this

investigation.

The variation of the specific conductivities of several sodium lignin sulfonate fractions with $\sqrt{c}$ at 25°C is shown in Fig. 16. Curves A and B represent fractions having molecular weights of 58,000 and 19,200 respectively and are typical of polyelectrolytes. Curves C, D and E obtained for fractions with molecular weights 5,200 , 3,700 and 3,650 are not smooth; this may indicate association, as generally observed for colloidal electrolytes, but not for polyelectrolytes. The specific conductivity vs. $\sqrt{c}$ plot for a colloidal electrolyte shows very sharp discontinuity at the critical micelle formation concentration. At lower colloidal electrolyte concentration, the plot is linear and descends slightly; at higher concentration it drops very markedly and quite often passes through a minimum (2, 58). The molecular weights of colloidal electrolytes however, are in the range of several hundreds and about 20 to 200 molecules associate to form a micelle; abrupt changes are therefore shown in the properties at the critical concentration of micelle formation. Considerably greater molecular weights were found for the lignin sulfonates investigated than for conventional colloidal elctrolytes. Consequently it is improbable that aggregates consisting of a great number of

Fig. 16.

Specific conductivities of sodium lignin sulfonate fractions having molecular weights 58,000 (Curve A), 19,200 (B), 4,600 (C), 3,700 (D) and 3,650 (E).

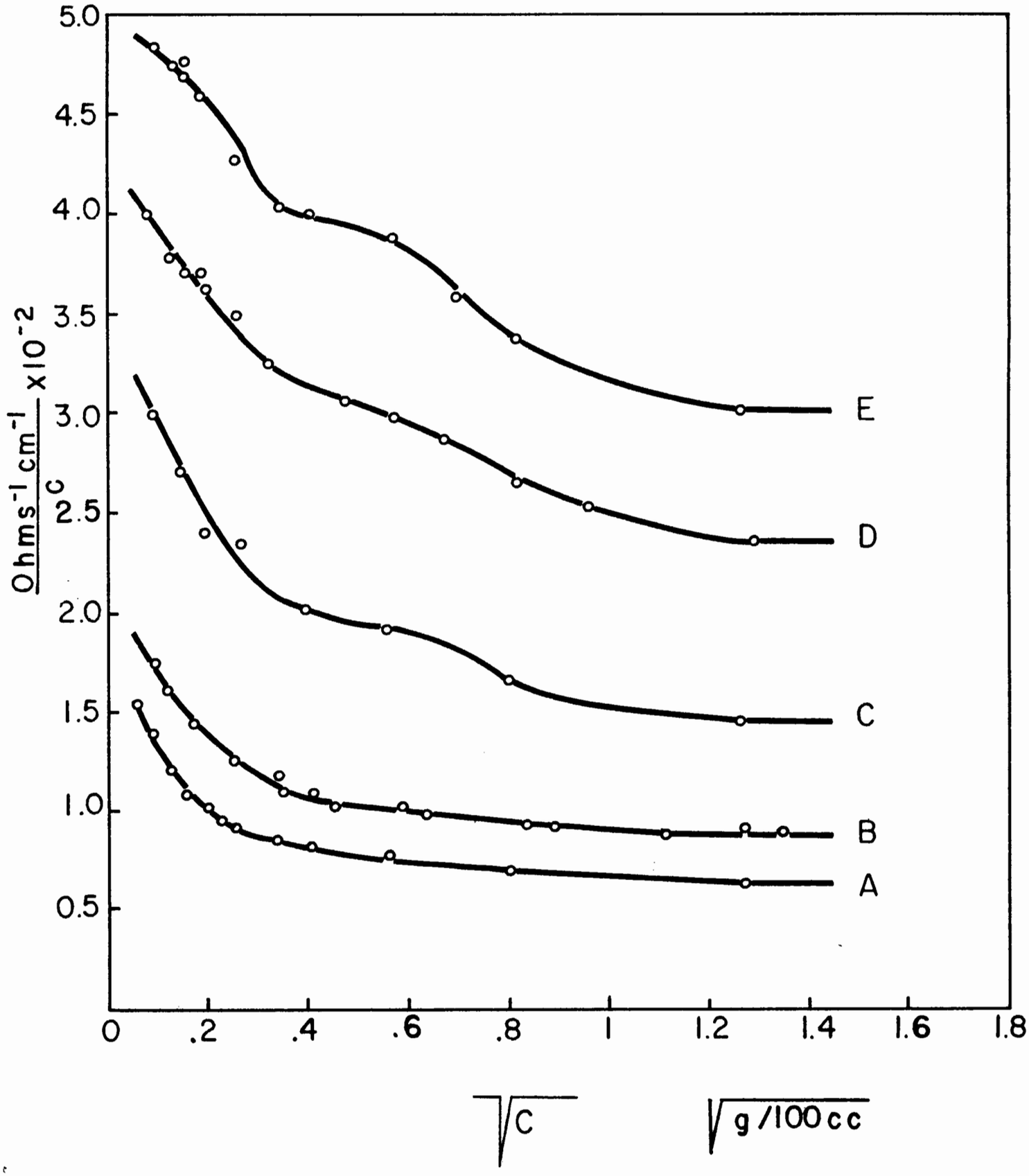
5.0
4.5
4.0
3.5
3.0
2.5
2.0
1.5
1.0
0.5
$\frac{Ohms^{-1}cm^{-1}}{c} \times 10^{-2}$
E
D
C
B
A
0
.2
.4
.6
.8
1
1.2
1.4
1.6
1.8
$\sqrt{c}$
$\sqrt{g/100cc}$

lignin sulfonate molecules will be formed. Hence the lignin sulfonate solutions do not show such sharp discontinuities as the solutions of colloidal electrolytes around the critical micelle formation concentration. The shape of curves C, D and E may be considered as evidence that the low molecular weight lignin sulfonates are intermediate between polyelectrolytes and colloidal electrolytes. As will be shown, the reduced viscosity curves of all fractions and the dyestuff adsorption curves of all but the lowest molecular weight fractions were smooth. Hence the conductivity curves cannot be considered as absolute proof for association in the low molecular weight range; this matter requires further study.

C. DYESTUFF ADSORPTION MEASUREMENTS

It has been observed (98) that the optical absorption spectra of aqueous solutions of certain dyestuffs shift in the presence of micelles of colloidal electrolytes. According to Corrin and Harkins (15), this is due to adsorption or incorporation of the dyestuff on, or into, the micelle and to the different colors of the dyes in a polar medium e.g. water, and in a non-polar medium as the non-charged micelle. They suggested the use of this phenomenon

to detect the critical micelle formation concentration.

The influence of the uncharged coiled polyelectrolyte molecules on the colour of indicator dyes has not yet been investigated. The experiments here described indicate that, as was to be expected, they changed the light adsorption spectra of such dyes just as the micelles of the colloidal electrolytes.

Pinacyanole is blue when dissolved in pure water and green in the presence of uncharged aggregates (15). This cationic dyestuff was found to be suitable for experiments with lignin sulfonates. In Fig. 17 light absorption curves of solutions containing 1.2 mg./ 100 cc. dye (A), the same amount of dye and 0.5 gm./ 100 cc. lignin sulfonate (B) and 0.5 gm./ 100 cc. lignin sulfonate alone (C) are shown. The maximum at 620 mμ in curve (B) is characteristic of the dyestuff discharged aggregate complex, but the pure dyestuff solution also absorbs light at this wavelength appreciably. However, the light absorption of both pure dye and pure lignin sulfonate at 630 mμ wavelength is negligibly small. The optical density at 630 mμ can be considered as a measure for the amount of discharged aggregate-dye complex present in the solution.

Fig. 17.

Absorption curves of (A) 1.2 mg./100 cc. pinacyanole

(B) 1.2 mg./100 cc. pinacyanole and 0.5 gm./100 cc. lignin sulfonate (molecular weight 19,200)

(C) 0.5 gm./100 cc. lignin sulfonate

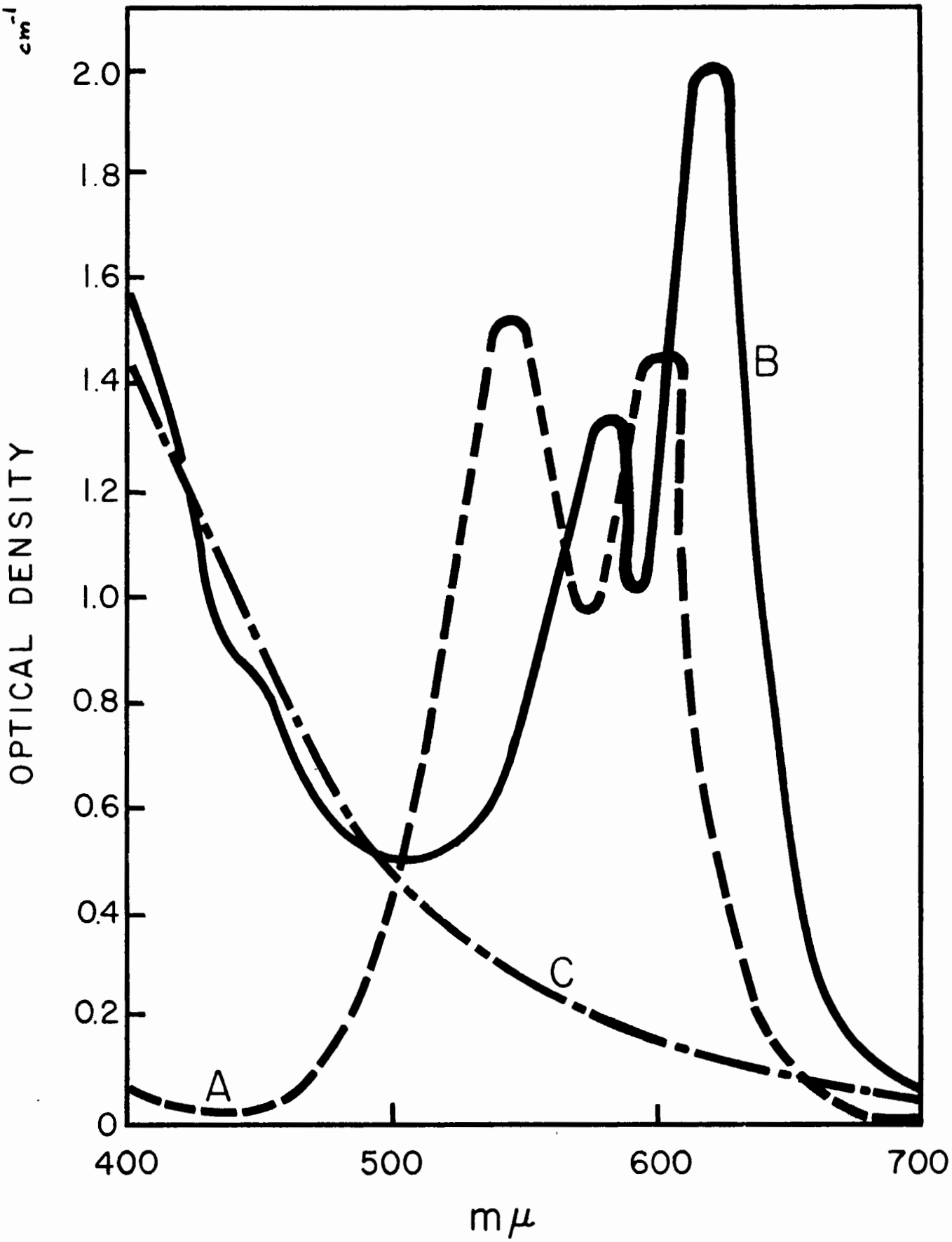
cm⁻¹
2.0
1.8
1.6
1.4
1.2
1.0
0.8
0.6
0.4
0.2
0
OPTICAL DENSITY
400
500
600
700
mμ
A
B
C

Fig. 18.

Optical densities at 630 mμ of solutions containing 1.2 mg./100 cc. pinacyanole and various amounts of lignin sulfonates. The molecular weights of the lignin sulfonates are 58,000 and 15,500 (curve A), 4,500 (B), 3,700 (C), and 3,650 (D).

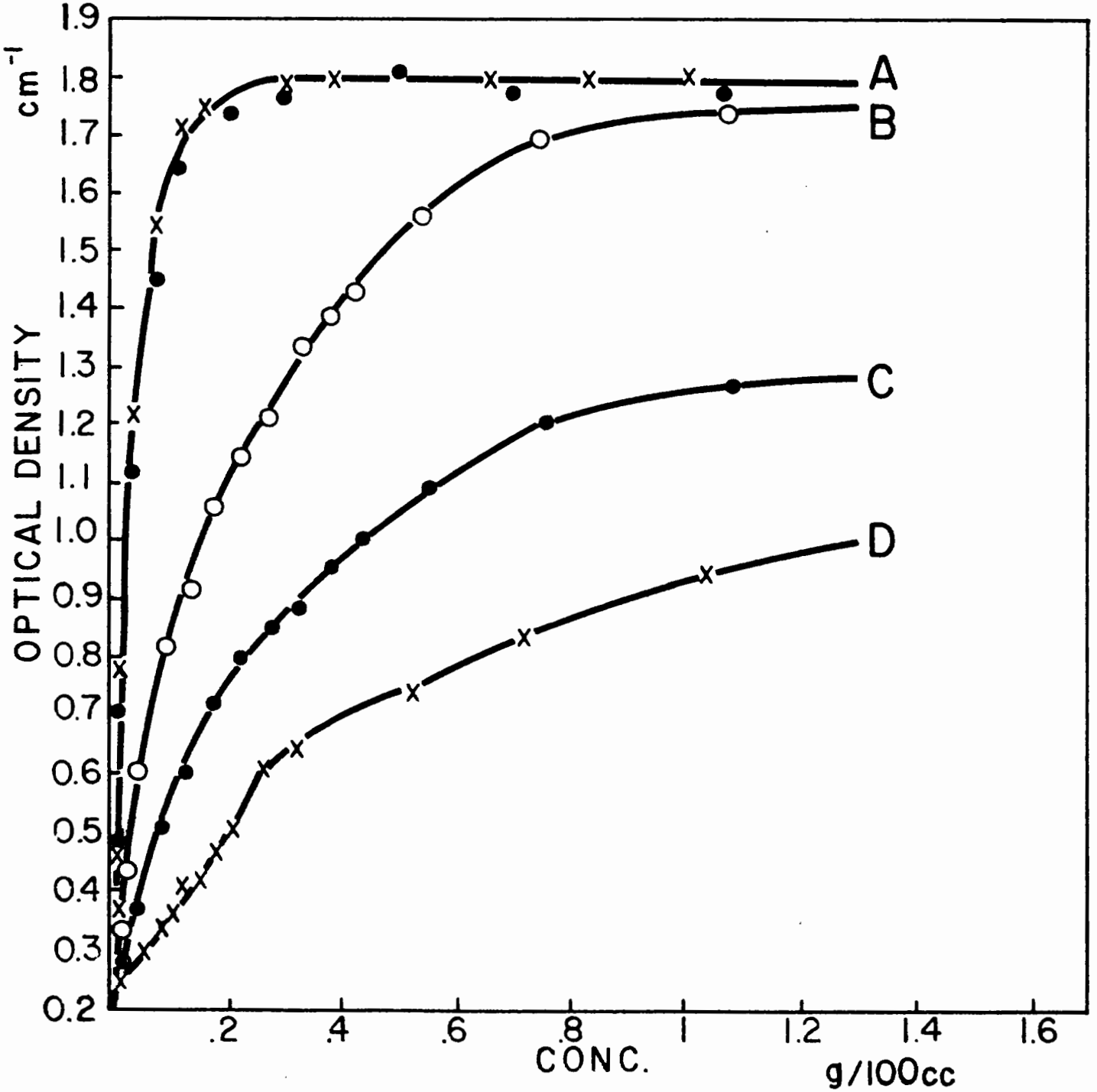
OPTICAL DENSITY
cm⁻¹
1.9
1.8
1.7
1.6
1.5
1.4
1.3
1.2
1.1
1.0
0.9
0.8
0.7
0.6
0.5
0.4
0.3
0.2
A
B
C
D
.2
.4
.6
.8
1
1.2
1.4
1.6
CONC.
g/100cc

The optical densities of solutions containing a fixed amount of dyestuff at various concentrations of lignin sulfonates, measured in a Beckman Model DU spectrophotometer at 630 mμ, are shown in Fig. 18.

As the molecules progressively lose their charge with increasing concentration, they adsorb increasing amounts of dyestuff. The high molecular weight fractions adsorb all the dyestuff present in the solution at around 0.2% concentration. The shape of curve A representing fractions with molecular weights 58,000 and 15,500 corresponds well to the pattern demonstrated by the conductivity and viscosity measurements.

The curves (B), (C) and (D) indicate that the ability of the lower molecular weight fractions to adsorb dye is smaller than that of the high molecular weight fractions. The uncharged particles of the low molecular weight fractions are probably smaller than those of the high molecular weight fractions and, if they contain associated molecules, the number of the molecules per aggregate is probably small. The discontinuity in curve (D) may indicate that the lowest molecular weight fraction associates in solution.

D. VISCOSITY MEASUREMENTS

The viscosities were determined at 25°C in Ostwald-Cannon type (12) viscometers with flow times for water about 400 seconds. The kinetic energy corrections were negligible.

The dependence of the reduced viscosities of sodium lignin sulfonate fractions on their concentrations in distilled water are shown in Figs. 19 and 20. The shape of these curves is typical for polyelectrolytes; at low concentrations the reduced viscosities are high as the molecules are extended, and at high concentrations they are low since the molecules are coiled. The dependence of the reduced viscosities of sodium lignin sulfonates does not follow the empirical equation of Fuoss (31) given below:

$$z = \frac{\eta_{sp}}{c} = \frac{A_\eta}{1 + B_\eta \sqrt{c}} + D_\eta \qquad \ldots \text{ V (1)}$$

In the above equation, z is the reduced viscosity, c' is the concentration, B_η is a constant depending on the dielectric properties of the solvent, (A_η + D_η) is the intrinsic viscosity of the polyelectrolyte when the molecules are extended and D_η is a measure of the intrinsic viscosity of

the randomly coiled molecules. According to this equation $1/(z - D_\eta)$ vs. $\sqrt{c'}$ plot should be linear. No such linear plot could be obtained for the lignin sulfonates. If, however, the term $c^{1/2}$ was replaced in equation V (1) by c^x, then

$$z = \frac{\eta_{sp}}{c} = \frac{A_\eta}{1 + B_\eta c'^x} + D_\eta \qquad \ldots V\ (2)$$

linear plots of $1/(z - D_\eta)$ vs. c^x were obtained for the three highest molecular weight fractions (Fig. 21). The value of D_η was taken equal to the reduced viscosity of a 4% solution. The error in doing so was very small as the reduced viscosities of solutions with concentrations higher than 2% were practically constant. The constant x was established by trial and error. With an approximate value of A_η, $\log[1/(z - D_\eta) - 1/A_\eta]$ was plotted against log c'. The value of A_η was so chosen that this plot yielded a straight line, the slope of which was x. When D_η and x were known, the curves of Fig. 21 could be plotted. The intercepts on the vertical axes obtained by extrapolation were equal to $1/A_\eta$. Since this extrapolation was uncertain, the values of A_η thus obtained were not precise; values of $(A_\eta + D_\eta)$ are estimated to lie within the limits given in Table XII. The values of x and D_η are also tabulated.

Fig. 19.

Reduced viscosities of the five highest molecular weight sodium lignin sulfonate fractions in water. The molecular weights of the numbered fractions are given in Table XII.

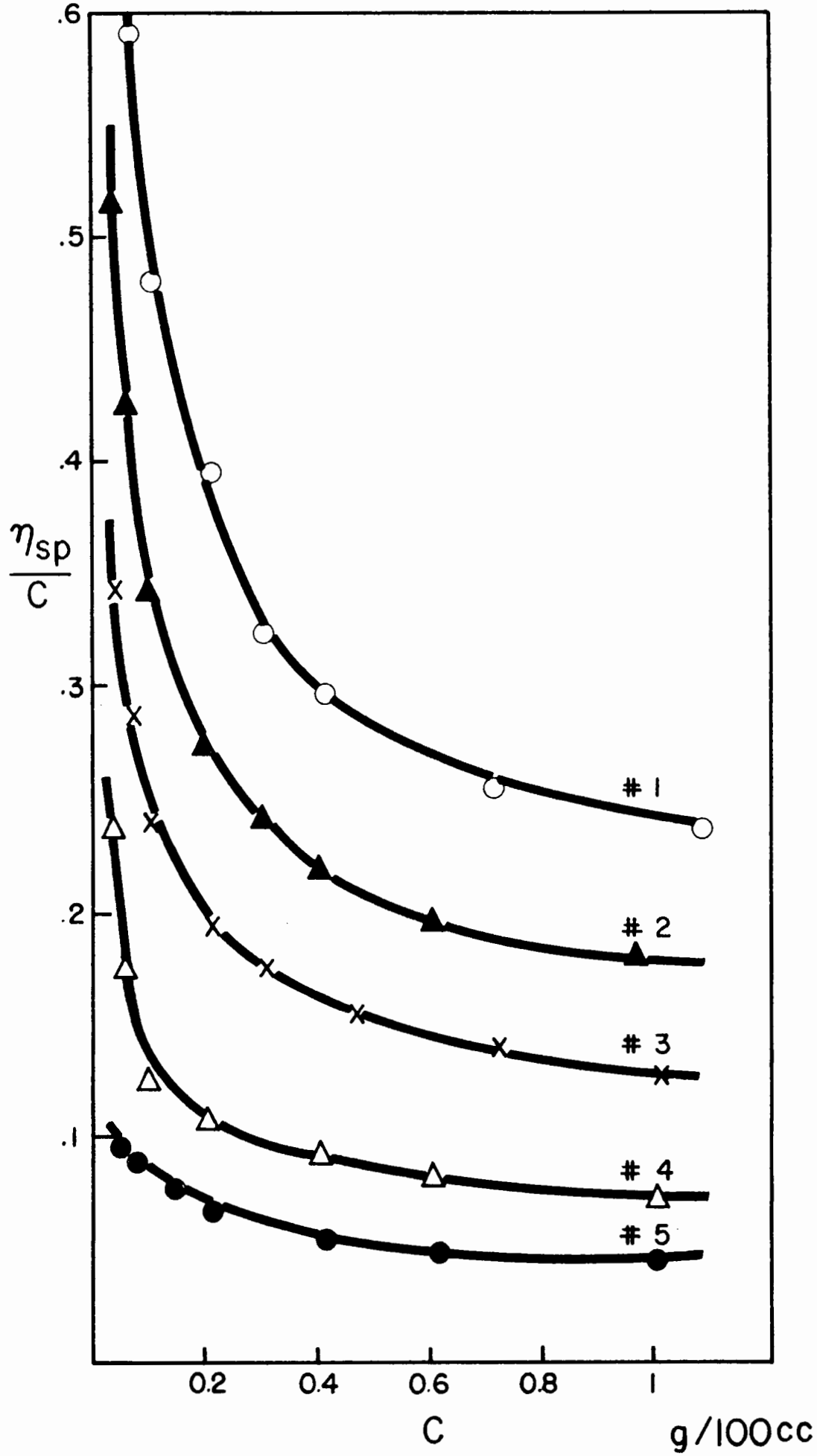
.6
.5
.4
.3
.2
.1
$\frac{\eta_{sp}}{C}$
#1
#2
#3
#4
#5
0.2
0.4
0.6
0.8
1
C
g/100cc

Fig. 20.

Reduced viscosities of the five lowest molecular weight sodium lignin sulfonate fractions in water. The molecular weights of the numbered fractions are given in Table XII.

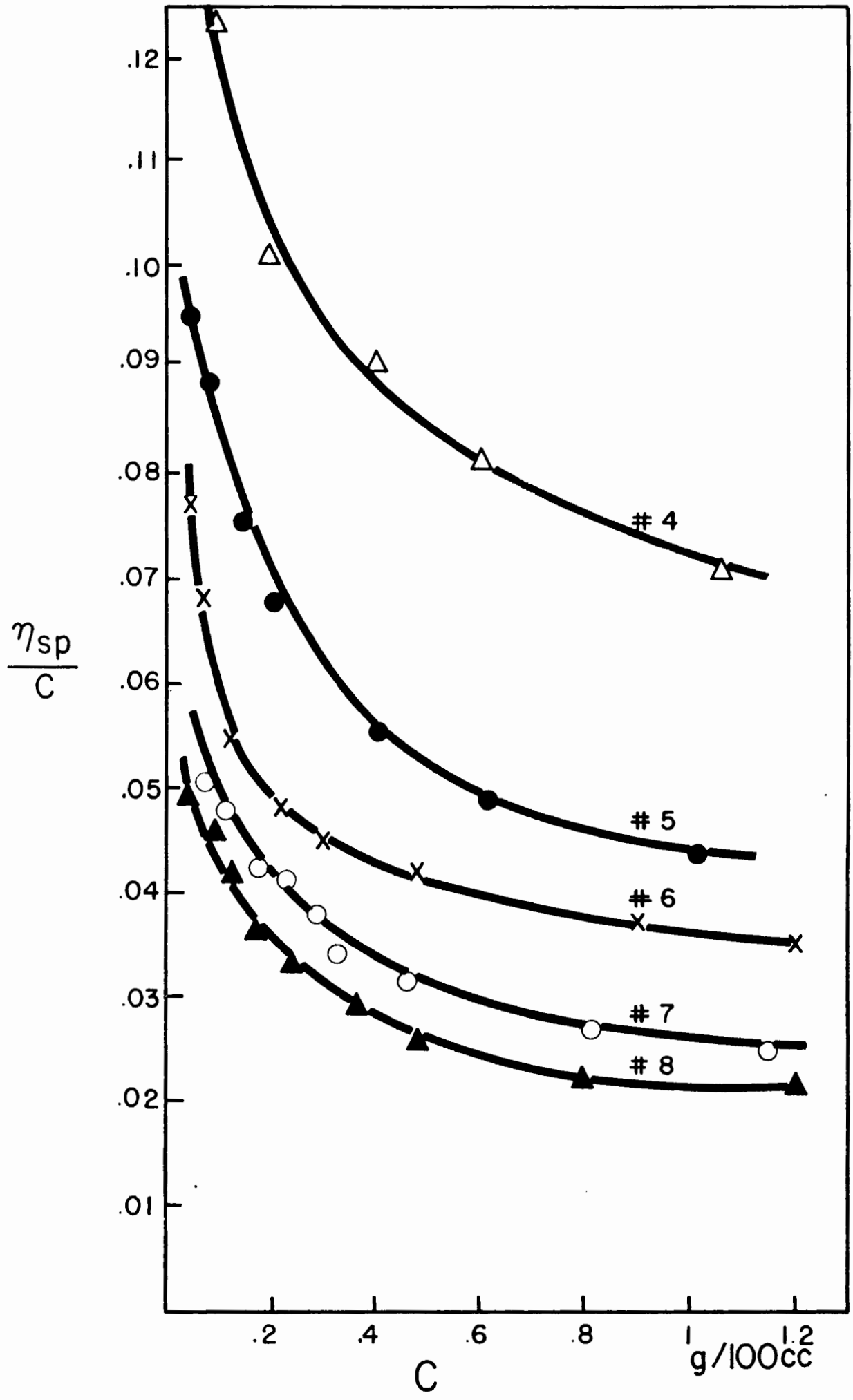
.12
.11
.10
.09
.08
.07
.06
.05
.04
.03
.02
.01
$\frac{\eta_{sp}}{C}$
4
5
6
7
8
.2
.4
.6
.8
1
1.2
C
g/100cc

Fig. 21.

$1/(z - D_\eta)$ vs. c^x plots for the three highest molecular weight fractions.

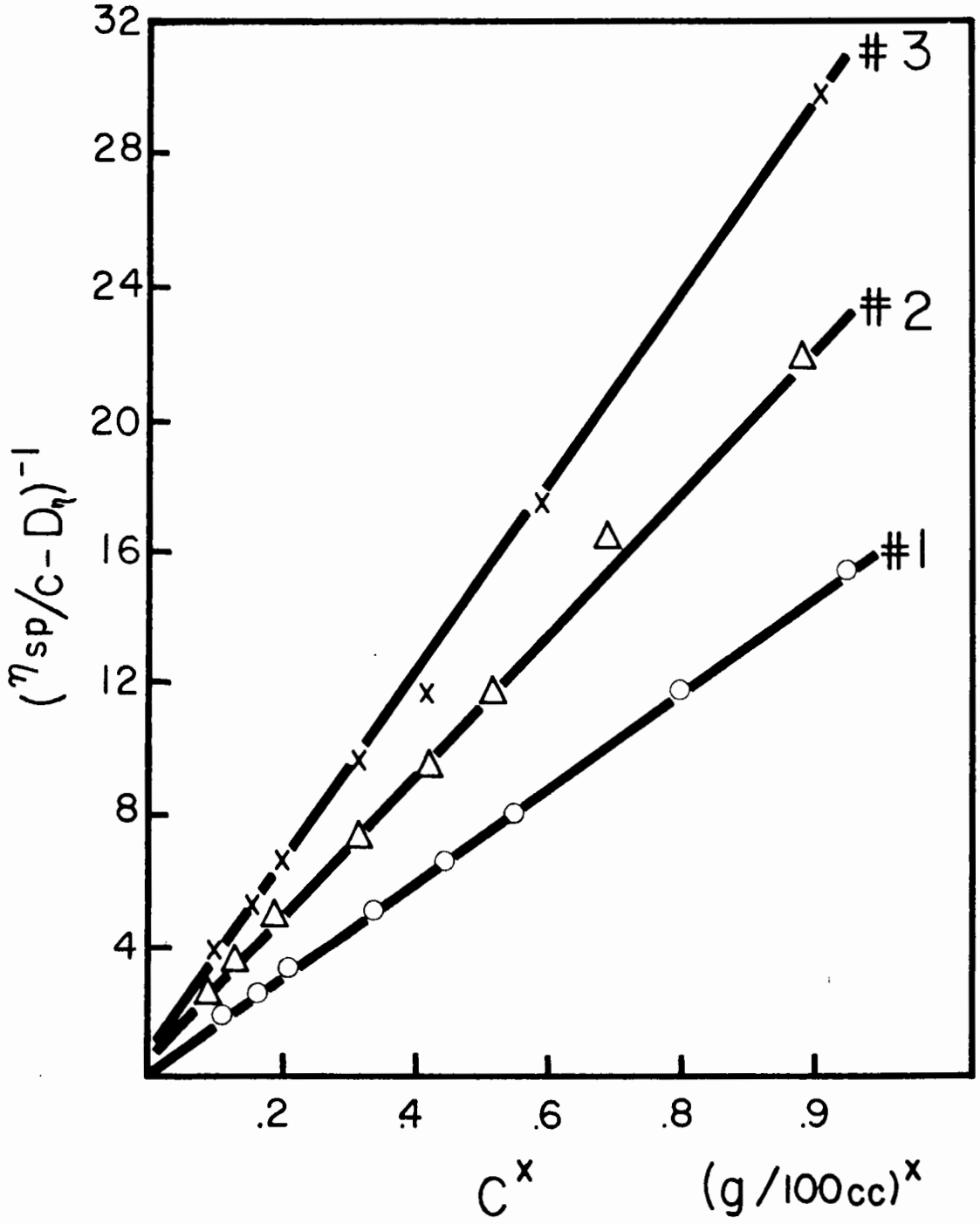
32
28
24
20
16
12
8
4
$(\eta_{sp}/c - D_\eta)^{-1}$
#3
#2
#1
.2
.4
.6
.8
.9
C^x
$(g/100cc)^x$

Equation V.(2) is empirical and does not have the theoretical significance of equation 1. It is probable that the proportionality between $1/(z - D_\eta)$ and c^x is fortuitous and the true equation describing the dependence of the reduced viscosity of the lignin sulfonates on their concentration is that of Schaffgen quoted by Katchalsky (46):

$$z = \frac{\eta_{sp}}{c'} = \frac{A_\eta}{1 + B_\eta\sqrt{c'} + B'_\eta c'} + D_\eta \qquad \ldots V\ (3)$$

The concentration dependence of the reduced viscosities of the other fractions cannot be expressed by equation 2. Thus, the intrinsic viscosities of the extended molecules could not be determined. The D_η values determined at a 4% concentration are given in Table XII.

The reduced viscosities of the fractions in 2N sodium chloride are shown in Fig. 22. The concentration dependence of the reduced viscosities can be expressed by the equation of Simha (85) and Huggins (41) derived for non-charged interacting particles:

$$\eta_{sp}/c' = [\eta] + k[\eta]^2 c' + \ldots \qquad V\ (4)$$

Figure 22.

Reduced viscosities of sodium lignin sulfonates in 2N sodium chloride. The molecular weights of the various fractions are listed in Table XII.

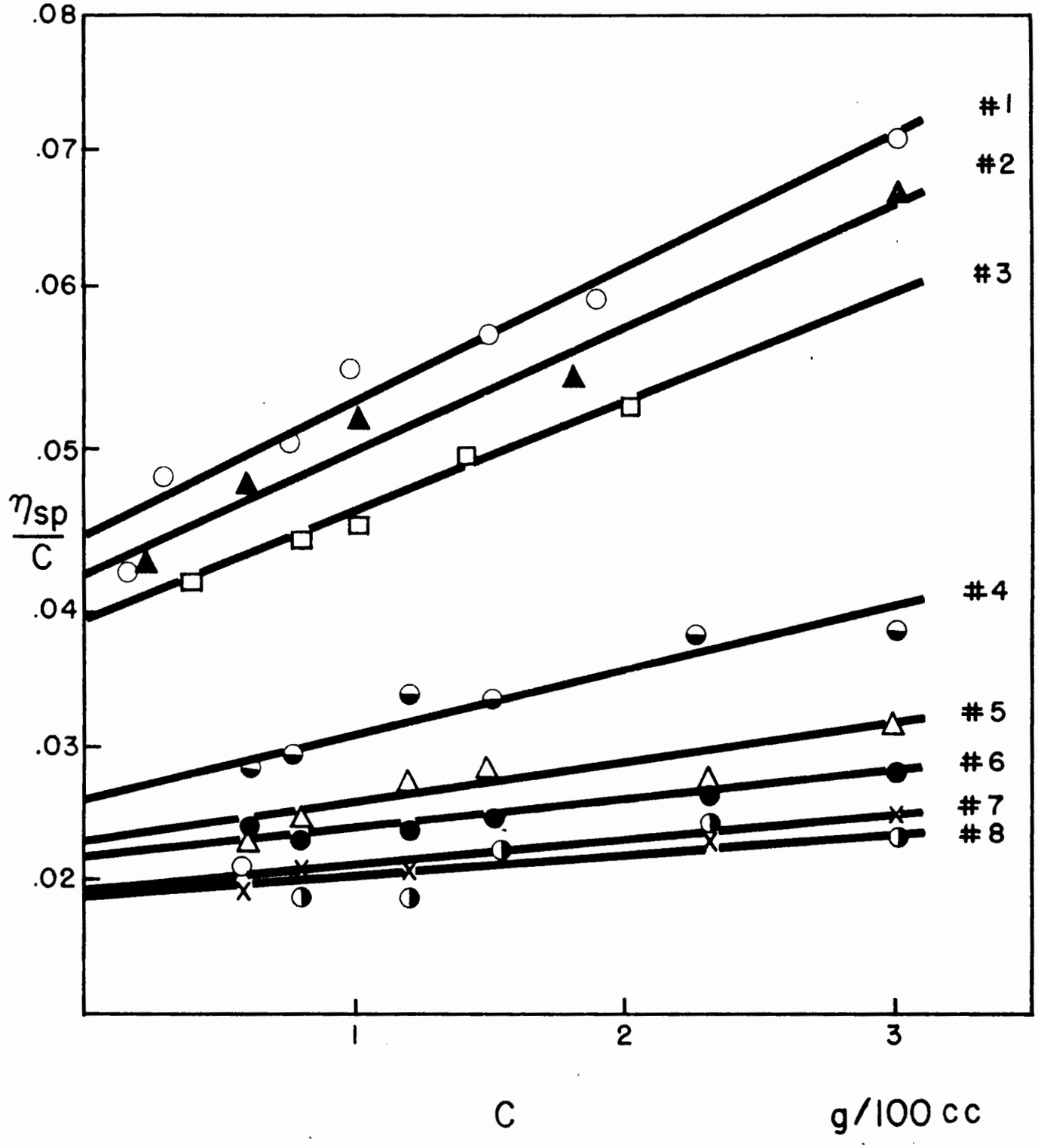
.08
.07
.06
.05
.04
.03
.02
$\frac{\eta_{sp}}{C}$
#1
#2
#3
#4
#5
#6
#7
#8
1
2
3
C
g/100 cc

In this equation $[\eta]$ is the intrinsic viscosity and k is a constant characteristic for the homologous polymer series. Both $[\eta]$ and k are given for all fractions in Table XII. As can be seen, k changes between 4.2 and 6. Lignin sulfonates are approximately, but not truly, members of a homologous series and this may account for the variation of k.

E. RELATIONS BETWEEN INTRINSIC VISCOSITIES, DIFFUSION COEFFICIENTS AND MOLECULAR WEIGHTS.

According to the theories of Kuhn (49), Kirkwood and Riesman (47) and Debye and Bueche (17), the constants a and b in the equations:

$$[\eta] = k_2 M^a \qquad \ldots V\ (5)$$

$$D_1 = k_1 M^{-b} \qquad \ldots V\ (6)$$

describing the dependence of the intrinsic viscosities and the diffusion coefficients D_1 on the molecular weights are both equal to unity, if the molecules are linear flexible chains, randomly coiled and permeable to the solvent, and equal to 0.5, if the randomly coiled flexible molecules are impermeable to the solvent. The constants k_1 and k_2

are characteristic of the homologous series. Kuhn and Kuhn (51) showed that these theories are also applicable to branched molecules if these chains are flexible and randomly coiled. The intrinsic viscosities of branched-chain molecular structures are lower than those of linear molecules of comparable size. Huggins (loo, 40) has shown that a = 2 when molecules behave as rigid rods.

It has been experimentally verified for a number of polyelectrolytes (32, 46) that the values of "a" for the intrinsic viscosities (A_η + D_η), corresponding to the extended molecules, approach 2 if the polyelectrolytes are linear, and are higher than unity but less than 2 if the polyelectrolytes are branched (86). As mentioned before, D_η is a measure of the intrinsic viscosity of a randomly coiled polyelectrolyte. Depending on the degree of ionization D_η changes linearly with, or proportionally to the square root of, the molecular weight (46).

The diffusion coefficients, D_η values, and intrinsic viscosities in 2N sodium chloride are plotted on a logarithmic scale against the number average molecular weights of the lignin sulfonate fractions on Fig. 23 . From the slopes of these plots it can be concluded that the value of "a" is approximately unity for the molecular weight dependence of

TABLE XII.

Viscosity data, diffusion coefficients and number average molecular weights of the sodium lignin sulfonate fractions.

Fraction No.	Dimension	Solvent	1	2	3	4	5	6	7	8
Molecular Weight	gm.	1/2N NaCl	58,000	19,200	15,500	8,500	5,200	4,600	3,700	3,650
Diffusion Coefficient	$\frac{cm^2}{day}$	1/2N NaCl	0.0314	0.0849	0.113	0.134	0.178	0.194	0.219	0.221
$D = \left[\frac{\eta_{sp}}{c}\right]_{c=4\%}$	$\frac{100cc.}{gm.}$	Water	0.172	0.134	0.0905	0.0563	0.0389	0.0328	0.0242	0.0211
$[\eta] = A + D$	$\frac{100cc.}{gm.}$	Water	4 - 7	1.35 - 1.6	0.8 - 1.2	-	-	-	-	-
x	-	Water	0.71	0.73	0.78	-	-	-	-	-
$[\eta]$	$\frac{100cc.}{gm.}$	2N NaCl	0.0455	0.0425	0.0394	0.0262	0.0235	0.0220	0.0197	0.0190
K	-	2N NaCl	4.9	5.0	5.42	6.00	4.75	4.15	4.6	4.6

Figure 23.

Correlations between molecular weights, diffusion coefficients and viscosity data.

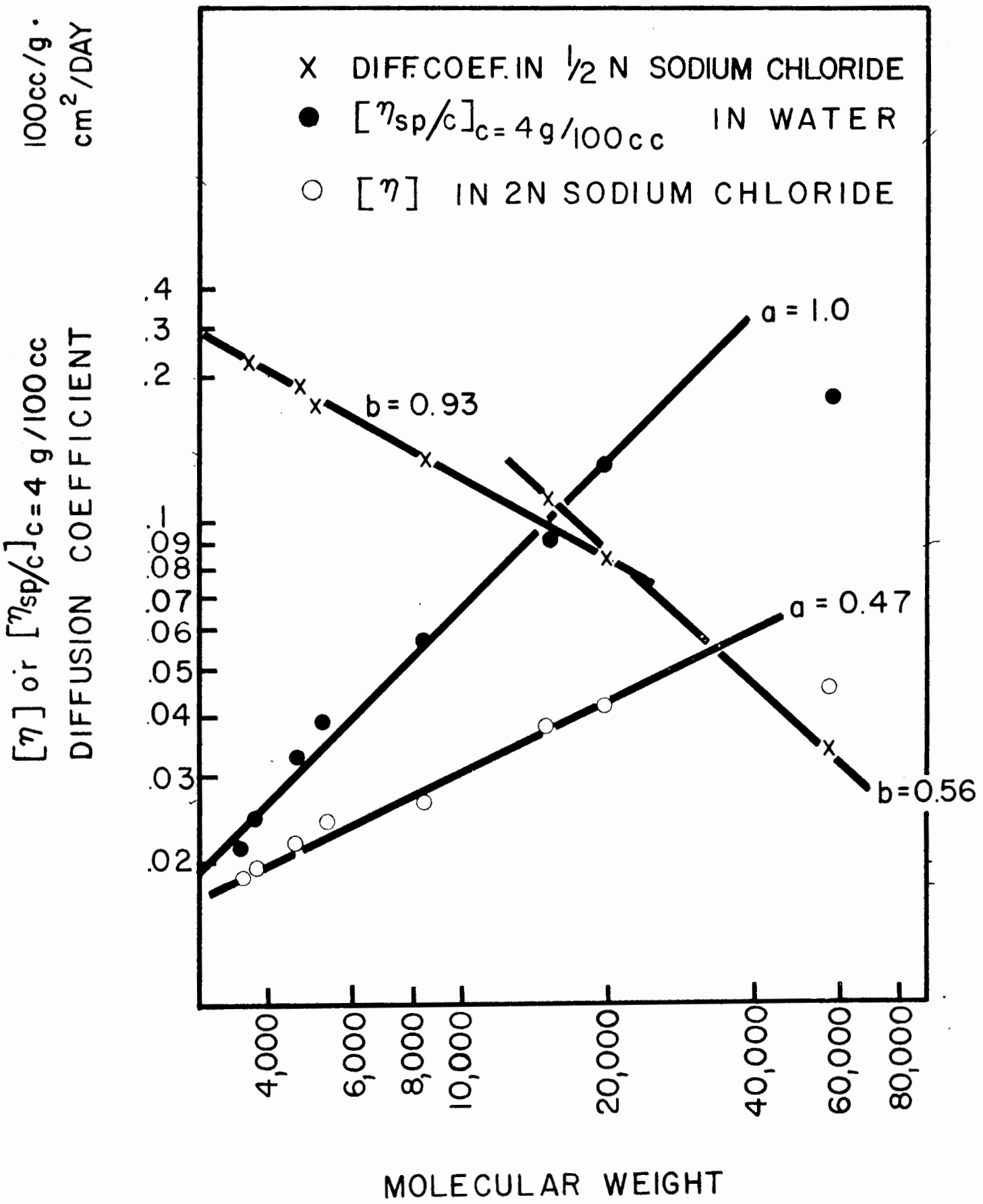
X DIFF. COEF. IN ½ N SODIUM CHLORIDE
● $[\eta_{sp}/c]_{c=4g/100cc}$ IN WATER
○ $[\eta]$ IN 2N SODIUM CHLORIDE
100cc/g · cm²/DAY
$[\eta]$ or $[\eta_{sp}/c]_{c=4\,g/100cc}$
DIFFUSION COEFFICIENT
.4
.3
.2
.09
.08
.07
.06
.05
.04
.03
.02
a = 1.0
b = 0.93
a = 0.47
b = 0.56
4,000
6,000
8,000
10,000
20,000
40,000
60,000
80,000
MOLECULAR WEIGHT

D_η and 0.47 for the intrinsic viscosities in 2N sodium chloride if the highest molecular weight fraction is disregarded. According to Debye (16), the intrinsic viscosity is a measure of the true partial specific volume. As can be seen, the intrinsic viscosities in salt solution are smaller than the D_η values. Consequently, probably owing to the osmotic pressure of the sodium chloride, the coils in the sodium chloride solution are compressed while the structure of the coils in pure water is looser. The compressed coils are impermeable to water, the loose coils are permeable and hence the values of "a" are in the range of 0.5 and 1 respectively.

Both the intrinsic viscosity in 2N sodium chloride and the D_η value of fraction no. 1 are lower than predicted by the regularities described above. The integral molecular weight distribution of the lignin sulfonates (Fig. 15) indicates that this fraction is more heterodisperse than the others and probably contains lignin sulfonates with molecular weights as high as 100,000. It is fair to assume that the probability for branching, during polymerization in the sulfite cook, is greater the higher the degree of polymerization. If so, the reason for the relatively low D_η and low intrinsic viscosity of the highest molecular weight

fraction is its higher degree of branching.

The diffusion coefficients were determined in 1/2 N sodium chloride as previously described. It seems that there are two "b" values for the dependence of the diffusion coefficients on the molecular weights: $b = 0.56$ corresponds to all fractions but No. 1 and No. 3, while $b = 0.93$ corresponds to fractions Nos. 1, 2 and 3; this matter requires further investigation.

In connection with these results it is of interest to mention the work of Olleman, Pennington and Ritter (69), who determined the diffusion coefficient, intrinsic viscosity and partial specific volume of ammonium lignin sulfonates in 1 N ammonium acetate solution. Using the Polson-Kuhn equation (74), they calculated the axial ratio to be 4.6. The frictional coefficient was evaluated according to Perrin (73). The weight-average molecular weight 21,000 calculated by them for a lignin sulfonate with 0.080 sq.cm./day diffusion coefficient compares favourably with the diffusion coefficient 0.0847 and number average molecular weight 19,200 of fraction No. 2.

F. CONCLUSIONS

The results presented above show that the lignin

sulfonates are flexible polyelectrolytes. In aqueous solution the molecules are coiled at sufficiently high lignin sulfonate concentration and in the presence of a suitable electrolyte. The structure of the coiled sodium lignin sulfonate molecules in the absence of sodium chloride is looser than in its presence. There is indication that the low molecular weight fractions associate in solution and that the molecules of the highest molecular weight fraction are more branched than those of the other fractions.

Simha et al. (84) showed that the adsorption of any polymer on solid surfaces is greatly favoured if the polymer is flexible because the number of anchorage points per molecule is increased. A functional property of adhesives and dispersants is their ability to be adsorbed on solid surfaces. The applicability of flexible polyelectrolytes, such as natural gums, carboxy-methyl-cellulose and also lignin sulfonates as adhesives and dispersants, may be explained by their molecular flexibility and good solubility.

VI. CLAIMS TO ORIGINAL RESEARCH

(1) Lignin sulfonates were separated into eight fractions of different molecular weights by means of fractional dialysis and ultrafiltration. Changes in analytical data of the residual liquor and dialysate were closely controlled during the dialysis and indicated that the reducing power of the lignin sulfonates under investigation was inherent and not due to impurities. The ultrafiltration was carried out in a new type of ultrafilter.

(2) All fractions had analogous ultraviolet spectra, the ratios between the maximum and minimum extinctions being the same. The ultraviolet extinctions per methoxyl bearing unit were the same for all but the lowest molecular weight fractions.

(3) A new type of supported membrane osmometer for aqueous solutions was designed.

(4) The theory and practice for correcting osmotic pressure measurements for membrane leakage was developed. This technique makes possible the evaluation of molecular

weights as low as 5,000 with membranes which are impermeable only to substances with molecular weights higher than 20,000. It is in principle also possible to determine the molar volumes of solvated solutes by this method.

(5) The integral molecular weight distribution of the lignin sulfonates was determined and found that the molecular weights of the lignin sulfonates range from about 3,500 to an excess of 60,000.

(6) The experimental evidence presented suggests that lignin sulfonates are flexible polyelectrolytes. Some results also indicate that the lower molecular weight fractions associate in solution and that the degree of branching of the highest molecular weight fraction is higher than that of the other fractions.

VII. SUGGESTIONS FOR FURTHER WORK

A. FRACTIONATION OF LIGNIN SULFONATES

(1) Methods other than ethanol precipitation of the barium salts could be used for the separation of the lignin sulfonates from the carbohydrates. In this connection, Erdtman's (19) work on the precipitation of lignin sulfonates with various amines is of interest.

(2) Membranes with larger ranges of pore sizes than used in the present investigation could be used for the fractionation of the higher molecular weight fractions. The ultrafiltration could be speeded up by moderately heating the liquor and thus reducing its viscosity. It would also be of interest to compare the average pore sizes of the membranes used, and the partition coefficients and molecular weights of the fractions.

(3) The carbohydrates present in the spent sulphite liquor were not investigated in the present work. The non-ionic sugars and the non-lignous acids could be separated by electrodialysis using ion exchange membranes. The non-lignous acids could be investigated by methods similar to

those employed with lignin sulfonates.

B. RESEARCH ON THE PHYSICAL STRUCTURE OF LIGNIN SULFONATE MOLECULES.

(1) The degree of solvation of the lignin sulfonates in salt solution could be established by ultra-filtration experiments as suggested by McBain (62).

(2) Correlating these results with partial specific volume determinations, the true effective volumes of the lignin sulfonates in salt solutions can be determined. Either from the effective volumes, diffusion coefficients and ultra-centrifuge sedimentation measurements, or from the effective volumes, diffusion coefficients and intrinsic viscosities, weight average molecular weights and shape factors can be determined. It would be of interest to compare the results obtained by these two ways with each other and also to compare the weight average molecular weights with the number average molecular weights established by osmotic pressure measurements.

(3) The reduced viscosities of the fractions in water at different degrees of neutralization could be

examined to determine how stronger ionization influences the flexible coiling of the molecules.

(4) Reduced viscosities of the sodium lignin sulfonates with different amounts of sodium chloride added could be measured and to obtain the intrinsic viscosities corresponding to the fully stretched molecules, the results could be extrapolated to zero sodium chloride concentration by the method of Paals and Hermans (71, 72).

(5) Whether lignin sulfonates associate or not may be clarified by light scattering experiments. By such measurements dimensions of the molecules could also be established (32, 70).

(6) The intrinsic dissociation constant of the ionizable groups and the electrostatic potential of the lignin sulfonates could be determined from potentiometric titration or even better from the combination of the results obtained from potentiometric titration and electrophoresis experiments (46, 32).

C. RESEARCH ON THE SURFACE ACTIVE PROPERTIES OF LIGNIN SULFONATES

Investigations on the surface active properties of

the lignin sulfonates would have both practical and theoretical significance. Ways for the improvement of the present practical applications of the lignin sulfonates may be found. Finding correlations between the ability of the lignin sulfonates to adsorb in interfaces and their molecular size, shape, charge and flexibility would be of general interest. Surface tension lowering, foam stabilizing, interfacial tension lowering, solubilizing, deflocculating and dispersing properties of the different fractions could be investigated. Experimental methods are described by Alexander and Johnson (2, 3), McBain (58, 59), Moillet and Collie (67) and Adam (1).

D. IMPROVEMENTS IN THE TECHNIQUE OF OSMOTIC PRESSURE MEASUREMENTS WITH MEMBRANES PERMEABLE TO THE SOLUTE.

A new supported membrane osmometer should be designed in which the contents of both half cells can be stirred. This design can be similar to the one used in the present work. The stirring can be accomplished by circulating the solutions in the half cell by magnet governed propellers in closed tubes attached to the inlets of the half cells. By putting small reservoirs into the path of the solutions, the half cell volumes could be changed, allowing

greater variations in the values of K_s, α and β, than was done in the present work. It would also be advantageous if this instrument could be filled right in the thermostat with previously temperature-adjusted solvent and solution.

Using such an instrument it should be possible to measure osmotic pressures more accurately, to extend the applicability of the method into lower molecular weight regions and to determine molar volumes of hydrated substances. The latter results could be compared to the partial specific volumes corrected for hydration in accordance with ultrafiltration experiments previously described.

BIBLIOGRAPHY

(1) Adam, N.K., The Physics and Chemistry of Surfaces, Oxford University Press, London (1941).

(2) Alexander, A.E. and Johnson, P., Colloid Science, p.667-696 Oxford University Press, London (1949).

(3) Alexander, A.E. and Johnson, P., ibid. p.611-667.

(4) Aulin-Erdtman, G., Tappi, 32, 160 (1949).

(5) Aulin-Erdtman, G., Svensk Papperstidn. 56,287 (1953).

(6) Aulin-Erdtman, G., Bjorkman, A., Erdtman, H., Hagglund, S.E., Svensk Papperstidn. 50:11B, 81 (1947).

(7) Adler, E. and Lindgren, B.O., Svensk Papperstidn. 55, 563 (1952).

(8) Brauns, F.E., Chemistry of Lignin, p. 114-125 Academic Press, New York (1952).

(9) Brauns, F.E., ibid., p.191-197.

(10) Brauns, F.E., ibid., p.621-669.

(11) Bechhold, H., Z. Physik. Chem. 60, 257 (1907)

(12) Cannon, M.R. and Fenske, M.R., Ind. Eng. Chem. Anal. Ed. 10, 297 (1938).

(13) Conner, W.P., J. Chem. Phys. 9, 591 (1941).

(14) Cummings, A.P., Technique of Organic Chemistry, Ed. by Weissberger, p.558-563, Interscience Publishers, New York (1950).

(15) Corrin, M.L. and Harkins, W.D., J. Am. Chem. Soc. 69, 679 (1947).

(16) Debye, P., J. Chem. Phys. 14, 636 (1946).

(17) Debye, P., and Bueche, M., J. Chem. Phys. 16, 573 (1948).

(18) Elford, W.J. and Ferry, J.D., Biochem. J. 28, 650 (1935).

(19) Erdtman, H., Svensk Papperstidn. 45, 315, 374, 392 (1942).

(20) Erdtman, H., Svensk Kem. Tid. 53, 201 (1941).

(21) Erdtman, H. and Lingren, B.O. and Petersson, T. Acta Chem. Scand. 4, 228 (1950).

(22) Eastham, A.M., Fisher, H.E., Kulka, M. and Hibbert, H., J. Am. Chem. Soc. 66, 26 (1944)

(23) Ernsberger, F.M. and France, W.G., J. Phys. Coll. Chem. 52, 267 (1948).

(24) Freudenberg, K., Holz abs Roh. und Werkstoff. 11, 267 (1953).

(25) Freudenberg, K., Svensk Kem. Tid. 55, 201 (1943).

(26) Freudenberg, K. and Dietrich, G., Ann. 146, 563 (1949).

(27) Freudenberg, K., Lautsch, W. and Piazolo, G. Cellusochem. 22, 97 (1948).

(28) Flory, P.J., Principles of Polymer Chemistry p.629-637 Cornell University Press, (1953).

(29) Ferry, J.D., Chem. Rev. 18, 374 (1936)

(30) Fuoss, R.M., Disc. Farad. Soc. 11, 125 (1951)

(31) Fuoss, R.M., J. Polymer Sci. 3, 603 (1948)

(32) Fuoss, R.M. and Strauss, U.P., Die Physik der Hochpolymeren. Ed. by H.A. Stuart, Vol. II., p.680-700. Springer Verlag, Berlin (1953).

(33) Fuoss, R.M. and Mead, D.J., J. Phys. Chem. 47, 59 (1943).

(34) Hagglund, E., Chemistry of Wood, p.292-297, Academic Press, New York (1951).

(35) Hagglund, E., ibid. p. 306-324.

(36) Hengstenberg, J., Die Physik der Hochpolymeren, Ed. By H.A. Stuart, Vol. II. p.483-484 Springer Verlag, Berlin (1953).

(37) Goldschmied, O., Analitical Chem. 26, 1421 (1954).

(38) Gralen, N., J. Colloid Sci., 1, 453 (1946).

(39) Hagglund, E., Chemistry of Wood, p.221-226 Academic Press, New York (1951).

(40) Huggins, M.L. J. Phys. Chem. 43, 439 (1939).

(41) Huggins, M.L, J. Am. Chem. Soc. 64, 2716 (1942)

(42) Hibbert, H., Am. Rev. Biochem., 11, 183 (1942).

(43) Ivarsson, B., Svensk Papperstidn. 51, 1 (1951).

(44) International Critical Tables, I. ed. Vol.V. p.68.

(45) Klason, P., Beitrage zur Kenntniss der Zussammensetzung des Fichtenholzes p. 34 (1911).

(46) Katchalsky, A., J. Polym. Sci., 12, 159 (1954).

(47) Kirkwood, J.G. and Riseman, J., J. Chem. Phys. 16, 565 (1948).

(48) Koenig, F., Cellulosechemie, 2, 100 (1921).

(49) Kuhn, W., Kolloid Z. 68, 2 (1934).

(50) Kuhn, W., Z. fur Electrochem. 55, 207 (1951).

(51) Kuhn, W. and Kuhn, H., Helv. Chem. Acta 30, 159 (1947).

(52) Lindgren, B.O., Svensk Papperstidn. 55, 633 (1952).

(53) Leopold, B., Acta Chem. Scand. 6, 65 (1952).

(54) Lautsch, W., Die Chemie, 57, 149 (1949).

(55) Lautsch, W., and Piazolo, G., Cellulosechemie 22, 48 (1944).

(56) Loughborough, D.L. and Stamm, J., J. Phys. Chem. 40, 1113 (1936).

(57) Loughborough, D.L. and Stamm, J., J. Phys. Chem. 45, 1137 (1941).

(58) McBain, J.W., Colloid Science, p. 240-274 Heath & Co., Boston, (1950).

(59) McBain, J.W., ibid., p.14-38, 174-187.

(60) McBain, J.W., ibid., p.121-130.

(61) McBain, J.W. and Liu, T.H., J. Am. Chem. Soc. 53, 59 (1931).

(62) McBain, J.W., Kawalzami, Y. and Lucas, H.P., J. Am. Chem. Soc. 55, 2762 (1933).

(63) Marshall, H.B., Pulp and Paper Mag. of Can. 54, 113 (1953).

(64) Melander, K.A.H., Cellulosechemie, 2, 41 (1921).

(65) Markham, A.E., Peniston, Q.P. and McCarthy, J.L., J. Am. Chem. Soc. 71, 3599 (1949).

(66) McCarthy, J.L., private communication.

(67) Moillet, J.L. and Collie, B., Surface Activity, p.11-221, Spon Ltd., London.

(68) Northop, J.H. and Anson, M.L. J. Gen. Physiol. 12, 543 (1929).

(69) Olleman, E.D., Pennington, D.E. and Ritter, D.M., J. Coll. Sci. 3, 185 (1948).

(70) Oth, A. and Doty, A., J. Phys. Chem. 56, 43 (1952).

(71) Paals, D.T.F. and Hermans, P.H., Rec. Trav. Chi. Pays-Bas 71, 433 (1952).

(72) Paals, D.T.F. and Hermans, P.H., J. Polym. Sci. 5, 733 (1950).

(73) Perrin, F., J. Phys. radium. 7, 1 (1936).

(74) Polson, A., Kolloid Z. 88, 51 (1939).

(75) Peniston, Q.P. and McCarthy, J.L., J. Am. Chem. Soc. 70, 1324 (1948).

(76) Peniston, Q.P. and Hibbert, H., Paper Trade J. 109, 231 (1939).

(77) Pennington, D.E. and Ritter, D.M., J. Am. Chem. Soc. 69, 665 (1941).

(78) Racky, G., Papierfabrikant 39, 121 (1941).

(79) Racky, G., Cellulosechem. 20, 22 (1942).

(80) Samec, M. and Ribaric, I., Kolloidchemische Beihefte, 24, 157 (1928).

(81) Samec, M. and Pirkenmayer, B., Kolloid Z. 72, 336 (1935).

(82) Schwabe, K. and Hahn, E., Holzforschung 2, 42 (1947).

(83) Schwabe, K. and Hasner, L., Cellulosechem. 20, 61 (1942).

(84) Simha, R., Frisch, H.L., Erich, F.R., J. Phys. Chem. 57, 585 (1953).

(85) Simha, R., J. Res. Natl. Bur. Standards, 42, 409 (1944).

(86) Schaeffgern, J.R. and Trivisonno, C.F., J. Am. Chem. Soc. 74, 2715 (1952).

(87) Samuelson, O. and Westlin, A., Svensk Papperstidn. 50:11B, 149 (1947).

(88) Samuelson, O. and Westlin, A., Svensk Papperstidn. 51 179 (1948).

(89) Stauffer, R.E., Technique of Organic Chemistry, Ed. by Weissberger, Vol. III. p.323-376 Interscience Publishers, New York (1950).

(90) Schulz, G.V., Die Physik der Hochpolymeren, Ed. by H.A. Stuart, Vol. II. p.387, Springler Verlag, Berlin, (1953).

(91) Vjebock, F. and Schwappach, A., Ber. 63, 2818 (1930).

(92) Wagner, R.H., Technique of Organic Chemistry,
Ed. by Weissberger, Vol. I., Part I.
p.518-540, Interscience Publishers, New York (1949).

(93) Wagner, R.H., ibid. p.500-503.

(94) Yorston, F.H., Pulp & Paper Mag. of Can.,
47:3, 74 (1947).

(95) Gierer, J., Lindgren, B.O. and Mikawa, H.,
Svensk Papperstidn. 57, 633 (1954).

(96) Glasstone, S., Textbook of Physical Chemistry,
p.654-657, 664-670. McMillan, London (1948).

(97) Gordon, A.R., Annals N.Y. Acad. of Sci.,
46, 785 (1945).

(98) Hartley, G.S., Trans. Far. Soc. 30, 444 (1934).

(99) Hearon, W.M., Tappi, 636:9 14A (1953).

(100) Huggins, M.L., J. Phys. Chem. 42, 911 (1938).